

THE MOLECULAR MECHANISM OF ACTION OF THE
ANTIANGIOGENIC NATURAL PRODUCT, CREMASTRANONE

Halesha Dhurvigere Basavarajappa

Submitted to the faculty of the University Graduate School
in partial fulfillment of the requirements
for the degree
Doctor of Philosophy
in Department of Biochemistry and Molecular Biology
Indiana University

July 2016

Accepted by the Graduate Faculty, Indiana University, in partial
fulfillment of the requirements for the degree of Doctor of Philosophy

Timothy W. Corson, Ph.D., Chair

Doctoral Committee

Maria B. Grant, MD.

May 16, 2016

Thomas D. Hurley, Ph.D.

Lawrence A. Quilliam, Ph.D.

Rebecca J. Chan, MD, Ph.D.

DEDICATION

This thesis is dedicated to my mother Subhadra Arehalli and my wife Ragadeepthi Tunduguru. Without their support and encouragement I would not have reached this point. I am also dedicating this thesis to my daughter Spoorthi Dhurvigere.

ACKNOWLEDGEMENTS

I would first like to thank my adviser, Dr. Timothy W Corson, for providing a conducive research environment that enabled me to carry out and successfully complete my dissertation with critical thinking. It has been an absolute pleasure working in his laboratory. He is an inspiring supervisor with so much positive attitude towards life and research that he has been my role model. I thank him for his unending support to my work.

I thank all the current and former members of the Corson lab. In particular, I would like to thank Kamakshi Sishtla and Rania Sulaiman for their help with my project, cheerful and engaging conversations in the laboratory and supporting me throughout my graduate work. Kamakshi Sishtla cannot be credited enough for her technical advice, scientific support and help in ordering reagents. I would also like to thank Mehdi Shadmand who as an LHSI undergraduate student helped me with some of the experiments.

This project would not be possible without the help from chemistry collaborators, Dr. Seung-Yong Seo, Bit Lee and Xiang Fei (College of Pharmacy, Gachon University, Incheon, South Korea). They are the synthetic chemists who synthesized all of the homoisoflavanones and affinity reagents used in the project. I would also like to acknowledge the insight and assistance from other coauthors, Dr. Michael Boulton, Dr. Maria Grant, Dr. Gangaraju Rajashekhar. These scientists helped me understand the ocular diseases in detail.

I thank the members of my thesis committee, Dr. Thomas D. Hurley, Dr. Lawrence A. Quilliam, Dr. Rebecca J. Chan and Dr. Maria B. Grant. They have provided useful suggestions and ideas that benefited my project greatly.

I would also like to thank Kemin Industries for providing me the Ausich graduate student research scholarship for two years.

I consider myself fortunate to have made good friends in Indianapolis who have supported me through the ups and downs of this journey. Kamakshi Sishtla, Rania Sulaiman, Michael O'Hare, Mehdi Shadmand, Sasha Vayl, Judith Quigley and Breedge Callaghan were of great support. I will cherish friendship and all the happier times spent together with Latha Ramalingham, Abhirami Iyer, Sridhar Nonavinakere, Isha Singh, Akaash Mishra, Siddarth Rangpariya, Sudha Savant, Kishore Mahalingam and Lakshmipalam Reddy. They have helped me mould my character during my stay in Indianapolis.

I would like to thank my father Basavarajappa, brothers Dhananjaya and Rudresha and sister Manjula who have always given me unrelenting encouragement and love.

Halesha Dhurvigere Basavarajappa

The molecular mechanism of action of the antiangiogenic natural product,
cremastranone

Prevention of pathological angiogenesis is a key strategy for treatment of common blinding ocular diseases such as retinopathy of prematurity, proliferative diabetic retinopathy, and wet age-related macular degeneration. The current treatment strategies are associated with partial vision loss and are ineffective in a significant patient population. Hence novel drugs as well as new ways to target ocular angiogenesis are needed for treating these diseases. I pursued a natural antiangiogenic compound, cremastranone, to develop novel drug leads and to find new targets. The objective of my doctoral thesis project was to elucidate cremastranone's molecular mechanism of action and optimize its structure-activity relationship (SAR).

In order to achieve this goal, with the help of chemistry collaborators cremastranone was synthesized for the first time. I showed that cremastranone has 50-fold more potency against endothelial cells as compared to non-endothelial cells, and also tested a novel active isomer, SH-11052. By SAR studies I identified a potent molecule, SH-11037, that has 10-fold more selectivity against retinal endothelial cells as compared to macrovascular endothelial cells. I then elucidated cremastranone's molecular mechanism using a chemical proteomic approach. I identified ferrochelatase (FECH) as a specific interacting protein partner of cremastranone using photoaffinity chromatography. Hence, I

hypothesized that cremastranone exerts its antiangiogenic activities through modulation of the functions of FECH.

Cremastranone inhibited the enzymatic activity FECH in endothelial cells. Therefore, I investigated the role of FECH in ocular angiogenesis. Partial loss of FECH, using a siRNA-based knock down approach, decreased retinal angiogenesis both in vitro and in vivo in mouse models. Knock down of FECH decreased the expression levels of key proangiogenic proteins HIF-1 α , eNOS, and VEGFR2. This work suggests that ferrochelatase plays an important, previously undocumented role in angiogenesis and that targeting of this enzyme by cremastranone might be exploited to inhibit pathological angiogenesis in ocular diseases.

Timothy W. Corson, Ph.D., Chair

TABLE OF CONTENTS

List of Tables	xiv
List of Figures	xv
List of Abbreviations	xvii
Chapter 1. Introduction	1
1.1 Chapter summary	2
1.2 Overview of angiogenesis	2
1.2.1 Histology of blood vessels	3
1.2.2 Formation of blood vessels	5
1.2.3 Vasculogenesis	6
1.2.4 Angiogenesis	8
1.3 Molecular mechanism of angiogenesis	12
1.3.1 Vascular endothelial growth factor (VEGF)	12
1.3.2 VEGF receptors	13
1.3.3 VEGF/VEGFR2 signaling	14
1.3.4 Basic fibroblast growth factor (bFGF)	15
1.3.5 Platelet derived growth factor (PDGF)	16
1.3.6 Notch signaling	16
1.4 Ocular diseases arising from pathological angiogenesis	17
1.4.1 Anatomy of the human eye	17
1.4.2 Retinopathy of prematurity	18
1.4.3 Diabetic retinopathy	19
1.4.4 Age-related macular degeneration	21

1.4.5 Anti-VEGF biologic drugs	22
1.5 Natural products as inhibitors of ocular angiogenesis	23
1.6 Cremastranone	26
1.7 Summary, hypothesis and specific aims	27
Chapter 2. Synthesis and mechanistic studies of a novel	
homoisoflavanone inhibitor of endothelial cell growth	30
2.1 Chapter summary	31
2.2 Introduction	32
2.3 Materials and methods.....	33
2.3.1 Materials used	33
2.3.2 Cell proliferation assay	34
2.3.3 EdU incorporation assay	34
2.3.4 In vitro angiogenesis assay	35
2.3.5 Caspase-3 expression assay	35
2.3.6 NF- κ B nuclear translocation assay	36
2.3.7 VCAM-1 expression assay	37
2.3.8 qRT-PCR	37
2.3.9 Immunoblot	38
2.3.10 Statistical analysis	39
2.4 Results	39
2.4.1 SH-11052 inhibits proliferation of HRECs	39
2.4.2 SH-11052 inhibits in vitro angiogenesis without inducing	
apoptosis	40

2.4.3 SH-11052 inhibits the TNF- α mediated NF- κ B pathway	43
2.4.4 SH-11052 decreases levels of NF- κ B targets	45
2.4.5 SH-11052 inhibits VEGF-mediated activation of PI3K/Akt signaling	45
2.5 Discussion.....	46
Chapter 3. First synthesis of the anti-angiogenic homoisoflavanone cremastranone	
56	
3.1 Chapter summary	57
3.2 Introduction	57
3.3 Methods	58
3.3.1 Cell proliferation assay	58
3.3.2 EdU incorporation assay	58
3.3.3 In vitro scratch assay	58
3.3.4 In vitro angiogenesis assay	59
3.4 Results	59
3.5 Discussion.....	63
Chapter 4. Synthesis and biological evaluation of novel homoisoflavonoids for retinal neovascularization	
65	
4.1 Chapter summary	66
4.2 Introduction	66
4.3 Methods	69
4.3.1 Chemistry methods	69
4.3.2 Materials	69

4.3.3 Cell proliferation assay	69
4.3.4 EdU incorporation assay	69
4.3.5 Apoptosis assay	69
4.3.6 TUNEL assay	70
4.3.7 In vitro scratch-wound assay	70
4.3.8 In vitro angiogenesis assay	70
4.3.9 Oxygen induced retinopathy mouse model	71
4.3.10 Statistical analysis	72
4.4 Results and Discussion.....	72
4.4.1 Biological evaluation of A-ring modified homoisoflavanones	72
4.4.2 Biological evaluation of B-ring modified homoisoflavanones	73
4.4.3 Biological evaluation of homoisoflavanones coupled with amino acids on the C3' position	78
4.4.4 Validation of a potent cremastranone derivative in vitro	82
4.4.5 In vivo efficacy of a potent cremastranone derivative	89
4.5 Conclusion	91
Chapter 5. Ferrochelatase is a therapeutic target for ocular neovascularization	92
5.1 Chapter summary	93
5.2 Introduction	93
5.3 Methods	94

5.3.1 Materials	94
5.3.2 Preparation of photoaffinity reagents	94
5.3.3 Photoaffinity pulldown experiments	95
5.3.4 Recombinant FECH	97
5.3.5 Immunoblot assay	97
5.3.6 siRNA knock down of FECH in cells	98
5.3.7 Cell proliferation assay	98
5.3.8 Migration assay	98
5.3.9 In vitro Matrigel tube formation assay	99
5.3.10 Animals	99
5.3.11 L-CNV model	99
5.3.12 Immunostaining	100
5.3.13 Choroidal sprouting assay	101
5.3.14 Griseofulvin feeding	102
5.3.15 eNOS assay	102
5.3.16 Hemin pulldown	103
5.3.17 PPIX build-up assay	104
5.3.18 Iron chelation	105
5.3.19 Apoptosis assays	105
5.3.20 qRT-PCR	105
5.3.21 Statistical analyses	106
5.4 Results	106
5.4.1 Ferrochelatase is a target of an antiangiogenic compound	106

5.4.2 Ferrochelatase is required for angiogenesis in vitro	110
5.4.3 Ferrochelatase is upregulated during neovascularization	113
5.4.4 Ferrochelatase is required for neovascularization in vivo	113
5.4.5 Ferrochelatase-targeting therapy treats neovascularization	116
5.4.6 Ferrochelatase depletion decreases the VEGF receptor via eNOS	119
5.5 Discussion.....	125
Chapter 6. Discussion	131
6.1 Overall summary	131
6.2 Ferrochelatase overview	136
6.3 Role of FECH in angiogenesis	141
6.4 FECH inhibition as a therapy	143
6.5 Experimental approach	144
6.6 Potential limitations of the study	151
6.7 Future directions	153
6.7.1 Understanding the role of FECH in angiogenesis	153
6.7.2 FECH functions in endothelial and non-endothelial cells	154
6.7.3 Study of CNV and RNV in FECH mutant mice	155
6.7.4 Therapeutic potential of FECH inhibitors	156
6.8 Conclusion	157
Chapter 7. References	158
Curriculum vitae	

LIST OF TABLES

Table 4.1	Growth inhibitory activity (GI_{50} , μM) of A-ring modified homoisoflavanones	74
Table 4.2	Growth inhibitory activity (GI_{50} , μM) of B-ring modified 3-benzylidene-4-chromanone analogs	75
Table 4.3	Growth inhibitory activity (GI_{50} , μM) of B-ring modified 3-benzyl-4-chromanone analogs	77
Table 4.4	Growth inhibitory activity (GI_{50} , μM) of homoisoflavonoids comprising amino acids on the C3' position of the B-ring	79
Table 6.1	GI_{50} values of cremastranone, SH-11052 and SH-11037 on various cell on lines tested in AlamarBlue proliferation assay	136

LIST OF FIGURES

Figure 1.1	Pictorial representation of vasculogenesis and angiogenesis	7
Figure 1.2	VEGF receptor and its signaling pathways	14
Figure 2.1	Homoisoflavanone SH-11052 inhibits proliferation of endothelial cells	41
Figure 2.2	SH-11052 blocks DNA synthesis in endothelial cells	42
Figure 2.3	SH-11052 inhibits <i>in vitro</i> angiogenesis without causing apoptosis	44
Figure 2.4	SH-11052 inhibits TNF- α mediated NF- κ B signaling	47
Figure 2.5	SH-11052 decreases the expression of NF- κ B target genes	48
Figure 2.6	SH-11052 inhibits VEGF mediated Akt signaling	49
Figure 3.1	The structure of cremastranone (1) and its congeners	60
Figure 3.2	Synthetic cremastranone (1) blocks in vitro angiogenesis of HRECs in a dose-dependent manner	62
Figure 4.1	Homoisoflavonoid analog design	68
Figure 4.2	Compound 14a inhibits angiogenic behavior of HRECs in vitro ...	84
Figure 4.3	Compound 14a (SH-11037) inhibits in vitro proliferation of HRECs as measured by EdU incorporation assay	85
Figure 4.4	Compound 14a (SH-11037) arrests HRECs at G2/M cell cycle stage	86
Figure 4.5	Compound 14a does not induce apoptosis	87
Figure 4.6	Viability of HRECs is not significantly altered by compound 14a .	88
Figure 4.7	Homoisoflavonoid 14a inhibits retinal neovascularization in the	

	OIR mouse model	90
Figure 5.1	Ferrochelatase (FECH) is a target of the antiangiogenic natural product, cremastranone	108
Figure 5.2	Peptide mass fingerprinting analysis of proteins pulled down with a cremastranone affinity reagent	109
Figure 5.3	Role of PDXK in angiogenesis in vitro	109
Figure 5.4	FECH is an essential protein for angiogenesis in vitro	111
Figure 5.5	Validation of cremastranone's inhibition of FECH	112
Figure 5.6	FECH is an essential protein for angiogenesis in vivo	114
Figure 5.7	Effect of FECH-siRNA, NMPP and griseofulvin on HRECs in apoptosis assays	115
Figure 5.8	Chemical inhibition of FECH inhibits angiogenesis in vitro	117
Figure 5.9	FECH knockdown has no significant effects on proliferation of other cell types	118
Figure 5.10	Antifungal drug griseofulvin inhibits ocular neovascularization in vivo	120
Figure 5.11	Oral griseofulvin's systemic effects	121
Figure 5.12	FECH depletion suppresses VEGFR2 via eNOS and HIF-1 α	123
Figure 5.13	Effect of <i>FECH</i> knockdown on mRNA expression in HRECs	124
Figure 5.14	Effect of Griseofulvin on FECH activity.	127
Figure 6.1	Overview of the mechanistic study of cremastranone.....	134
Figure 6.2	The heme biosynthetic pathway in mammals	140

LIST OF ABBREVIATIONS

AMD	Age related macular degeneration
Ang	Angiopoietin
ANOVA	Analysis of variance
bFGF	Basic fibroblast growth factor
DAG	Diacyl glycerol
DAPI	4', 6-diamidino-2-phenylindole
DLL4	Delta like ligand 4
DR	Diabetic retinopathy
Cdc/CDK	Cyclin dependent kinase
EBM	Endothelial basal medium
EC	Endothelial cell
ECM	Extracellular matrix
EdU	5-Ethynyl-2'-deoxyuridine
EGM	Endothelial growth medium
EPC	Endothelial progenitor cells
FBS	Fetal bovine serum
FECH	Ferrochelataase
hEGF	Human epidermal growth factor
HIF-1	Hypoxia inducible factor 1
HUVEC	Human umbilical vein endothelial cells
HPLC	High pressure liquid chromatography
HREC	Human retinal microvascular endothelial cells

IGF	Insulin-like growth factor
IgG	Immunoglobulin G
IL8	Interleukin 8
JNK	Jun N-terminal kinase
MAPK	Mitogen activated protein kinase
LCMS	Liquid chromatography mass spectrometry
NCID	Notch intracellular domain
NF- κ B	Nuclear factor κ B
NP-40	Non-ionic P-40 detergent
NPDR	Non-proliferative diabetic retinopathy
NRP	Neuropilin
PAGE	Polyacrylamide gel electrophoresis
PBS	Phosphate buffered saline
PCs	Pericytes
PDR	Proliferative diabetic retinopathy
PDGF	Platelet derived growth factor
PDXK	Pyridoxal kinase
PI3K	Phosphatidylinositol-3-kinase
PKC	Protein kinase C
PLC	Phospholipase C
PVDF	Polyvinylidene difluoride
PPIX	Protoporphyrin IX
ROP	Retinopathy of prematurity

SDS	Sodium dodecyl sulfate
TGF	Transforming growth factor
TNF- α	Tumor necrosis factor α
TUNEL	Terminal deoxynucleotidyl transferase (TdT) dUTP nick end labeling
VEGF	Vascular endothelial growth factor
VEGFR	Vascular endothelial growth factor receptor
vSMC	Vascular smooth muscle cells
VCAM	Vascular cell adhesion molecule

CHAPTER 1. INTRODUCTION

1.1 CHAPTER SUMMARY

In this introductory chapter an overview of angiogenesis and its molecular mechanism with special emphasis on pathological angiogenesis in the eye is discussed. Formation of new blood vessels in the eye (also called ocular neovascularization) underlies numerous diseases such as retinopathy of prematurity (ROP) in infants, proliferative diabetic retinopathy (PDR) in adults and wet age-related macular degeneration (wet AMD) in elderly people. These ocular diseases arising from pathological angiogenesis and current treatments including the development of new therapies are explained in detail. Further, as a part of discovering novel drugs for treating ocular diseases arising from ocular angiogenesis, natural products with special emphasis on homoisoflavanones are discussed. Towards the end of the chapter an antiangiogenic homoisoflavanoid, cremastranone is emphasized along with the context and rationale for my dissertation work. The overall goal of this study is to improve the knowledge on novel ways to inhibit ocular angiogenesis and thereby pave the way for discovering new and effective therapies for ocular diseases.

1.2 OVERVIEW OF ANGIOGENESIS

Vertebrates have developed an elaborate network of blood vessels to nourish all the organs of the body. This network enables every cell of the body to get enough oxygen and nutrients along with the waste disposal system. In addition cells of the immune system patrol for immune surveillance through this network. As blood vessels nourish every organ of the body, deviation from the normal pattern of vessel growth contributes to numerous diseases. Insufficient

blood vessel formation leads to stroke, myocardial infarction, ulcerative disorders and neurodegeneration. Excessive or abnormal blood vessel formation is associated with cancer, inflammatory disorders, pulmonary hypertension and blinding eye diseases such as retinopathy of prematurity (ROP), diabetic retinopathy (DR) and wet-age related macular degeneration (Alitalo and Carmeliet, 2002; Carmeliet, 2003; Carmeliet and Jain, 2011). These ocular diseases will be discussed further, below. Before getting into the details of the molecular events of blood vessel formation it is imperative to understand the cellular composition and organization of blood vessels.

1.2.1 Histology of blood vessels

Blood vessels are composed of endothelial cells, perivascular cells and extracellular matrix (including collagen and elastin) organized into three layers – Tunica intima, Tunica media and Tunica adventitia.

1.2.1A. Tunica intima (tunica intern): It is the thinnest layer facing the lumen of the blood vessel. It is composed of a single layer of endothelial cells and is separated from tunica media by a dense elastic lamina (also called basal lamina).

1.2.1B. Tunica media: It is the thickest layer and provides structural support, vasoreactivity and elasticity to blood vessels. It is composed of perivascular cells, elastic fibers and connective tissue. Perivascular cells, general term used for cells enveloping the blood vessels, are contractile cells and referred to as vascular smooth muscle cells (vSMCs), pericytes (PCs) or mural

cells based on the type of blood vessels – in large blood vessels such as arteries, veins and arterioles they are called vascular smooth-muscle cells and in small blood vessels such as capillaries and venules they are termed as pericytes (Hughes and Chan-Ling, 2004). Thickness of tunica media depends on size of the blood vessels. While small blood vessels contain scarcely distributed pericytes, large blood vessels contain multiple layers of vascular smooth-muscle cells, elastic and collagen fibers. Perivascular cells maintain communications with endothelial cells through both physical contact and paracrine signaling. They play crucial roles in regulating the flow of blood by contracting and relaxing the blood vessels. Perivascular cells are also required for maturation of vasculature and loss of these cells results in regression of blood vessels as observed in ocular complications such as macular edema and diabetic retinopathy (Carmeliet, 2000).

1.2.1C. Tunica adventitia (Tunica externa): It is mainly made up of connective tissue, nutrient vessels (called vasa vasorum), autonomous nerves (nervi vasorum) fibroblasts and macrophages.

While all the above three layers are present in larger blood vessels, tunica media and tunica adventitia are absent in capillaries. Capillaries are made up of a single layer of endothelial cells surrounded by basal lamina, in which are embedded pericytes.

1.2.2 Formation of blood vessels

Cells required for the formation of blood vessels originate from the mesodermal layer of the embryo. During embryonic development, new blood vessels are formed by the differentiation of endothelial precursor cells (called 'angioblasts') into endothelial cells. These differentiated endothelial cells then assemble into a primitive vascular labyrinth. This process is called vasculogenesis (Swift and Weinstein, 2009). Further formation of new blood vessels from vascular labyrinth occurs through a process called 'angiogenesis'.

Angiogenesis is a process of formation of *new blood vessels* from *preexisting* ones (Carmeliet and Jain, 2011). Angiogenesis during embryonic development creates a network that remodels into arteries and veins. Later pericytes and vSMCs are recruited to nascent blood vessels to provide stability and to regulate perfusion. In adults, blood vessels are quiescent and rarely form new branches. However, endothelial cells (ECs) retain high plasticity to sense and respond to angiogenic signals to form new vessels (Potente et al., 2011).

Earlier it was believed that vasculogenesis occurs only during embryonic development, however later reports indicate occurrence of vasculogenesis in adults by endothelial progenitor cells (EPCs) circulating in the blood (Asahara et al., 1997; Grant et al., 2002; Shi et al., 1998). However, angiogenesis remains the major pathway of new blood vessel formation in adults. As the major goal of this study is based on angiogenic process, in the following sections

vasculogenesis is briefly described whereas the cellular and molecular events of angiogenesis are described in detail.

1.2.3. Vasculogenesis

ECs and hematopoietic cells have common progenitor cells called 'hemangioblasts'. During embryonic development, in the yolk sac, hemangioblasts aggregate. The inner cells develop into hematopoietic precursor cells and the outer population into angioblasts (Figure 1.1). Angioblasts proliferate and migrate extensively before de novo differentiation into endothelial cells and formation of vascular labyrinth (Potente et al., 2011). The differentiation of angioblasts into ECs is influenced by basic fibroblast growth factor (bFGF), vascular endothelial growth factor (VEGF), and VEGF receptor 2 (VEGFR2) (Carmeliet et al., 1996; Ferrara, 1999; Ferrara et al., 1996; Shalaby et al., 1997). This vascular labyrinth then undergoes stabilization and maturation by the recruitment and enwrapping of pericytes around the vessels. Pericytes are derived from mesenchymal stem cells or neural crest cells and the recruitment takes place through chemotaxis process wherein ECs secrete platelet derived growth factor –B (PDGF-B) and pericytes expressing PDGF-B receptors are attracted to the vessel formation site (Bergers and Song, 2005; Hellstrom et al., 1999). The vascular labyrinth then remodels into an organized network of arteries, capillaries and veins. Notch signaling plays a key role in deciding the fate of ECs to become arteries or veins. Notch pathway components are highly expressed in arteries whereas venous ECs express low levels of Notch components (Gridley, 2010; Potente et al., 2011; Swift and Weinstein, 2009).

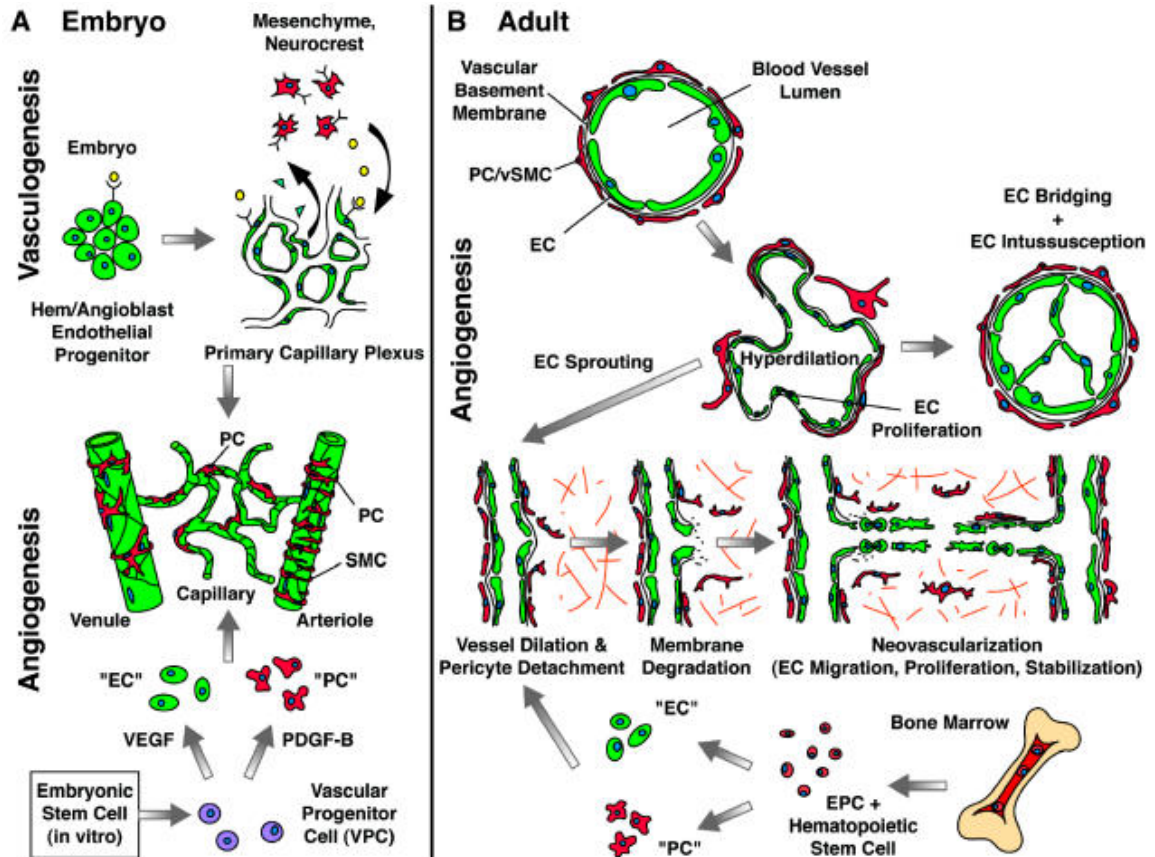


Figure 1.1. Pictorial representation of vasculogenesis and angiogenesis. Reproduced with permission from Oxford University Press (Bergers and Song, 2005).

1.2.4. Angiogenesis

Angiogenesis is a tightly controlled process guided by a set of pro-angiogenic and antiangiogenic molecules. Angiogenesis occurs during growth, wound repair and reproduction (ovulation, follicular development, implantation and placentation during pregnancy) (Tahergorabi and Khazaei, 2012).

Although angiogenesis can occur through intussusception (splitting of pre-existing vessels), under physiological conditions angiogenesis occurs through a process called sprouting. The key molecular events during sprouting were identified using mouse retina wherein the development of vasculature occurs postnatally (Walti et al., 2013). Sprouting angiogenesis takes place in the following steps:

- Vasodilation and increased vascular permeability
- Tip and stalk cell selection
- Endothelial cell proliferation and migration
- Vessel branch fusion
- Vessel maturation, stabilization and quiescence

1.2.4A. Vasodilation and increased vascular permeability: The sprouting process begins with vasodilation, a process involving nitric oxide. VEGF increases vascular permeability in order to allow extravasation of plasma proteins that lay down a scaffold for migrating ECs.

In order for ECs to emigrate from their resident site, they need to loosen cell-cell contacts between them and with pericytes. In other words, mature vessels need to be destabilized. This occurs by the detachment of pericytes from blood vessels promoted by angiopoietin 2 (Ang2), an inhibitor of Tie2 signaling, released from ECs (Walti et al., 2013). This is followed by degradation of basement membrane by matrix metalloproteinases (MMPs) such as MMP1 secreted by ECs. These MMPs also liberate proangiogenic growth factors that are sequestered in the matrix. During this process antiangiogenic molecules such as plasminogen activator inhibitor are also released to prevent abnormal sprouting and to coordinate branching of vessels (Potente et al., 2011; Walti et al., 2013).

1.2.4B. Tip and stalk cell selection: Attracted by proangiogenic signals, ECs become motile, invasive and protrude filopodia. These ECs are called 'Tip cells'. These tip cells spearhead new sprouts and probe the surrounding environment for guidance cues. Tip cells then play a master role in formation of the vessel. Tip cells dissociate from the capillary and move towards the proangiogenic signal gradient. Then, the surrounding endothelial cells, called "stalk cells", proliferate and migrate along with tip cells. The specification of ECs into tip and stalk cells is controlled by the Notch pathway. Stalk cells exhibit

higher Notch activity as compared to tip cells. Blockade of Notch signaling is observed in tip cells that express higher levels of DLL4 ligand (Carmeliet, 2000; Potente et al., 2011; Welte et al., 2013).

VEGF/VEGFR2 enhances DLL4 expression in tip cells. DLL4-mediated activation of Notch in neighboring ECs inhibits tip cell behavior in these cells by downregulating VEGFR2, VEGFR3 and neuropilin 1 (NRP1), a co-receptor of VEGFR2. Following exposure to VEGF, all ECs upregulate DLL4. However, ECs that express DLL4 more quickly or at higher levels have a competitive advantage to become tip cells as they activate Notch signaling in neighboring cells more effectively. Hence ECs at the angiogenic front dynamically compete for the tip position through DLL4/Notch signaling (Potente et al., 2011; Welte et al., 2013).

1.2.4C. Endothelial cell proliferation and migration: Compared to tip cells, stalk cells have fewer filopodia and they are more proliferative. Stalk cells have the ability to form tubes and branches. VEGF/VEGFR2 signaling is the key driver for proliferation and migration of ECs. Along with VEGF, other growth factors such as Insulin-like growth factor (IGF-1), placental growth factor (PLGF), bFGF, PDGF, TGF- β 1, TNF- α and $\alpha_v\beta_3$ integrin also promote proliferation and migration of ECs (Carmeliet, 2000; Potente et al., 2011).

1.2.4D. Vessel branch fusion: When two tip cells from opposite branches of capillaries meet then they fuse to become tubes. Once the contact between tip cells is established, VE-cadherin-containing junctions are formed between ECs to consolidate the connection.

1.2.4E. Vessel maturation, stabilization and quiescence: Maturation of newly formed blood vessel takes place wherein proliferation and migration of endothelial cells are halted, pericytes and vascular smooth muscle cells are recruited and basement membrane for blood vessels is laid out. Recruitment of pericytes to newly formed vessels is controlled by PDGF/PDGF-B signaling. ECs secrete PDGF-B and pericytes, which express receptors for PDGF-B, are attracted to the site of the newly formed blood vessel (Carmeliet and Jain, 2011; Taherghorabi and Khazaei, 2012; Welte et al., 2013). In turn, pericytes produce Ang1, which activates Tie2 signaling in ECs to promote pericyte adhesion to ECs and tightening of endothelial junctions. Once the vessel is matured the blood flows through newly formed vessels. This exposure to oxygenated blood suppresses hypoxia-inducible factors (HIFs) in ECs and proliferative activity is decreased. As endothelial proliferation decreases during maturation, ECs adopt survival properties to maintain integrity of the vessel lining. Autocrine and paracrine survival signals from endothelial and support cells protect the vessel from environmental stresses. VEGF is the main survival factor for ECs through the activation of the PI3K/AKT pathway (Potente et al., 2011; Welte et al., 2013).

Until now, I have briefly discussed key cellular events of angiogenesis with mention of key signaling pathways in each of the step. In the following section, key molecular players of angiogenesis are discussed.

1.3. MOLECULAR MECHANISM OF ANGIOGENESIS

The main trigger for initiation of angiogenesis is hypoxia (Das and McGuire, 2003). Under low oxygen concentration, hypoxia Inducible factor-1 (HIF-1) is stabilized in endothelial cells (ECs). This stabilized transcription factor HIF-1 then upregulates expression of many proangiogenic molecules including vascular endothelial growth factor (VEGF), angiopoietin-2 (ang-2) and fibroblast growth factor (FGF) (Das and McGuire, 2003). Apart from this Notch, Tie2 and PDGF signaling play important roles in angiogenesis (Papetti and Herman, 2002). In the following sections each of these are described.

1.3.1 Vascular Endothelial Growth Factor (VEGF)

Among all the proangiogenic molecules, VEGF is the most potent one (Penn et al., 2008). VEGF is essential for angiogenesis and a lack of a single allele arrests angiogenesis and leads to embryonic lethality (Ferrara et al., 1996). VEGF is a dimeric glycoprotein of approximately 40 kDa size. In mammals, the VEGF family consists of seven members: VEGF-A (typically referred as VEGF), VEGF-B, VEGF-C, VEGF-D, VEGF-E, VEGF-F and placental growth factor (PlGF). Among these members, VEGF-A is the potent inducer of angiogenesis. The *VEGFA* transcript undergoes alternate splicing to produce several variants with different functions. These variants are VEGF₁₂₁, VEGF₁₄₅, VEGF₁₆₅,

VEGF₁₈₉ and VEGF₂₀₆. These variants differ in their ability to bind heparin. VEGF₁₈₉ and VEGF₂₀₆ have high heparin binding capacity and are hence sequestered in ECM while VEGF₁₂₁ lacks heparin binding ability and hence are highly soluble. VEGF₁₆₅ and VEGF₁₄₅ have less affinity for heparin but are associated with ECM. Among all the VEGF variants VEGF₁₆₅ is the predominant one (Penn et al., 2008).

The expression of VEGF is mainly induced by hypoxia (Carmeliet et al., 1998; Penn et al., 2008). HIF-1 is the key transcriptional factor, which under hypoxic conditions binds to the hypoxia responsive element (HRE) of the VEGF promoter and upregulates the production of VEGF mRNA. Apart from this, under hypoxia stability of VEGF mRNA is also increased 2-3 fold due to binding of HuR, a 36-kDa RNA-binding protein, to the 3' UTR of VEGF mRNA, protecting it from degradation from endonucleases (Brennan and Steitz, 2001).

1.3.2. VEGF receptors

VEGF receptors are tyrosine kinase family receptors in the membrane with seven immunoglobulin-like folds on the extracellular side of the protein, a single transmembrane region and a tyrosine kinase domain at the intracellular region of the protein. VEGF receptors contain three members; VEGFR-1/Flt-1, VEGFR-2/KDR/Flk-1 and VEGFR-3/Flt-4. VEGFR-1 and -2 are mainly involved in angiogenesis whereas VEGFR-3 is involved in lymphangiogenesis (Yancopoulos et al., 2000). VEGF₁₆₅ induces its angiogenic potential through binding to VEGFR-2 (Penn et al., 2008). Once activated, VEGFR-2 recruits a host of

different signaling proteins involved in proliferation, migration and survival of endothelial cells as depicted in Figure 1.2. Hypoxia does not directly upregulate VEGFR-2 expression. However VEGF, which is induced by hypoxia, potentiates the expression of VEGFR-2.

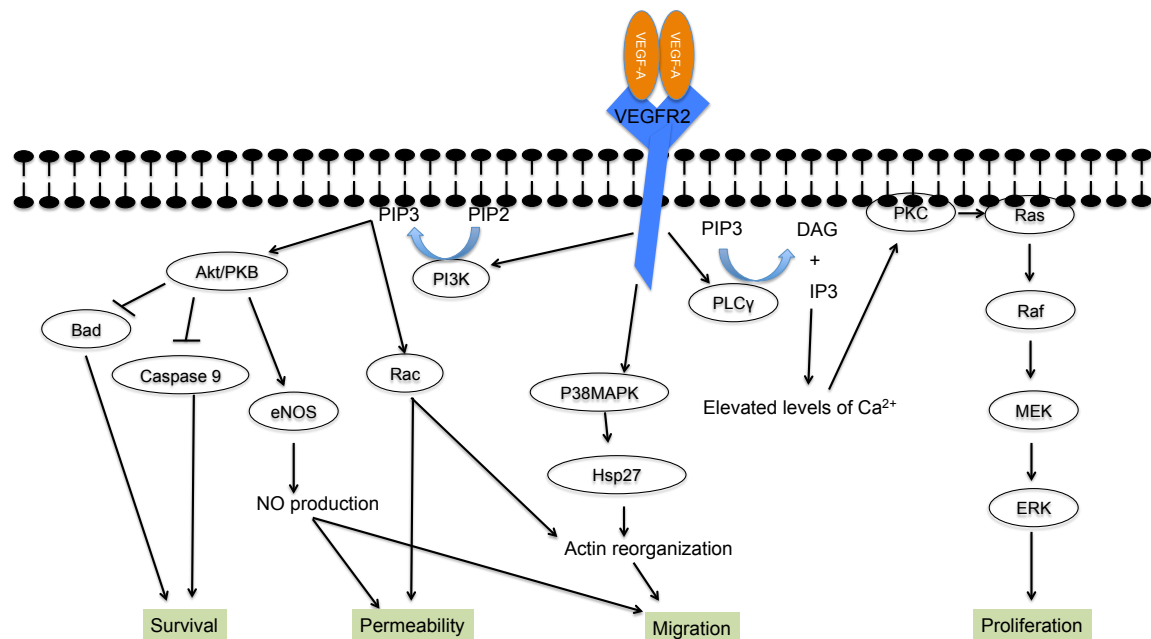


Figure 1.2. VEGF receptor and its signaling pathways.

1.3.3. VEGF/VEGFR-2 signaling

Once secreted, VEGF binds to VEGFR-2 leading to dimerization of VEGFR-2. The dimerized VEGFR-2 trans phosphorylate each other on the intracellular domain. To this phosphorylated VEGFR-2, a SH2 domain containing Phospholipase C- γ (PLC- γ) binds at Tyr1175 region and mediates a mitogen-activated protein kinase (MAPK) cascade, leading to proliferation of endothelial cells. PLC- γ activates protein kinase C (PKC) via production of diacylglycerol (DAG) and increased concentration of intracellular calcium. In addition to this

phosphorylated VEGFR-2, PI3K protein binds and activates AKT as well as p38MAPK pathway to promote both survival and migration of ECs respectively (Figure1.2) (Penn et al., 2008).

1.3.4. Basic fibroblast growth factor (bFGF)

FGFs are 18-25 kDa polypeptides and ubiquitously expressed. bFGF plays an important role in angiogenesis in vitro. bFGF strongly promotes proliferation, migration and tube formation ability of ECs in vitro. bFGF binds to heparin with high affinity and hence is sequestered in ECM. FGFs have been implicated in retinal neovascularization (Das and McGuire, 2003). However the role of bFGF in vivo seems to be redundant as mice lacking bFGF show normal vasculature (Tobe et al., 1998). Thus there is contradictory findings regarding the role of bFGF in ocular neovascularization wherein one school of researchers believe bFGF induces angiogenesis (Hanneken et al., 1991; Kimura et al., 1999; Sivalingam et al., 1990) while the other group believe bFGF plays little role in angiogenesis in vivo (Ozaki et al., 1998; Tobe et al., 1998).

1.3.5. Platelet derived growth factor (PDGF)

In order to avoid the regression of newly formed blood vessels, pericytes need to be recruited. This recruitment of pericytes to neovascularized areas is promoted by PDGF-B secreted by ECs. Loss of pericytes is a hallmark of diabetic retinopathy and a strong correlation between reduced pericyte density and low PDGF levels has been demonstrated in mice (Bergers and Song, 2005; Carmeliet, 2000).

1.3.6. Notch signaling

During the initiation of angiogenesis some ECs are destined to become “tip cells”. Selection of tip cells takes place through Notch signaling (Welti et al., 2013). ECs after activation by VEGF, compete for tip position by increasing the expression of the Notch ligand Delta-like 4 (DLL4), which binds to Notch receptors on adjacent ECs (stalk cells). Activated Notch receptors undergo protein cleavage and release Notch intracellular domain (NICD), which acts as a transcriptional regulator decreasing the expression of VEGFR2 and NRP-1 (neuropilin-1, coreceptor of VEGFR-2) while increasing the expression of VEGFR-1, which traps VEGF. Thus Notch signaling distinguishes ECs as tip cells and stalk cells. However, it is VEGF signaling that promotes proliferation, migration and tube formation abilities of ECs. Once the tip cells from opposing sides of the capillary fuse and form a nascent blood vessel, maturation and stabilization of the blood vessel takes place through recruitment of pericytes (Potente et al., 2011; Welti et al., 2013).

Mural pericytes reduce EC proliferation, migration and vessel leakage. TGF- β 1 promotes differentiation of precursor cells to pericytes and ECs secreting PDGF-B attract pericytes expressing PDGFR- β . Once the hypoxic tissue is perfused, ECs go into quiescence. Ang-1 signaling in ECs inhibits the permeability of new blood vessels by inducing DLL4 expression and NICD signaling. Basement membrane is laid around quiescent ECs to promote vessel stabilization.

Apart from the above described signaling pathways there are many new signaling pathways being linked to angiogenesis but their role in ocular angiogenesis is not clearly understood. In the following section, some of the ocular diseases arising from uncontrolled angiogenesis are discussed.

1.4. OCULAR DISEASES ARISING FROM PATHOLOGICAL ANGIOGENESIS

Pathological angiogenesis in the eye leads to several ocular diseases, including three prevalent ones: ROP, PDR and wet AMD. These three diseases together are a leading cause of vision loss in the world (Penn et al., 2008). Pathological angiogenesis links these ocular diseases. In order to understand the pathologies of these diseases, anatomy and histology of the human eye is briefly discussed below.

1.4.1 Anatomy of the human eye

The human eye is a fluid-filled sphere enclosed by three layers of tissues

- Outer layer – this is composed of tough white fibrous tissue called ‘sclera’. However, at the front of the eye this layer is transparent and the region is called ‘cornea’. The cornea permits the light rays into the eye.
- Middle layer – this layer includes three distinct but continuous structures: The iris, the ciliary body and the choroid. The iris is the colored portion of the eye and controls the amount of light to be

entered into the eye. The choroid is composed of a rich capillary bed that serves as the main source of blood supply for the photoreceptors of the retina.

- Inner layer – this layer, the retina, includes photoreceptors that are sensitive to light and neurons/glia that are capable of transmitting the visual signals to brain.

1.4.2 Retinopathy of prematurity

ROP arises from perturbation in the normal vascular development of retina (Sapieha et al., 2010). Retina is one of the last organs to be vascularized in the human fetus. ROP occurs in two distinct phases: the first phase is associated with inhibition of normal retinal vasculature due to exposure of the premature baby to hyperoxia environment (oxygen therapy). In this phase VEGF levels are decreased. The second phase is associated with rapid growth of abnormal leaky blood vessels into the vitreous, followed by vitreous hemorrhage and retinal detachment. This phase occurs due to transfer of the premature baby from hyperoxia to normoxia. This causes a relative hypoxic environment in the eye leading to triggering of upregulation of VEGF (Penn et al., 2008). The two distinct phases of this disease makes the treatment more complicated, as angiogenesis needs to be promoted in the first phase and inhibited in the second phase.

In the United States, 70% of the infants with very low birth weight develop ROP after exposure to postnatal hyperoxia. Around 1,300 infants per year in the United States develop complete vision loss due to this disease, and 500 more

are severely impaired (Faia and Trese, 2011). Overall, between 6% and 18% of childhood blindness is attributable to ROP (Gilbert et al., 1997). Moreover, as more and more children survive premature birth in middle-income countries due to improvements in neonatal intensive care, ROP is becoming more prevalent worldwide. The traditional therapies for ROP are laser photocoagulation, cryotherapy and surgical interventions. However the main drawbacks of these therapies are that they are all invasive therapies with partial loss of peripheral vision.

1.4.3 Diabetic retinopathy (DR)

Similar to ROP, in adults due to diabetic complications (because of high blood glucose levels) there is initially regression of retinal vasculature followed by abnormal growth of blood vessels in the retina. DR is the most common complication in diabetes and clinical symptoms of DR are seen in 75% of diabetic patients, with 10% of them eventually developing visual impairment (Penn et al., 2008). DR is currently the leading cause of blindness among working age adults and accounts for 8% of the legal blindness in the United States (Penn et al., 2008). Clinical progression of DR includes adhesion of leukocytes to the vessel wall (leukostasis), aggregation of platelets, altered blood flow, degeneration of pericytes and thickening of basement membranes. Blockage of retinal capillaries then causes localized hypoxia triggering increased production of angiogenic factors, mainly VEGF. Despite increased production of VEGF, a potent survival factor for ECs, microvascular retinal ECs degenerate, leading to capillary closure and formation of acellular non-perfused capillaries. With the disease progression,

vascular leakage increases and blood and fluid accumulate in the retinal tissue forming exudative deposits, a condition called non-proliferative diabetic retinopathy (NPDR).

In some patients NPDR progresses to proliferative diabetic retinopathy (PDR). PDR is characterized by new blood vessel formation on the surface of the retina, analogous to that seen in the second phase of ROP. These new blood vessels are fragile and may break, leaking blood into the vitreous thus clouding the vitreous and compromising vision. In advanced PDR fibrovascular scar tissue grows from the retinal surface into the vitreous cavity. If left untreated, this can cause retinal detachment and hence blindness (Penn et al., 2008). The specific reasons for disease progression and retinal injury in diabetic patients are not yet clear. But there is strong support for the concept that elevation of blood and tissue glucose levels stimulates production of proangiogenic factors, mainly VEGF, and upregulates VEGFR2 (Gilbert et al., 1998; Miller et al., 1997). High glucose, oxidative stress, hypoxia and inflammatory reactions occur in diabetes and all of these conditions are shown to promote the expression of VEGF. Hence blocking the action of VEGF might prevent PDR. The current treatment methods for PDR are laser therapy and administration of anti-VEGF biologics. While laser therapy is effective in many patients, the loss of retinal tissue during the process can lead to decreased peripheral vision, impair night vision and change color perception (Penn et al., 2008). Administration of anti-VEGF biologic drugs blocks the progression of PDR. The available anti-VEGF drugs for treatment are Avastin (bevacizumab), Lucentis (ranibizumab) and Eylea (aflibercept). Lucentis and

Eylea are approved by FDA for treatment of PDR while Avastin is approved for treating cancer but is commonly used in clinics to treat PDR.

1.4.4 Age-related Macular degeneration

Unlike ROP and PDR, which are caused by retinal neovascularization, AMD is associated with choroidal neovascularization. Age-related macular degeneration is one of the leading causes of vision loss worldwide (Resnikoff et al., 2004). AMD develops late in life and both genetic and environmental factors play key roles in pathogenesis. AMD can be categorized into dry and wet AMD forms. Dry AMD is a chronic disease caused by slow photoreceptor degeneration and nearly 90 % of AMD patients belong to this category. There is no treatment for these patients. However NIH clinical studies (age-related eye disease studies –AREDS) indicated that a combination of vitamins C, E, beta-carotene, zinc and copper can reduce the risk of progression by 25 %. Wet AMD affects approximately 2 million people in the United States and is estimated to engender a productivity burden of nearly \$5.4 billion (Fine et al., 2000). Although less common than dry AMD, wet AMD is responsible for causing approximately 90 % of the legal blindness associated with this disease (Fine et al., 2000). Wet AMD is characterized by pathogenic neovascularization of the choroid, projecting through Bruch's membrane and into the adjacent retinal pigment epithelium. Rupture of these new blood vessels causes hemorrhage, rapid photoreceptor degeneration and eventual fibrotic scarring, with rapid vision loss (Ehrlich et al., 2009). Established treatment modalities for wet AMD include photodynamic therapy, laser surgery and administration of anti-VEGF biologics. The most

common therapy for wet AMD patients is anti-VEGF drugs and photodynamic therapy is less commonly used, in conjunction with anti-VEGF therapy.

1.4.5 Anti-VEGF biologic drugs

Anti-VEGF biologic drugs work by interfering in VEGF binding to VEGF receptors and thereby blocking VEGF-VEGFR2 signaling. Currently there are three anti-VEGF drugs licensed for use in eye diseases – pegaptanib (brand name – Macugen), aflibercept (brand name – Eylea), ranibizumab (brand name – Lucentis) and one that is not licensed but used off-label – bevacizumab (brand name – Avastin). Pegaptanib, an aptamer, is a selective inhibitor of VEGF₁₆₅ and was the first anti-VEGF agent approved for eye diseases in 2004 (Gragoudas et al., 2004). This was followed in 2006 by ranibizumab, a monoclonal antibody (Rosenfeld et al., 2006) and in 2011 by aflibercept, a fusion protein containing VEGF-binding regions of VEGF receptors 1 & 2 fused to Fc portion of human IgG1 immunoglobulin (Heier et al., 2012). Off-label use of bevacizumab is robust since 2005 and it maintains the predominant market share due to similar efficacy to ranibizumab with a distinct pricing advantage (Avery et al., 2006).

However these medications face an unfavorable cost to benefit ratio (Hodge et al., 2010; Mitchell et al., 2011) and have the potential for significant acute systemic side effects such as non-ocular hemorrhage and myocardial infarction (Folk and Stone, 2010b). There is also a significant population that is refractory to these drugs; up to 45% in one series of AMD patients (Lux et al.,

2007). Hence targeting not only VEGF signaling but multiple proangiogenic signals is required to improve the efficacy of treatment for diseases arising from pathological angiogenesis. Thus, there is a critical unmet medical need to develop novel therapies to either replace or supplement the present therapies to increase the efficiency of treatment of these diseases. At present there is no small molecule drug to treat these ocular diseases on the market, although many investigational small molecule inhibitors of angiogenesis (such as TG10080, PTK787, PAN90806 and squalamine) are in various stages of clinical trials (Englander and Kaiser, 2013). Towards this end, our long-term goal is to identify and develop novel small molecules that not only inhibit angiogenesis in the eye but also might be delivered topically rather than by injection which is the main delivery route for all of the biologics (Folk and Stone, 2010).

1.5 NATURAL PRODUCTS AS INHIBITORS OF OCULAR ANGIOGENESIS

The medicinal use of natural products obtained from plants and animals dates back thousands of years (Ji et al., 2009). Different human civilizations across the world used these natural products as treatment for a majority of the diseases, wherein extracts of plants were either taken orally or applied topically. However only during the 19th century a systematic study of extracting active ingredients from these natural extracts were carried out, mainly because of advancements in analytical and structural chemistry. The discovery of the antibiotic penicillin revolutionized the medicinal chemistry field to identify active chemical compounds from natural products. As the technology for identifying and determining the structure of compounds became available there was an

explosion of drug discovery research based on natural products (Ji et al., 2009; Newman et al., 2003). In the 20th century more than 50 % of the approved drugs are either natural products or their derivatives such as antibiotics, immunosuppressants and anticancer drugs, which have revolutionized human medical history and improved the quality of life (Li and Vederas, 2009). The discovery and development of antibiotics not only saved millions of lives but also set the platform for big pharmaceutical companies to explore the field to develop drugs based on natural products for other diseases. One of the main reasons to investigate natural products is that over millions of years nature has perfected the interaction between natural product and its interacting partner (drug target). So understanding these interactions further gives us an avenue for exploring novel chemicals through rational design of drugs in target based drug discovery programs (Schmidt et al., 2007). As natural products offer specificity as well as chemical diversity they serve as lead molecules in drug discovery.

Despite these advantages, there was a decline in natural products-based drug discovery programs as there were technological revolutions in molecular biology, synthetic and computational chemistry, which made it easier to rationally design new synthetic drugs based on drug target structure. However in the past few years there is renewed interest in the use of natural products as a basis of drug development. This is partly because several natural products have undergone clinical evaluation and shown promising results especially in cancer, immunological and inflammatory diseases (Mishra and Tiwari, 2011). Interest in natural products will continue as advances in bioprospecting, separation and

structure determination technologies ensure natural products with more chemical diversity and hence novel chemical templates to synthesize new chemicals with intellectual patent (IP) properties. Natural sources may also provide lead molecules with favorable absorption, distribution, metabolism, excretion and toxicity (ADMET) characteristics (Corson and Crews, 2007; Koehn and Carter, 2005).

Several natural products have been tested for their antiangiogenic properties in context with cancer. However very few have been tested for their efficacy in ocular diseases (Sagar et al., 2006a, b). These tested natural products are chemically diverse and have promising effects.

Of these molecules polyphenols are of interest as they are abundant in nature and are constituents in many medicinal plants. They are recognized for their antioxidant properties and hence tested in animal models of diseases associated with oxidative stress such as cancer, inflammatory diseases and cardiovascular diseases (Manach et al., 2004). Polyphenols is a general term used to describe aromatic compounds containing several hydroxyl groups. Based on number of phenolic groups and arrangement of aromatic rings they are classified as phenolic acids, flavonoids, stilbenoids and lignans. Of particular interest are flavonoids as these have been studied for their beneficial role in ocular diseases (Majumdar and Srirangam, 2010; Manach et al., 2004). Flavonoids are further classified based on substitution on the heterocycle ring, position and length of the linker connecting cycle moieties. One of the flavonoids of interest to us is a homoisoflavanone, and is described in the following section.

1.6. CREMASTRANONE

The extract from the bulb of a plant *Cremastra appendiculata* is used in East Asia to treat several cancers and skin lesions. A South Korean research group isolated an active compound from this extract and gave it the generic name “homoisoflavanone” (Shim et al., 2004) (Figure 2.1). This compound, 5,7-dihydroxy-3(3-hydroxy-4-methoxybenzyl)-6-methoxychroman-4-one, is a member of a small group of known homoisoflavanones; we named it cremastranone. Shim et al. identified cremastranone as the component of *C. appendiculata* bulbs responsible for a blockade of the proliferation of human umbilical vein endothelial cells (HUVECs) (Shim et al., 2004). This potent compound also inhibits vascular tube formation and migration induced by basic fibroblast growth factor (bFGF) in tissue culture, without marked cytotoxicity (Kim et al., 2007; Shim et al., 2004). Further it was shown that the compound inhibits angiogenesis in vivo. Cremastranone showed efficacy in the laser photocoagulation murine model of choroidal neovascularization: here, cremastranone inhibited choroidal neovascularization (Kim et al., 2008). This model is widely used for testing the efficacy of drugs used for wet AMD. Cremastranone was also efficacious in an oxygen-induced retinopathy mouse model, a widely used model to understand the ROP disease, suggesting it inhibits retinal neovascularization (Kim et al., 2007). Reassuringly, injection of 10 μ M cremastranone into the vitreous of normal adult mice showed no cytotoxic or inflammatory effects on the retina, nor did it induce apoptosis of retinal cells (Kim et al., 2008).

1.7. SUMMARY, HYPOTHESIS AND SPECIFIC AIMS

In summary, blood vessels are formed through both vasculogenesis and angiogenesis during embryonic growth and in adults angiogenesis is the major route for new blood vessel formation. Although angiogenesis does not take place under normal physiological conditions except during wound repair and reproduction, under certain disease conditions such as ROP, PDR and wet AMD abnormal blood vessel formation occurs. To treat these diseases various antiangiogenic therapies have been employed and the most dominant drugs in the market are anti-VEGF biologic drugs. Although a few small molecule inhibitors of angiogenesis are being tested in both preclinical and clinical settings, the progress is limited. Hence there is a need to discover new drugs with less toxicity, high potency and specificity. Cremastranone is a candidate molecule with antiangiogenic effects in vitro and in vivo.

Given these impressive findings, our long term goal is to develop an understanding of how cremastranone acts as an antiangiogenic agent relevant to treating ocular diseases arising from pathological angiogenesis. In order to understand the molecular mechanism of cremastranone, I hypothesized that cremastranone binds to and modulates the activity of cellular proteins required for ocular angiogenesis. To address this hypothesis I designed three specific aims:

Specific Aim 1: To synthesize and biologically characterize cremastranone, its analogues and affinity reagents. This step is important to

understand if synthetic cremastranone has similar biological properties to its natural counterpart and helps in synthesizing enough quantities for use in mechanistic studies. Also this step is required for synthesizing affinity reagents for use in photo-affinity based pull down assay (Chapters 2, 3, and 4).

Specific Aim 2: To identify and validate cremastranone interacting proteins. This step helps in identifying the proteins with which cremastranone interacts and also testing if it is through these proteins that cremastranone exerts its antiangiogenic activity (Chapter 5).

Specific Aim 3: To understand the role of cremastranone binding proteins in ocular angiogenesis. This step helps us in knowing if the cremastranone binding protein(s) are required for ocular angiogenesis in vivo and also the molecular mechanisms through which the target protein(s) are involved in angiogenesis (Chapter 5).

This study proceeded as follows: our South Korean synthetic chemist collaborators synthesized cremastranone and an isomer of it. After assessing the biological functions of these compounds (Chapters 2 and 3) to be very similar to that of homoisoflavanones extracted from natural source, we set out to elucidate the structure-activity relationship studies of cremastranone to understand how to improve the potency of this compound and where to add chemical linker groups to synthesize a photoaffinity reagent. During this process I came across a potent homoisoflavanoid, which is very specific against retinal microvascular endothelial cells and inhibited retinal neovascularization in vivo (Chapter 4). Using the

photoaffinity chemical reagent synthesized, I was able to identify that cremastranone binds and modulates the activity of ferrochelatase, a heme synthesizing enzyme (Chapter 5). The functional roles of ferrochelatase and heme biosynthesis in reference to angiogenesis are further discussed in Chapters 5 and 6.

CHAPTER 2. SYNTHESIS AND MECHANISTIC STUDIES OF A NOVEL HOMOISOFLAVANONE INHIBITOR OF ENDOTHELIAL CELL GROWTH

[This chapter forms portion of previously published following research paper and reproduced here with permission from *PLoS ONE*:

Halesha Basavarajappa, Bit Lee, Xiang Fei, Daesung Lim, Breedge Callaghan, Julie A Mund, Jamie Case, Gangaraju Rajashekar, Seung-Yong Seo*, Timothy W Corson*. 2013. Synthesis and mechanistic studies of a novel homoisoflavanone inhibitor of endothelial cell growth. *PLoS One* 9(4): e95694.

*Equal contributors.]

2.1 CHAPTER SUMMARY

The main objective of this chapter is to demonstrate that a synthetic analogue of cremastranone shows biological activities which are similar to the natural product cremastranone. In this study, we present the synthesis of a novel homoisoflavanone isomer of cremastranone. Our compound, SH-11052, has antiproliferative activity against human umbilical vein endothelial cells, and also against more ocular disease-relevant human retinal microvascular endothelial cells (HRECs). Tube formation and cell cycle progression of HRECs were inhibited by SH-11052, but the compound did not induce apoptosis at effective concentrations. SH-11052 also decreased TNF- α induced p38 MAPK phosphorylation in these cells. Intriguingly, SH-11052 blocked TNF- α induced I κ B- α degradation, and therefore decreased NF- κ B nuclear translocation. It decreased the expression of NF- κ B target genes and the pro-angiogenic or pro-inflammatory markers VCAM-1, *CCL2*, *IL8*, and *PTGS2*. In addition SH-11052 inhibited VEGF induced activation of Akt but not VEGF receptor autophosphorylation. Based on these results we propose that SH-11052 inhibits inflammation induced angiogenesis by blocking both TNF- α and VEGF mediated pathways, two major pathways involved in pathological angiogenesis. Synthesis of this novel homoisoflavanone opens the door to structure-activity relationship studies of this class of compound and further evaluation of its mechanism and potential to complement existing antiangiogenic drugs.

2.2 INTRODUCTION

During pathological conditions, levels of inflammatory cytokines such as TNF- α and IL-1 are elevated and these cytokines in turn promote angiogenesis along with VEGF (Oh et al., 1999; Yoshida et al., 1998). Hence targeting not only VEGF signaling but multiple proangiogenic signals is required to improve the efficacy of treatment for ocular diseases arising from pathological angiogenesis. At present there is currently no small molecule drug on the market to specifically prevent angiogenesis in the eye, hence there is a pressing need to develop specific novel small molecule drugs to treat these blinding eye diseases.

In order to further explore the potential of homoisoflavanones as treatments for neovascular eye diseases, we synthesized a novel isomer of compound **1**, 5,6-dihydroxy-3-(3-hydroxy-4-methoxybenzyl)-7-methoxychroman-4-one, known as SH-11052 (compound **2**, Fig. 1A). In this chapter I report this synthesis and show the anti-angiogenic properties of compound **2** in human retinal microvascular endothelial cells (HRECs). I also demonstrate that compound **2** blocks TNF- α induced NF- κ B signaling and the VEGF-induced PI3K/Akt pathway, two major proangiogenic signaling pathways activated during inflammation induced angiogenesis. These results suggest that the compound exerts its anti-angiogenic properties by blocking inflammation-induced angiogenic pathways.

2.3. MATERIALS AND METHODS

2.3.1 *Materials Used*

Compound SH-11052 was synthesized by synthetic chemistry collaborators based in Gachon University, South Korea. The details of the synthesis are described elsewhere (Basavarajappa et al., 2014). HRECs and Attachment Factor were purchased from Cell Systems (Kirkland, WA, USA). Clonetics® HUVECs were purchased from Lonza (Walkersville, MD, USA). All cells were used between passages 5 and 7. Endothelial Growth Medium (EGM-2) was prepared by mixing the contents of an EGM-2 “Bullet Kit” (Cat no. CC-4176) with Endothelial Basal Medium (EBM) (Lonza). The EGM-2 “Bullet Kit” contains hydrocortisone, human fibroblast growth factor (hFGF), VEGF, R3-insulin like growth factor (R3-IGF-1), ascorbic acid, human epidermal growth factor (hEGF), gentamycin and heparin along with 2% fetal bovine serum (FBS). Compound BAY 11-7082, caffeic acid phenethyl ester (CAPE), TNF- α , and α -tubulin antibody were from Sigma (St. Louis, MO, USA), and human VEGF-165 was from BioLegend (San Diego, CA, USA). The antibodies for p38 MAPK, NF- κ B p65 and VCAM-1 were obtained from Santa Cruz (Dallas, TX, USA) while the cleaved caspase-3, phospho p38 MAPK, Akt, phospho-Akt, VEGFR2, phospho-VEGFR2, and I κ B- α antibodies were from Cell Signaling (Danvers, MA, USA). Secondary antibodies were from Thermo Fisher Scientific (Pittsburgh, PA, USA). The TaqMan probes and 5'-ethynyl-2'-deoxyuridine (EdU) incorporation assay kit were procured from Life Technologies (Carlsbad, CA, USA). AbD Serotec (Kidlington, UK) was the source of the alamarBlue, while BD Biosciences (San

Jose, CA, USA) supplied the Matrigel. The Bradford reagent for protein estimation was prepared by dissolving 0.3 g of Coomassie G-250 (Pierce) in 500 mL of 3 % perchloric acid.

2.3.2. Cell Proliferation Assay

In a 96-well clear bottom black plate, cells (2,500 cells per well) were seeded in a total volume of 100 μ L EGM-2. After 24 hours of incubation of the plate at 37°C and 5% CO₂, a DMSO solution of compound **2** was added in the concentration range of 0.5 nM to 500 μ M (final DMSO concentration = 1%). The plate was then further incubated for 48 hours before adding 11.1 μ L of alamarBlue reagent to each well. Four hours after the addition of alamarBlue, fluorescence readings with excitation and emission wavelengths of 560 nm and 590 nm respectively were taken and the data were analyzed in GraphPad Prism software (v. 6.0). The dose response curve was generated and the GI₅₀ value was calculated using the following equation: $Y = 100 / (1 + 10^{(X - \text{Log}(\text{GI}_{50}))})$.

2.3.3. EdU Incorporation Assay

Cells (25,000 per coverslip) were seeded onto coverslips coated with Attachment Factor placed in a 6-well plate and incubated with the indicated concentrations of compound **2** in EGM-2 for 24 hours at 37°C and 5% CO₂. The cells were then serum starved for 8 hours and the medium was replaced with EGM-2 containing 10 μ M EdU. The plate was further incubated for another 8 hours before processing the cells for detection of labeled DNA (according to the manufacturer's instructions for the Click-iT EdU assay kit). Images were taken

using an EVOS fluorescence microscope (AMG, Mill Creek, WA, USA) and the number of DAPI stained and EdU stained cells were counted in six randomly chosen fields using ImageJ software.

2.3.4. In Vitro Angiogenesis Assay

Matrigel assays were performed as previously described (Ponce, 2001), with slight modifications for the use of HRECs. Briefly, HRECs were starved overnight at 0.5% FBS in EBM-2 and plated on a 96-well plate at a density of 7,500 cells/well over 50 μ L of Matrigel high concentration basement membrane. Compound **2** was added at the indicated concentrations in EBM-2 + 1% FBS. Cells were observed every 2 hours by bright field microscopy at 40 \times magnification for tube formation. Closed units (polygons) were manually counted at 8 hours post plating and numbers normalized to the DMSO control. Assays were performed in triplicate.

2.3.5. Caspase-3 Expression Assay

Cells (25,000 per coverslip) were seeded onto coverslips coated with Attachment Factor and incubated at 37°C and 5% CO₂ in EGM-2 until ~80 % confluence was achieved. The cells were then incubated for 4 hours with the indicated concentrations of compound **2**. Staurosporine (SP; 1 μ M) was used as a positive control. After the incubation, the cells were fixed in 4% paraformaldehyde for 20 min at room temperature followed by three quick washes in Tris buffered saline pH 7.4 (TBS). The cells were permeabilized by incubating with 0.5% Triton X-100 for 10 minutes and then blocked in 10% block

solution (DAKO, Glostrup, Denmark) in TBS plus 1% bovine serum albumin (BSA) for 1 hour. The cells were then incubated with cleaved caspase-3 (D175) antibody (1:200 dilution) overnight at 4°C. Dylight 555 conjugated goat anti-rabbit secondary antibody (1:400) was used to probe the cleaved caspase-3 antibody. The coverslips were mounted using Vectashield mounting medium containing DAPI (Vector Labs, Burlingame, CA, USA) for nuclear staining. The cells were imaged using an LSM 700 confocal microscope (Zeiss, Thornwood, NY, USA).

2.3.6. NF- κ B Nuclear Translocation Assay

Cells (25,000 per coverslip) were seeded onto coverslips coated with Attachment Factor and incubated at 37°C and 5% CO₂ for 24 hours in EGM-2. The cells were starved in 0.1% serum-EBM-2 for 8 hours followed by 0.1% serum-EBM-2 medium for one hour in the presence of different concentrations of compound **2**. The cells were induced with 10 ng/ml TNF- α for 20 minutes and fixed with 4% paraformaldehyde solution for 20 min at room temperature. Cells were quickly washed three times in TBS and permeabilized by incubating with 0.5% Triton X-100 for 10 minutes. The cells were blocked in 10% block solution (DAKO) in TBS plus 1% BSA followed by incubation with an antibody against NF- κ B p65 (1:50 dilution). Dylight 488-conjugated goat anti-mouse secondary antibody (1:200 dilution) was used to probe the NF- κ B p65 antibody. The coverslips were mounted using Vectashield mounting medium containing DAPI (Vector Labs) for nuclear staining. The cells were imaged using an LSM 700 confocal microscope (Zeiss).

2.3.7. VCAM-1 Expression assay

Cells (25,000 per coverslip) were seeded onto coverslips coated with Attachment Factor and incubated at 37°C and 5% CO₂ for 24 hours in EGM-2. The cells were starved in 0.1% serum-EBM-2 for 8 hours followed by incubation in 0.1% serum-EBM-2 medium for an hour in the presence of different concentrations of compound **2**. The cells were challenged with 10 ng/ml of TNF- α for 24 hours and fixed with 4% paraformaldehyde solution for 20 minutes at room temperature. The coverslips were quickly washed three times in TBS and blocked using 10% block solution (DAKO) prepared in 1× TBS-1% BSA buffer. The coverslips were incubated with the antibody against VCAM-1 (1:100 dilution) for 16 hours at 4°C followed by three washes in TBS- 0.1% BSA buffer. Dylight555-conjugated secondary antibody (1:200) was used to probe for the VCAM-1 antibody. After three washes in TBS-0.1% BSA, the coverslips were mounted using Vectashield mounting medium containing DAPI nuclear stain. The cells were imaged using an LSM 700 confocal microscope. The images were analyzed for fluorescence signal intensity using MetaMorph software (Molecular Devices, Sunnyvale, CA, USA).

2.3.8. qRT-PCR

Cells (10⁵ per well) were seeded in a 6-well plate and incubated for 24 hours at 37°C and 5% CO₂. The cells were then starved in 0.1% serum-EBM-2 for 12 hours followed by incubation for an hour in the presence of different concentrations of compound **2**. The cells were then challenged for 24 hours with

10 ng/ml TNF- α . Following incubation, cells were lysed and RNA was isolated using Trizol reagent (Life Technologies). cDNA was prepared from 80 ng total RNA using random primers and M-MuLV Reverse Transcriptase (New England Biolabs, Ipswich, MA, USA). RT-PCR reactions were set up using the TaqMan Fast Gene Expression Assay Kit according to the manufacturer's instructions. FAM-labeled TaqMan probes for *PTGS2* (Hs00153133_m1), *CCL2* (Hs00234140_m1), *IL8* (Hs00174103_m1), and *TBP* (Hs99999910_m1) genes were used to monitor the expression levels of these genes. The qRT-PCR plate was read in a ViiATM 7 qPCR system (Life Technologies) and the data were analyzed using the $\Delta\Delta C_t$ method. The expression levels of genes were normalized to *TBP* gene expression and calibrated to the DMSO-treated, unstimulated sample.

2.3.9. Immunoblot

HRECs were seeded at 10^5 cells/well in a 6-well plate and after 24 hours of incubation at 37°C, cells were serum starved in 0.1% serum-EBM-2 for 8 hours. Cells were then treated with the indicated concentrations of compound **2** for one hour before the addition of 20 ng/ml of TNF- α or 100 ng/ml VEGF. After 20 minutes, cells were lysed in NP-40 Lysis buffer containing 25 mM HEPES pH 7.4, 1% NP-40, 150 mM NaCl, 10% glycerol, 1 mM sodium orthovanadate, 10 mM sodium fluoride, 1 mM sodium pyrophosphate, 1 mM PMSF, 2.5 mg/ml aprotinin, 1 mM pepstatin, and 1 mM leupeptin. Equal amounts of proteins (80 μ g), as measured by a Bradford assay, were run on 10% SDS-PAGE, transferred to PVDF membrane, blocked with 5% BSA in TBS-0.05% Tween-20 and

immunoblotted with the indicated primary antibodies (1:1000 in 1% BSA in TBS-0.05% Tween-20) overnight at 4°C. After three washes in TBS-0.05% Tween-20, HRP-conjugated secondary antibodies (1:5000 in 5% BSA in TBS-0.05% Tween-20) were applied for one hour at room temperature. After three washes, the protein bands were detected and densitized using ECL Prime western blot detection reagent (GE Life Sciences, Piscataway, NJ, USA) and an XRS gel documentation system running Quantity One software (Bio-Rad). Target protein band intensity was normalized to housekeeping gene α -tubulin. For phosphoprotein analysis, normalized signal of each phosphoprotein was expressed relative to the normalized total amount of that protein.

2.3.10. Statistical Analysis

EdU incorporation, tube formation, apoptosis, immunoblot, and VCAM-1 staining assay data were analyzed by ANOVA with Dunnett's post hoc tests for comparisons between drug treatments and control. All analyses were performed with GraphPad Prism (v. 6.0). A p -value <0.05 was considered statistically significant in all tests.

2.4. RESULTS

2.4.1. SH-11052 Inhibits Proliferation of HRECs

It has been reported that compound **1** isolated from *C. appendiculata* showed antiproliferative effects with a 50% growth inhibitory (GI_{50}) concentration value in the low micromolar range in a HUVEC proliferation assay (Kim et al., 2008; Shim et al., 2004). In order to test if SH-11052 (**2**) has similar effects, the

proliferation of HUVECs induced by complete medium was monitored in the presence of compound **2** in the concentration range of 0.5 nM to 500 μ M. As shown in Figure 2.1B, compound **2** inhibited HUVEC proliferation in a dose dependent manner with GI_{50} = 18 μ M. Once the antiproliferative activity of compound **2** against HUVECs was confirmed, the proliferation of the more disease-relevant HRECs was tested in the presence of compound **2** in the same concentration range. As shown in Figure 2.1C, HREC proliferation was significantly inhibited by compound **2** with GI_{50} = 43 μ M. In order to confirm the inhibition of cell proliferation, we monitored incorporation of 5-ethynyl-2'-deoxyuridine (EdU) into endothelial cells in the presence of compound **2** (Figure 2.2). DNA synthesis in both HRECs and HUVECs was significantly inhibited in a dose dependent manner by this compound.

2.4.2. SH-11052 Inhibits *In Vitro* Angiogenesis without Inducing Apoptosis

The effect of compound **2** on the angiogenic ability of HRECs was evaluated using an *in vitro* Matrigel tube formation assay. HRECs treated with compound **2** showed a significant reduction in their tube formation ability as compared to DMSO treated samples (Figure 2.3A). In the presence of compound **2** at the GI_{50} value, there was a significant reduction in tube formation and the network of tubes was disrupted (polygon spaces in Figure 2.3A) and at 120 μ M the tube formation ability was completely abolished (Figure 2.3B). However, even at 100 μ M, compound **2** caused negligible apoptosis of HRECs as determined by cleaved caspase-3 staining (Figure 2.3C and 2.3D).

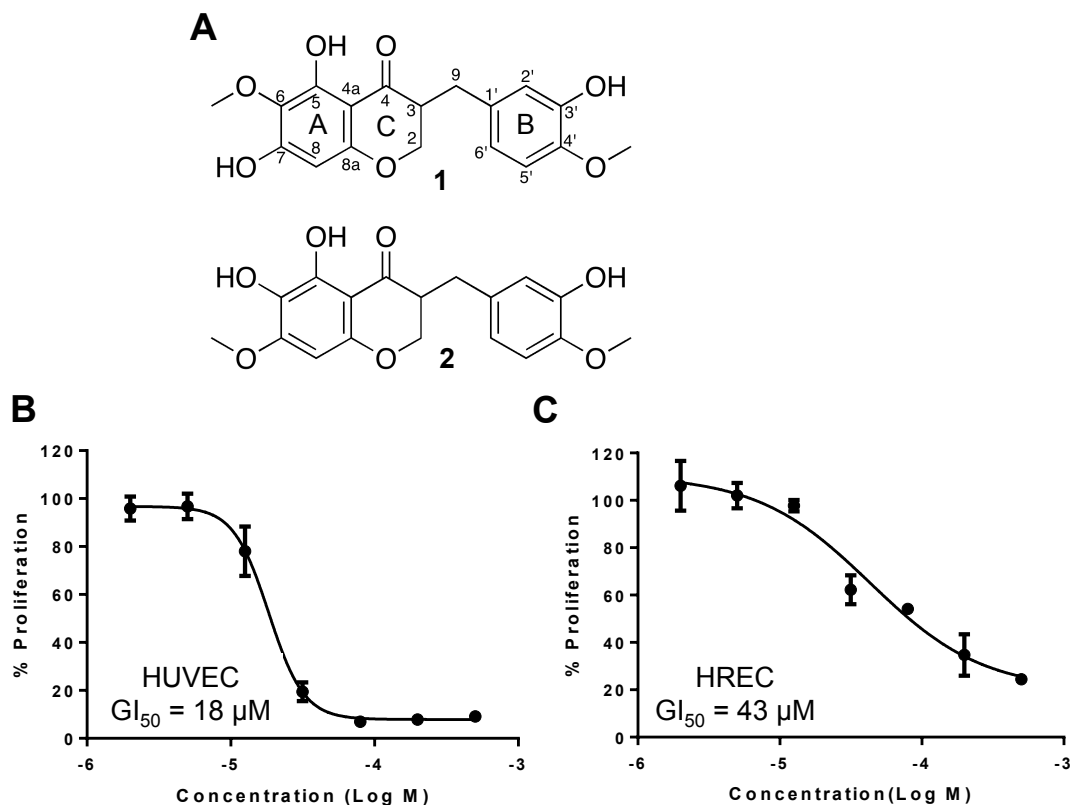


Figure 2.1. Homoisoflavanone SH-11052 inhibits proliferation of endothelial cells. The effects of SH-11052 (**2**), an isomer of the natural-source cremastranone **1** (A) on the proliferation of HUVECs (B) and HRECs (C) were tested by alamarBlue fluorescence in the concentration range of 0.5 nM to 500 μ M and shown as mean \pm SEM relative to DMSO control. Dose response curves and indicated GI_{50} values were generated using GraphPad Prism software.

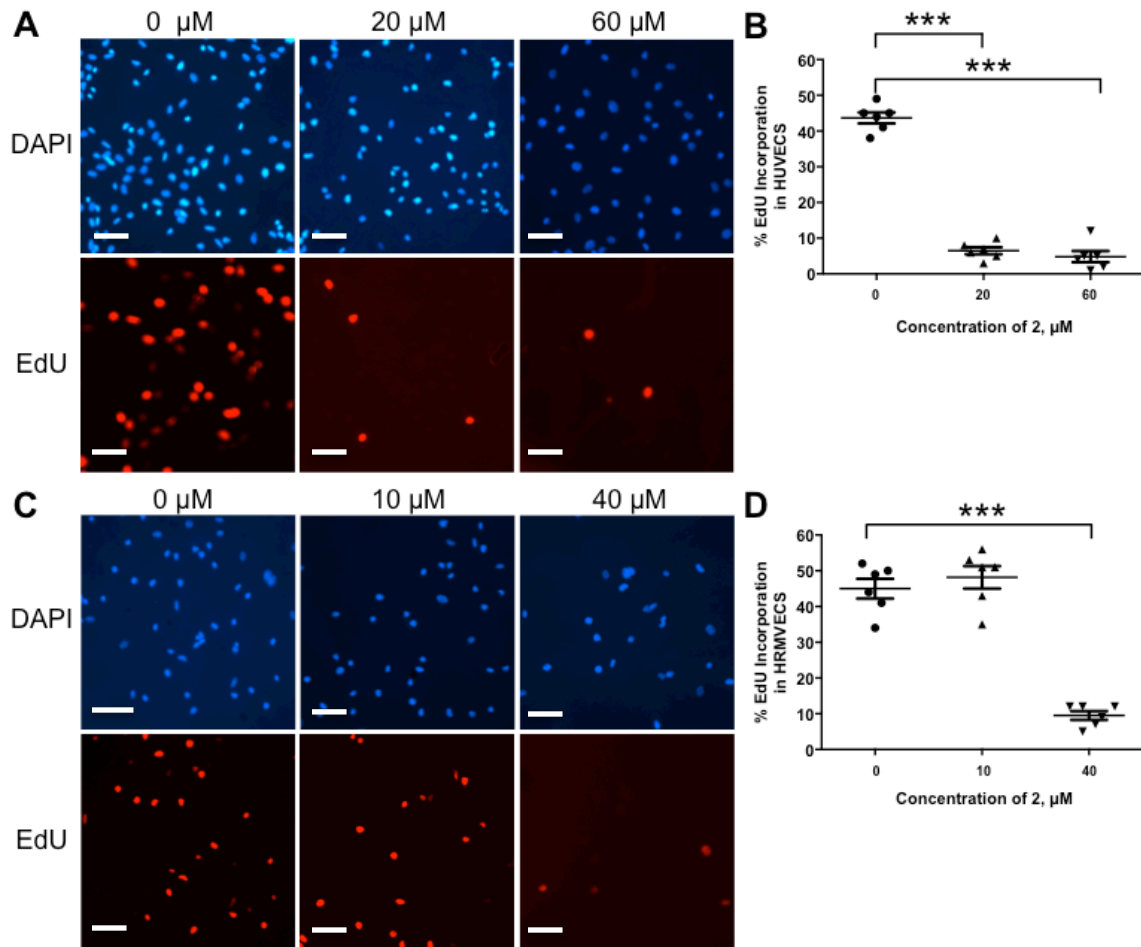


Figure 2.2. SH-11052 blocks DNA synthesis in endothelial cells. After treatment with the indicated concentrations of SH-11052 (**2**) and an EdU pulse, the HUVECs (A, B) and HRECs (C, D) were stained with DAPI (for nucleus - *blue*) and incorporated EdU (in proliferating cells - *red*) using a Click-iT kit (Life Technologies). The cells were counted from 6 different fields of a coverslip and the percentage of proliferating HUVECs (B) and HRECs (D) was calculated from the ratio of EdU stained cells to DAPI stained cells in each section (dots in the graphs) using ImageJ analysis software. Scale bars = 1 mm.

2.4.3. SH-11052 Inhibits the TNF- α Mediated NF- κ B Pathway

After establishing the anti-angiogenic activity of compound **2**, we examined the mechanistic details of its activity in HRECs. As inflammation plays a crucial role in pathological angiogenesis (Klein et al., 2002; Rajashekhar et al., 2011; Rajashekhar et al., 2006; Vanderslice et al., 1998), we examined the effect of compound **2** on inflammatory signaling in endothelial cells. HRECs were treated with different concentrations of compound **2** and then induced with TNF- α , a known pro-inflammatory cytokine and inducer of NF- κ B. Since NF- κ B exerts its transcriptional activity in the nucleus, blockade of stimulus-induced nuclear translocation of NF- κ B is an indication of NF- κ B pathway inhibition (Tomita et al., 1999). The nuclear translocation of NF- κ B upon TNF- α stimulation was inhibited by compound **2** in a dose dependent manner as monitored by immunofluorescence (Figure 2.4A). I κ B- α is an inhibitory protein that binds to NF- κ B and prevents its nuclear translocation. Upon TNF- α stimulation, I κ B- α is phosphorylated and degraded, freeing NF- κ B for nuclear translocation (Chen and Goeddel, 2002). In the presence of compound **2**, the TNF- α -mediated degradation of I κ B- α was significantly decreased in a dose dependent manner, further indicating that compound **2** is inhibiting NF- κ B signaling (Figure 2.4 B-C). In order to confirm inhibition of the TNF- α pathway, we monitored the activating phosphorylation of p38 mitogen activated

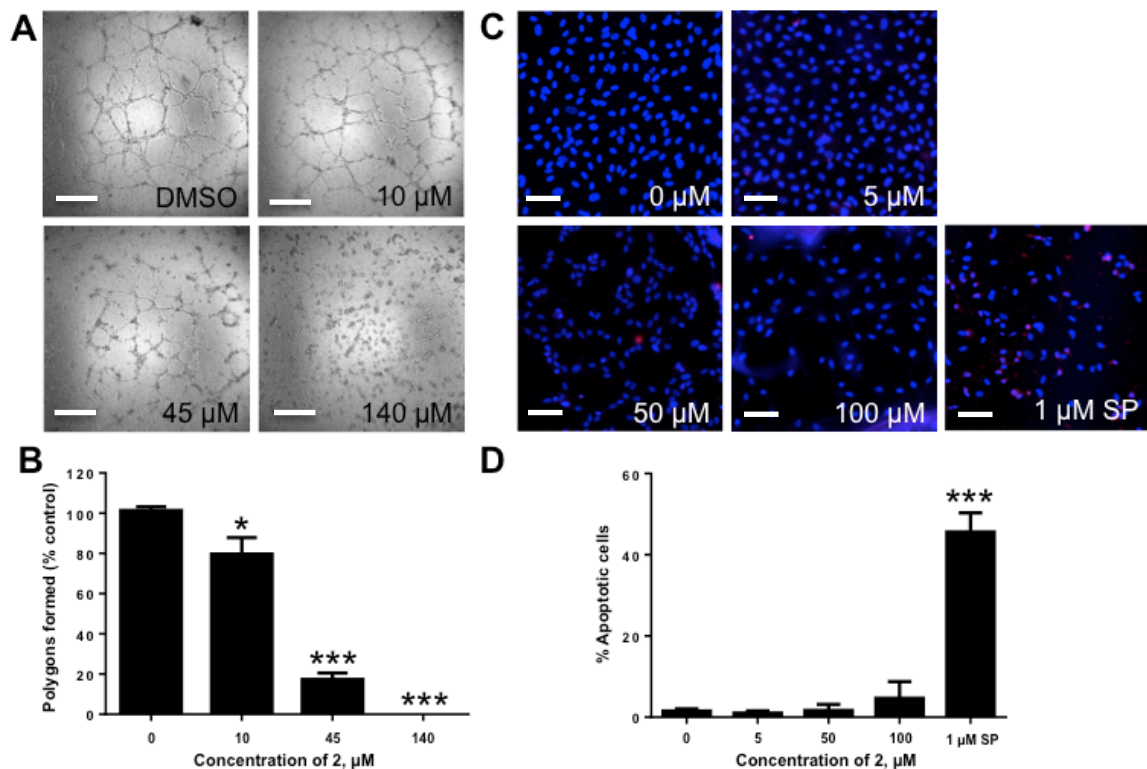


Figure 2.3. SH-11052 inhibits *in vitro* angiogenesis without causing apoptosis. (A) Tube formation on Matrigel by HREC cells in the presence of the indicated concentrations of **2**. (B) Polygons formed (open spaces) were counted. Mean \pm SEM of $n=3$ wells. *, $p<0.05$; ***, $p<0.001$ compared to DMSO control (ANOVA with Dunnett's post hoc test). (C) HREC cells were treated with indicated concentrations of **2** or staurosporine (SP) and stained with DAPI (for nucleus - blue) and activated caspase-3 antibody (red). (D). Percentage of HREC cells undergoing apoptosis was calculated by counting number of caspase (red) stained cells compared to total (blue) cells using ImageJ software. Scale bars = 1 mm.

protein kinase (MAPK), an important downstream target of the TNF- α pathway involved in cytokine induced cell proliferation (Liu et al., 2000). Compound **2** inhibited phosphorylation of p38 MAPK in a dose dependent manner (Figure 2.4 D-E).

2.4.4. SH-11052 Decreases Levels of NF- κ B Targets

We confirmed NF- κ B pathway inhibition by monitoring the expression of NF- κ B induced genes in the presence of compound **2** (Figure 2.5). VCAM-1 is a cell adhesion molecule specifically expressed on endothelial cells and its expression is induced by NF- κ B upon TNF- α signaling (Rajashekhar et al., 2007; Zhang et al., 2002). We monitored the expression of VCAM-1 in HRECs using immunofluorescence with increasing concentrations of compound **2**. There was a significant dose-dependent decrease in VCAM-1 protein expression in the presence of compound **2** (Figure 2.5A & 2.5B). Similarly the mRNA expression of the pro-inflammatory molecules *IL8*, *PTGS2* (COX2) and *CCL2* (MCP-1), inducible by NF- κ B, were decreased in the presence of compound **2**, as monitored by qRT-PCR (Figure 2.5C).

2.4.5. SH-11052 Inhibits VEGF-mediated Activation of PI3K/Akt Signaling

As VEGF signaling is a major contributor to angiogenesis, we tested if compound **2** can inhibit VEGF signaling along with inflammation induced TNF- α signaling. Upon VEGF stimulation, VEGF receptor 2 (VEGFR2) autophosphorylates, leading to activation of the PI3K/Akt pathway (Hoebe et al., 2004). Compound **2** did not inhibit phosphorylation of VEGFR2 but inhibited

activation of the downstream Akt in HRECs (Figure 2.6). Since TNF- α signaling also feeds through Akt to IKK α (Ozes et al., 1999), these results suggest that compound **2** might act at the level of PI3K or Akt to block both VEGF and TNF- α signaling.

2.5. DISCUSSION

In pathological ocular neovascularization such as that observed in ROP, DR and AMD, there is an increase in the levels of VEGF (Chen and Smith, 2007; Yoshida et al., 1997). Along with VEGF, inflammation plays a crucial role in pathological angiogenesis (Economopoulou et al., 2005; Rajashekhar et al., 2011; Yoshida et al., 1998; Yoshida et al., 1997). This suggests that pathologic vessel growth as observed in ocular diseases is not only under control of VEGF (Carmeliet, 2003), but also intimately linked with inflammation leading to endothelial activation (Rajashekhar et al., 2007; Rajashekhar et al., 2006). Of the several cell signal transduction pathways studied, NF- κ B pathways play an important role in inducing the expression of pro-angiogenic genes such as *VEGF*, *VEGFR*, *IL8*, *VCAM1*, *CCL2*, and *PTGS2* after activation through TNF- α signaling (Klein et al., 2002; Royds et al., 1998; Yoshida et al., 1997). Based on the clinical evidence that anti-VEGF antibody therapy led to arterial thromboembolic complications and suggested a role for endothelial damage and inflammation (Ratner, 2004), a combination of anti-VEGF and anti-inflammatory therapy might be more beneficial in treating neovascular eye disease as compared to monotherapy. In favor of this hypothesis, in ROP experimental models, a combination of inhibitors of different pathways was found to be

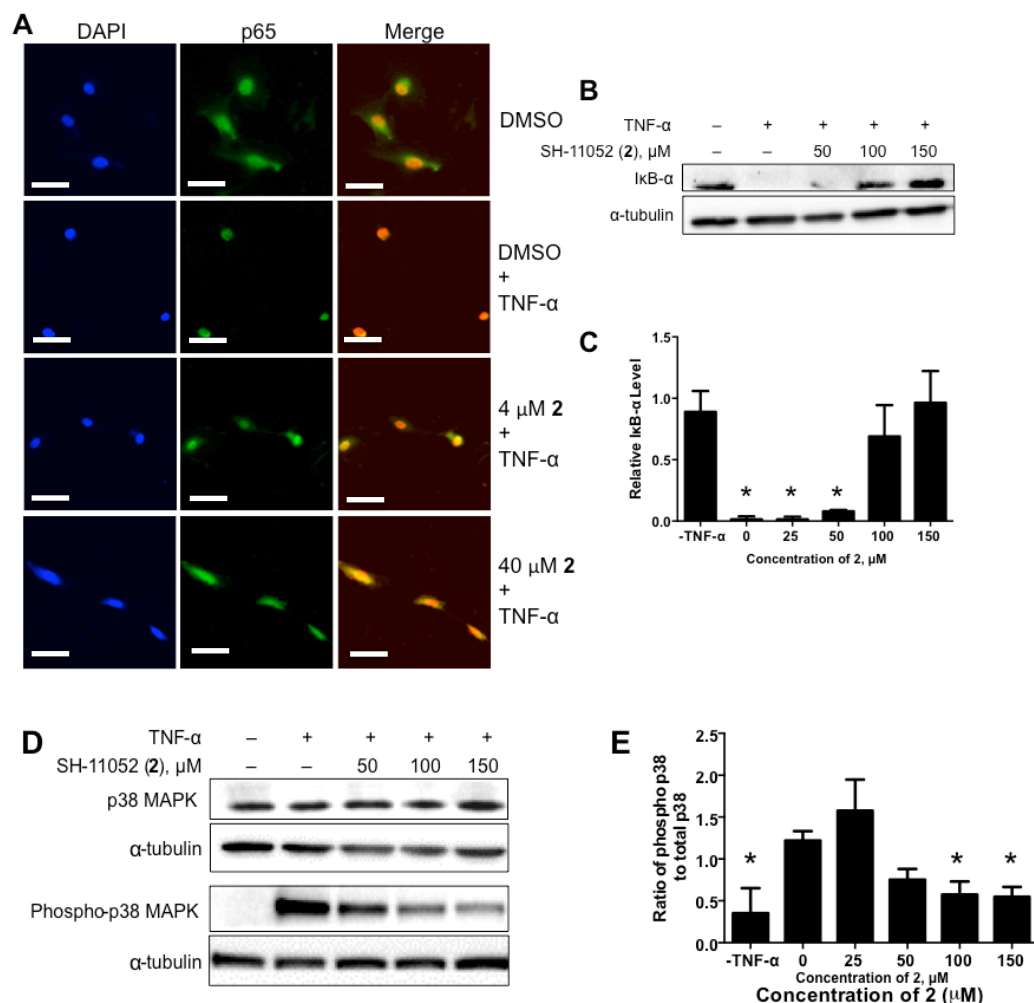


Figure 2.4. SH-11052 inhibits TNF- α mediated NF- κ B signaling. (A) After treating HRECs with the indicated concentrations of **2**, p65 (green) was detected by immunofluorescence and nuclei (blue) stained with DAPI. Representative data from three independent experiments. Scale bars = 1mm. (B) The protein levels of IkB- α were measured after TNF- α treatment in the presence of the indicated concentrations of compound **2** by immunoblot. (D) The phosphorylation level of p38 MAPK in HRECs stimulated with TNF- α was monitored in the presence of the indicated concentrations SH-11052 by immunoblot. (C & E) Densitometry was performed using Quantity One software and analyzed using GraphPad Prism.

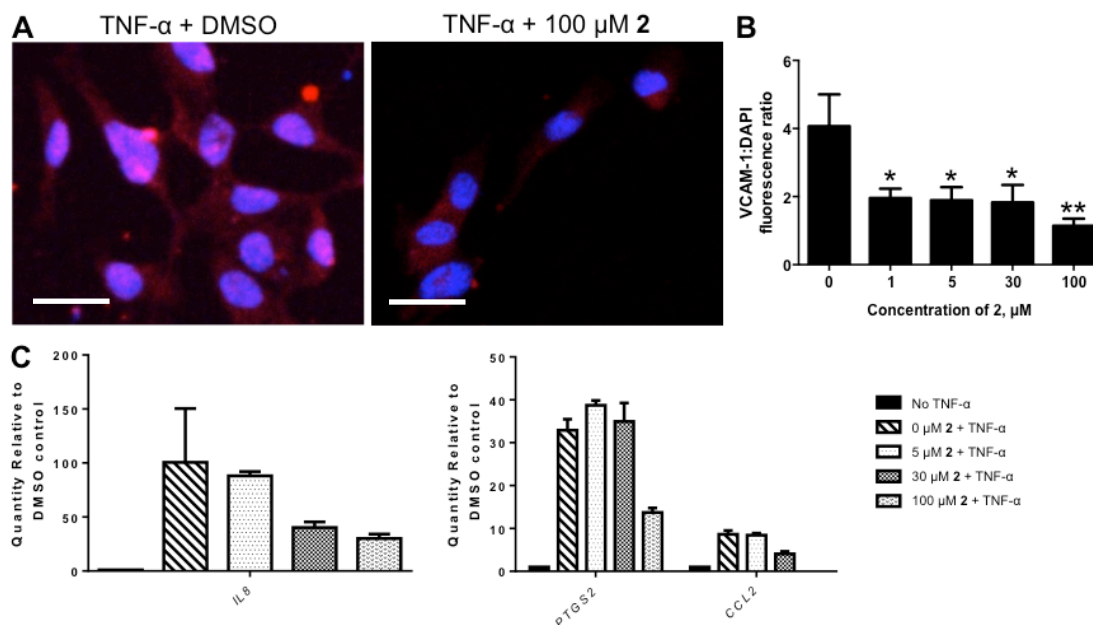


Figure 2.5. SH-11052 decreases the expression of NF- κ B target genes. (A) Endothelial activation marker VCAM-1 (red) was detected by immunofluorescence in HRECs exposed to TNF- α \pm **2**. Scale bars = 1mm. (B) MetaMorph fluorescence intensity analysis of VCAM-1 staining in the presence of TNF- α and the indicated concentrations of **2**, mean \pm SEM of n=5 fields; *, $p<0.05$ **, $p<0.01$ compared to DMSO control (ANOVA with Dunnett's post hoc test); representative data from two independent experiments. (C) qRT-PCR using TaqMan probes showed that mRNA levels of NF- κ B target genes *IL8* (interleukin-8) (left panel), *CCL2* (MCP-1) and *PTGS2* (COX2) (right panel), all induced by TNF- α , were decreased in the presence of **2** in a dose dependent manner.

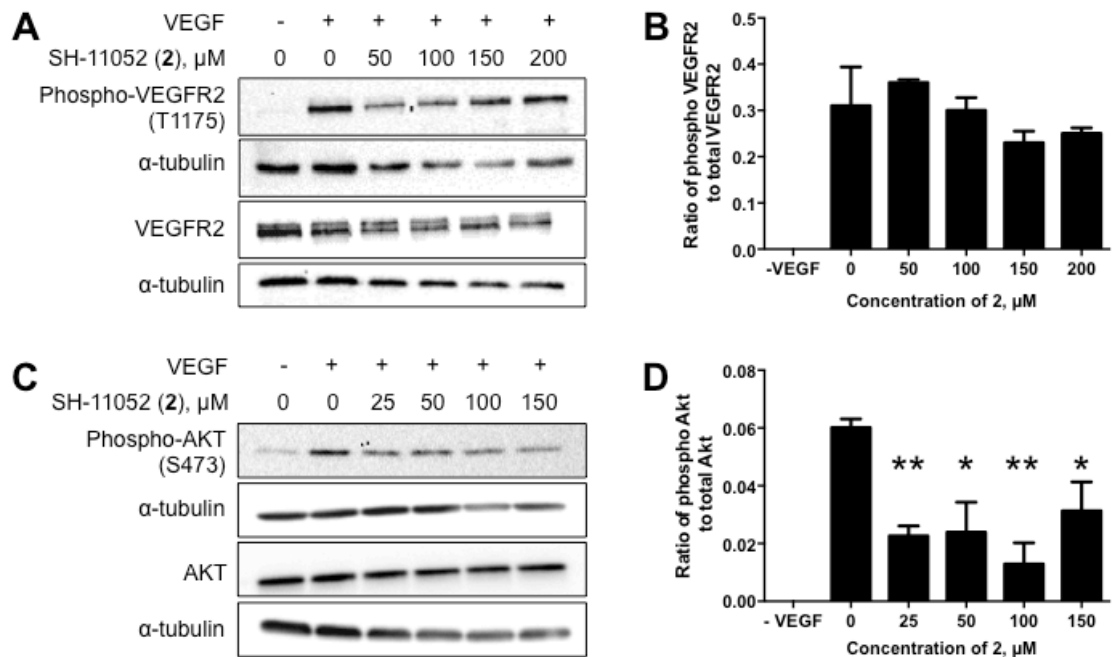


Figure 2.6. SH-11052 inhibits VEGF mediated Akt signaling. Phosphorylation of VEGFR2 (A) and Akt (C) was monitored in HRECs upon VEGF stimulation in the presence of varying concentrations of 2. (B & D) Densitometry was performed using Quantity One software and analyzed using GraphPad Prism. The lines indicate the mean \pm SEM of three biological replicates, * indicates $p < 0.05$ and ** indicates $p < 0.01$ compared to VEGF treatment alone (ANOVA with Dunnett's post hoc test).

highly significant in blocking new vessel formation (Friedlander, 2009). At present, the current antiangiogenic biologics only target VEGF signaling at the level of the receptor, therefore, the development of drugs targeting inflammatory signals provides an opportunity for new, combination anti-angiogenic therapies. Developing small molecules to include in such cocktails is therefore of significant interest and development of drugs which can inhibit multiple angiogenic pathways would greatly increase the efficacy of therapies. Towards this goal we have pursued SH-11052 as a small molecule inhibitor of retinal neovascularization, building on previous reports of the efficacy of a related homoisoflavanone (**1**) in animal models of ROP and choroidal neovascularization (Kim et al., 2007; Kim et al., 2008).

In the present study our collaborator used a novel method based on a chalcone intermediate and a regioselective demethylation to synthesize the novel homoisoflavanone **2**. This methodology adds to the diversity of homoisoflavanones that are synthetically tractable and will readily allow synthesis of novel analogs in future. I confirmed that our synthetic SH-11052 has similar effects on HUVECs to the natural-source compound **1** (Figure 1B). GI_{50} of the natural product **1** was reported as 0.5 $\mu\text{g/mL}$, or approximately 1.5 μM (Shim et al., 2004).

Endothelial cells from different tissues have different gene expression patterns suggesting different physiological effects (Hesse and Moser, 2003). HUVECs are macrovascular endothelial cells which do not have specific relevance to the microvascular endothelial cells that are present in retinal

capillaries of the eye. Therefore, we tested SH-11052 in HRECs, where it proved similarly potent as an anti-proliferative molecule (Figure 2.1C), albeit at higher GI_{50} , consistent with the hypothesis that microvascular endothelial cells differ from macrovascular endothelial cells. SH-11052 blocks proliferative progression through DNA synthesis in both HUVECs and HRECs (Figure 2.2). This is consistent with the documented G_2/M phase cell cycle arrest induced by **1** in HUVECs (Kim et al., 2007). We have also demonstrated the *in vitro* anti-angiogenic activity of **2** in a Matrigel HREC tube formation assay, similar to the effects of **1** in HUVECs (Kim et al., 2007).

The novel anti-angiogenic mechanism of homoisoflavanones remains largely unexplored. In HUVECs, compound **1** induced expression of $p21^{WAF1}$ (*CDKN1A*), an inhibitor of the cyclin-dependent kinase Cdc2 (*CDK1*), which in turn is downregulated by compound **1** (Kim et al., 2007). Homoisoflavanone **1** also blocked prostaglandin synthesis from arachidonic acid in a microsome assay, without marked effects on function of cyclooxygenases 1 and 2 as purified enzymes (du Toit et al., 2005). In keratinocytes, compound **1** inhibited the nuclear translocation of NF- κ B under ultraviolet light-induced inflammatory conditions, suggesting a role of the compound in modulating inflammatory signals in these cells (Hur et al., 2010b). In this context, compound **1** also decreased phosphorylation of the MAPKs Jun N-terminal kinase (JNK), p38 MAPK, and ERK.

We examined if the activity of SH-11052 in HRECs may likewise be mediated through modulation of inflammatory signals. As NF- κ B is the principal

mediator of inflammation induced signals (Tak and Firestein, 2001), we monitored NF- κ B activation upon TNF- α stimulation in the absence or presence of compound **2** in HRECs. NF- κ B is a transcription factor sequestered in the cytoplasm by association with I κ B- α protein. Upon TNF- α stimulation, I κ B- α is phosphorylated and degraded by the proteasome, releasing free NF- κ B. The free NF- κ B is then translocated into the nucleus and aids in the transcription of its target genes. Hence monitoring the protein levels of I κ B- α and nuclear translocation of NF- κ B upon TNF- α treatment are measures of the activation of the NF- κ B pathway by inflammatory signals (Tak and Firestein, 2001). Indeed, we show that I κ B- α degradation and nuclear translocation of NF- κ B in HRECs are inhibited by compound **2** (Figure 2.4). Furthermore, compound **2** also inhibited the expression of NF- κ B inducible pro-angiogenic and pro-inflammatory genes (Figure 2.5), suggesting a role for compound **2** in the inhibition of inflammation-induced pro-angiogenic signaling in HRECs.

SH-11052's suppressive effects on expression of *IL8* and *PTGS2* in HRECs are consistent with the observed effects of the natural product **1** in keratinocytes. To our knowledge, we show for the first time an effect of a homoisoflavanone on the endothelial activation marker and NF- κ B target, VCAM-1, and on the inflammatory marker *CCL2*. Thus, the data presented here are consistent with a function for compound **2** as an inhibitor of NF- κ B signaling in HRECs. NF- κ B has previously been implicated in pathological ocular angiogenesis (Omar et al., 2013; Yoshida et al., 1999).

This assertion of an NF- κ B-dependent role for compound **2** can integrate others' findings regarding the activities of the related compound **1** in other cell types as well. bFGF can act by signaling through phospholipase $\text{C}\alpha$ (Meyer et al., 2003; Raffioni et al., 1999), which activates protein kinase C (PKC) α via diacylglycerol. In turn, PKC α binds and activates IKK α , which phosphorylates and inactivates I- κ B (Lallena et al., 1999). Thus, blockade of this pathway would inhibit cellular responses to bFGF, as seen with compound **1** in HUVECs (2004). NF- κ B is a major transcription factor for inflammatory cytokines, and also for transcription of *PTGS2* (Kang et al., 2007), consistent with the negative transcriptional effects of compound **1** on these genes and consequent inhibition of prostaglandin production in keratinocytes. Mitochondrial superoxide dismutase (*SOD2*) transcription is also activated by NF- κ B (Maehara et al., 2000), potentially explaining increased reactive oxygen species generation after NF- κ B inhibition mediated by compound **1** (Hur et al., 2010b). Moreover, blockade of the NF- κ B pathway can deactivate MAPKs, as seen with compound **1** (Hur et al., 2010b) in keratinocytes and compound **2** in HRECs (Figure 2.4). This may occur via sequestration of the MAPK kinase kinase TPL2 (tumor progression locus 2) by (inactive) p105^{NF κ B1} (Yang et al., 2012). Finally, NF- κ B inhibition can lead to upregulated p53-mediated transcription (Webster and Perkins, 1999), which could increase levels of p21^{WAF1} and decrease Cdc2 expression in response to treatment with compound **1** as previously seen in HUVECs (Kim et al., 2007). A role for both compounds **1** and **2** in the NF- κ B pathway is also consistent with possible mechanisms for related isoflavones (Gupta et al., 2010), and NF- κ B

pathway inhibition can block pathogenic ocular neovascularization (Yoshida et al., 1999).

Compound **2** may be acting at the level of PI3K or Akt, since compound **2** can inhibit VEGF-induced Akt phosphorylation, but not VEGFR2 phosphorylation (Fig. 2.6), and since PI3K/Akt serves as a point of integration of both VEGF and TNF signaling (Ozes et al., 1999). As a post-receptor VEGFR signaling inhibitor and TNF- α pathway inhibitor, compound **2** may serve as a lead molecule for targeting multiple proangiogenic pathways to improve the efficacy of treatment. Development of such molecules which target both VEGF and other inflammation induced proangiogenic signaling pathways might help in replacing or reducing the dose of anti-VEGF biologics. Future studies identifying the direct molecular interacting partners of homoisoflavanones in HRECs will be crucial for elucidating their precise anti-angiogenic mechanism as described in chapter 5, as well as optimizing the structures of these molecules prior to future therapeutic use (discussed in chapter 4), via a target-based drug discovery approach.

In summary, we have synthesized a novel homoisoflavanone **2** and demonstrated its anti-angiogenic activity in retinal endothelial cells, and provided partial characterization of its molecular mechanism. Given SH-11052's anti-angiogenic properties, it will be important to fully elucidate the molecular mechanism of action of this compound. Our synthetic method also enables structure-activity profiling to obtain more potent anti-angiogenic molecules that can be tested in animal models of ocular neovascularization, both alone and in combination therapies.

Based on the success of synthesizing this compound, SH-11052, our synthetic chemistry collaborators attempted to synthesize cremastranone. In the next chapter I report the biological characterization of synthetic cremastranone.

CHAPTER 3. FIRST SYNTHESIS OF THE ANTI-ANGIOGENIC HOMOISOFLAVANONE, CREMASTRANONE

[This chapter forms portion of previously published research paper and reproduced here with permission from the Royal Society of Chemistry: Bit Lee, Halesha D. Basavarajappa, Rania S. Sulaiman, Timothy W. Corson* and Seung-Yong Seo*. 2014. First synthesis of the antiangiogenic homoisoflavanone, cremastranone. *Organic and Biomolecular Chemistry*, 12, 7673. * Equal contributors]. My role in this project was to evaluate the biological properties of cremastranone.

3.1 CHAPTER SUMMARY

An antiangiogenic homoisoflavanone, cremastranone, was synthesized for the first time. This scalable synthesis, which includes selective demethylation, could be used to develop lead molecules to treat angiogenesis-induced eye diseases. Synthetic cremastranone inhibited the proliferation, migration and tube formation ability of human retinal microvascular endothelial cells, important steps in pathological angiogenesis. The objective of this chapter is to characterize the biological activities of synthetic cremastranone in order to use it in mechanistic studies.

3.2 INTRODUCTION

So far, the syntheses of 5,7-dihydroxy-6-methoxyflavones and 5,7-dihydroxy-6-methoxyhomoisoflavanone have been reported (Fig. 3.1) (Farkas et al., 1971; Farkas and Strelisky, 1970). In spite of its interesting biological activities and the synthesis of congeners, to the best of our knowledge, the synthesis of the anti-angiogenic natural product **1** (Fig.3.1) was not reported yet. To allow future profiling and development of this homoisoflavanone and its analogs, we need to develop a scalable synthesis suitable for quickly securing multi-gram quantities. During our previous synthetic approach toward cremastranone (Chapter 2), the regioisomer (SH-11052) was generated due to the challenge of selective deprotection of methyl phenyl ethers (Basavarajappa et al., 2014). In this chapter, we describe a short and efficient synthesis of cremastranone (**1**) featuring a solution to the issue of selective deprotection of

the methyl phenyl ether. Moreover, we show for the first time that synthetic cremastranone has biological properties consistent with the natural-source compound.

3.3 METHODS

3.3.1. Cell proliferation assay

Alamar blue-based cell proliferation protocol was performed as described in chapter 2 (Section 2.3.2).

3.3.2. EdU incorporation assay

The EdU incorporation assay was performed as described in chapter 2 (Section 2.3.3).

3.3.3. In vitro scratch assay

HRECs (10^5) were seeded in each well of a 6-well plate coated with attachment factor. The cells were incubated in EGM-2 medium until confluent (~24 hours). The cells were then starved for 12 hours in serum free EBM-2 medium. After starvation, using a sterile fine 10 μ L micropipette tip, a straight scratch was introduced in the well and rinsed twice using EBM-2 medium to remove unbound cells and debris. Then cells were incubated in EGM-2 medium in the presence of the indicated concentrations of 1 at 37°C and 5% CO₂. After 8 hours, images were taken using the EVOS microscope and the number of migrated cells into the scratched area was counted.

3.3.4. *In vitro* Angiogenesis assay

The tube formation assay was performed as described in Chapter 2 (Section 2.3.4).

3.4 RESULTS

Synthetic chemist collaborator Dr. Seung-Yong Seo's group based in South Korea carried out the synthesis of cremastranone and other intermediates. Our plan for the preparation of cremastranone entailed chromanone formation and demethylation of a methyl aryl ether. This strategy would permit significant flexibility in the synthesis of **1** and thereby adapt a platform that leads to a variety of derivatives for further structure-activity relationship studies. In addition, we envisioned our synthesis would become very useful for the synthesis of similar interesting homoisoflavanones. The details of synthesis and methods are described in the published paper (Lee et al., 2014). Previously, cremastranone isolated from *C. appendiculata* was tested for its anti-proliferative activity against an endothelial cell model, human umbilical vein endothelial cells (HUVEC), and the 50% growth inhibitory concentration (GI₅₀) value was reported to be 1.5 μ M (Shim et al., 2004). Hence, we tested the anti-proliferative activity of synthetic cremastranone **1** (Fig. 3.1) on HUVECs in an alamar blue fluorescent cell proliferation assay and the GI₅₀ was observed to be 377 nM. The slightly higher potency of synthetic **1** might be attributed to a difference in the proliferation assays used.

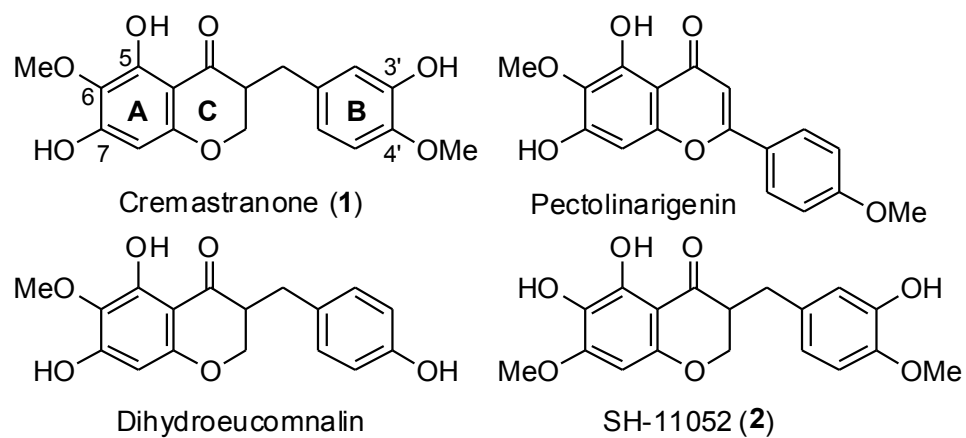


Figure 3.1. The structure of cremastranone (1) and its congeners.

Further, we tested the anti-proliferative activity of **1** against a more ocular disease relevant endothelial cell model, human retinal microvascular endothelial cells (HRECs). We observed clear dose dependent inhibition of HREC proliferation by **1** in complete medium with GI₅₀ of 217 nM (Fig. 3.2a). In addition we also tested the proliferation of HRECs induced by vascular endothelial growth factor, a potent inducer of angiogenesis, in presence of **1** and measured the GI₅₀ to be comparable (276 nM). In chapter 2, I reported a GI₅₀ of 43 μM for regioisomer SH-11052 (**2**), which differed in the positions of hydroxyl and methoxy groups on the 'A' ring at C6 and C7 as compared to **1**. The importance of positions of the groups on the 'A' ring suggests that a structure-activity relationship can be established.

We then measured the endothelial cell specificity of **1** by measuring the proliferation of non-endothelial ocular cell lines, Y79 (retinoblastoma), 92-1 (uveal melanoma) and ARPE-19 (retinal pigmented epithelium). The anti-proliferative potency of **1** on these non-endothelial cell lines was significantly lower than that of endothelial cells with GI₅₀ values of 9.8 μM, 47 μM and >250 μM on Y79, 92-1 and ARPE-19 cells respectively, indicating that compound **1** is highly specific toward endothelial cells.

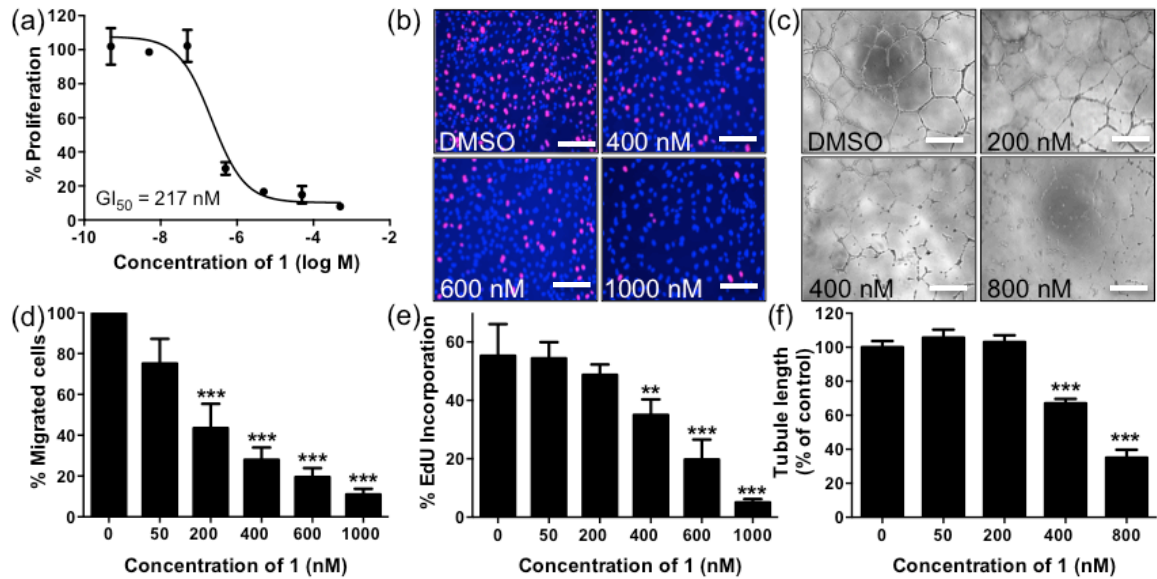


Figure 3.2. Synthetic cremastranone (1) blocks in vitro angiogenesis of human retinal microvascular endothelial cells (HREC) in a dose-dependent manner. (a) The effect of 1 on proliferation of HREC was tested using an alamar blue fluorescence assay. (b, e) In an EdU incorporation assay, 1 blocked DNA synthesis as evidenced by a decrease in incorporation of EdU (pink) into the nuclei of HREC (nuclei, blue). (c, f) Tube formation by HREC on Matrigel was blocked by 1; the extent of tube formation was measured as tubule length. (d) Migration of HREC in a scratch-wound assay was inhibited by 1. Scale bars = 1mm. The data points in all graphs indicate mean \pm SEM; ** represents $P < 0.01$; *** $P < 0.001$ (ANOVA with Dunnett's post hoc tests). Each of the panels is representative of three independent experiments.

We further confirmed the inhibition of HREC proliferation by **1** in a secondary assay by monitoring the incorporation of EdU into DNA of endothelial cells in the presence of different concentrations of **1**. In this EdU incorporation assay, compound **1** inhibited the DNA synthesis of HRECs in a dose dependent manner (Fig 3.2c).

After establishing the inhibition of HREC proliferation by **1**, we tested its anti-angiogenic activity in vitro. Migration is an important step in the angiogenesis process, wherein endothelial cells move from pre-existing capillaries to the site of blood vessel formation. We measured this ability of HRECs to migrate using the standard scratch-wound assay, in which HRECs were allowed to grow to confluency, then a scratch was introduced and movement of endothelial cells into the scratched area from the surrounding population was measured in presence of various concentrations of **1** (Fig 3.2b). The migration of HRECs was inhibited by **1** in a dose dependent manner. We also tested the ability of HRECs to form tubes in vitro in a Matrigel tube formation assay, which recapitulates in vitro all events of physiological angiogenesis. Cremastranone **1** prevented the formation of closed tube structures in a dose dependent manner as measured by both tube length (Fig. 2d) and number of polygons formed. This is consistent with previous findings with the natural-source cremastranone in HUVECs (Shim et al., 2004).

3.5 DISCUSSION

In summary, a novel, scalable strategy to synthesize biologically active cremastranone was developed by our collaborator, and the resulting compound

was tested in cell models. Together, these results confirm the anti-angiogenic activity of synthetic cremastranone **1** in a disease-relevant cell type, and thereby pave the way for development of analogues with higher potency and better pharmacological properties to treat blinding ocular diseases caused by pathological angiogenesis.

The scalable synthesis of synthetic cremastranone is very important to decipher the biological mechanism of action of cremastranone. Most of the biological methods used in understanding the mechanism of action require moderate to high quantities of cremastranone, which is difficult to obtain from plant sources as described in literature. The chemical synthesis of cremastranone removed this obstacle and also paved the way to synthesize more analogues to improve the potency and selectivity. Towards this end we pursued structure-activity relationship studies as described in chapter 4 in order to find potent and selective compounds which have high potency on HRECs and less activity on other endothelial and non-endothelial ocular cells.

CHAPTER 4. SYNTHESIS AND BIOLOGICAL EVALUATION OF NOVEL HOMOISOFLAVONIDS FOR RETINAL NEOVASCULARIZATION.

[This chapter was previously published in the following research article and reproduced here with permission from the American Chemical Society: Halesha D. Basavarajappa, Bit Lee, Hyungjun Lee, Rania S. Sulaiman, Hongchan An, Carlos Magaña, Mehdi Shadmand, Alexandra Vayl, Gangaraju Rajashekhar, Eun-Yeong Kim, Young-Ger Suh, Kiho Lee, Seung-Yong Seo, Timothy W. Corson. 2015. Synthesis and biological evaluation of novel homoisoflavonoids for retinal neovascularization. *Journal of Medicinal Chemistry*. 58(12):5015-27].

4.1 CHAPTER SUMMARY

Eye diseases characterized by excessive angiogenesis such as wet age-related macular degeneration, proliferative diabetic retinopathy, and retinopathy of prematurity are major causes of blindness. Cremastranone is an anti-angiogenic, naturally occurring homoisoflavanone with efficacy in retinal and choroidal neovascularization models and antiproliferative selectivity for endothelial cells over other cell types. We undertook a cell-based structure-activity relationship study to develop more potent cremastranone analogs, with improved antiproliferative selectivity for retinal endothelial cells. Phenylalanyl-incorporated homoisoflavonoids showed improved activity and remarkable selectivity for retinal microvascular endothelial cells. A lead compound inhibited angiogenesis in vitro without inducing apoptosis, and had efficacy in the oxygen-induced retinopathy model in vivo.

4.2 INTRODUCTION

In chapters 3 and 2 I showed that a natural product homoisoflavanone, cremastranone (**1**; Figure 1), and a regioisomer SH-11052 (**2**) inhibit angiogenesis in vitro, with some selectivity for blocking proliferation of endothelial cells over other ocular cell types. Selectivity for antiproliferative effects on microvascular endothelial cells (such as those in the eye) over macrovascular endothelial cells and non-endothelial cell lines is suggestive of a desirable lack of off-target cytotoxicity in vivo (Sulaiman et al., 2014). Indeed, cremastranone inhibits ocular angiogenesis, without obvious toxicity, in mouse models of laser-induced choroidal neovascularization (Kim et al., 2008) and oxygen-induced

retinopathy (OIR) (Kim et al., 2007), animal models recapitulating some of the features of wet AMD and ROP respectively.

Even though cremastranone's antiangiogenic activity is well established, other homoisoflavonoids have not been extensively explored for their effects on endothelial cells. One compound, (*E*)-3-(3-hydroxy-4-methoxybenzylidene)-6-methyl-4-chromanone was shown to have submicromolar antiangiogenic effects in vitro and efficacy in a laser-induced choroidal neovascularization model (Kim et al., 2008), while a related compound (*E*)-3-(2-methoxybenzylidene)-4-chromanone was shown to have antiproliferative effects on human umbilical vein endothelial cells (HUVECs) (Ivanova et al., 2013). Of natural-source homoisoflavanones, methylophiopogonanone B blocked HUVEC angiogenesis and the hypoxic response in vitro (Hasebe et al., 2003), while very recently methylophiopogonanone A was shown to block brain endothelial cell activation (Lin et al., 2015). In addition, considerable work has documented antiangiogenic effects of the related chalcones, flavones and flavanones (Fotsis et al., 1997). However, to our knowledge no systematic exploration of this class of compounds as antiangiogenic agents has been reported.

Multiple signaling pathways are modulated by cremastranone (Kim et al., 2007). It induces expression of p21^{WAF1} (*CDKN1A*), an inhibitor of the cyclin-dependent kinase Cdc2 (*CDK1*). It also blocks prostaglandin synthesis from arachidonic acid (du Toit et al., 2005); and decreases phosphorylation of the mitogen activated protein kinases. Finally, it blocks nuclear translocation of NF- κ B and production of inflammatory cytokines (Hur et al., 2010). The search for

direct molecular targets is underway. However, its exact mechanism of action remains unknown, rendering a cell-based analysis of efficacy the most appropriate route to developing novel derivatives. Here, we describe development of a structure-activity relationship of homoisoflavonoids for inhibiting proliferation of endothelial cells, which resulted in identification of potent, microvascular endothelial-cell specific antiangiogenic molecules for lead optimization. Using **1** as our primary scaffold, we envisioned homoisoflavonoid analog design by which several substituents on the A and B rings could be varied as shown in Fig. 4.1. We planned to synthesize homoisoflavonoids with highly oxygenated substitutions such as methoxy and hydroxy on the A ring (du Toit et al., 2010; Mulholland et al., 2013), whereas those with a wide range of substitution patterns on the B ring would be anticipated to exhibit more efficient and selective antiproliferative activity than natural product homoisoflavonoids.

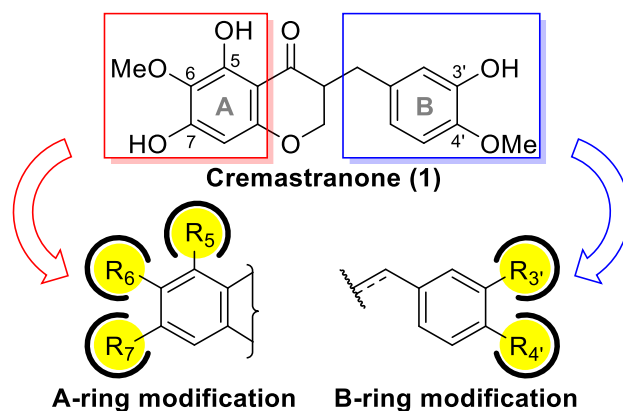


Figure 4.1. Homoisoflavonoid analog design.

4.3 METHODS

4.3.1 Chemistry Methods

Synthetic chemistry collaborator Dr. Seung-Yong Seo's group carried out the syntheses of all the homoisoflavonoid analogues. The details of the chemistry methods and results have been published (Basavarajappa et al., 2015).

4.3.2 Materials

The cells and culture media used are as described in chapter 2 (Section 2.3.1).

4.3.3 Cell proliferation assay

The detailed protocol for monitoring the cell proliferation is described in chapter 2 (Section 2.3.2).

4.3.4 EdU incorporation assay

A complete Protocol for monitoring the EdU incorporation in HRECs has been described in chapter 2 (Section 2.3.3).

4.3.5 Caspase-3 immunofluorescence assay

The assay was carried out as described in chapter 2 (Section 2.3.5).

4.3.6 TUNEL assay

Cells (25,000 per coverslip) were seeded on each coverslip coated with attachment factor in a 6-well plate and grown overnight in EGM-2 medium. Next day, fresh medium with the indicated concentrations of compound was added to cells and they were incubated for 4 hours. Cells were then fixed in 4% paraformaldehyde prepared in PBS for 20 minutes at room temperature. The coverslips were washed twice in PBS and incubated further for 20 min in 0.25% Triton X-100 in PBS. Then coverslips were washed in PBS twice and apoptotic cells were visualized using the Click-iT TUNEL assay kit as per the manufacturer's instructions, with DAPI counter-stain. The percentage of apoptotic cells was counted on three low-power fields per coverslip using Image J software and analysed using GraphPad Prism software (v. 6.0).

4.3.7 *In vitro* scratch-wound assay

The assay was carried out as described in chapter 3 (Section 3.3.3).

4.3.8 *In vitro* Angiogenesis assay

A Matrigel based tube formation assay was performed to monitor the tube-formation ability of HRECs in the presence of compound as described in chapter 2 (Section 2.3.4).

4.3.9 Oxygen induced retinopathy (OIR) mouse model

All animal experiments were approved by the Indiana University School of Medicine Institutional Animal Care and Use Committee and adhered to all standards set forth in the Association for Research in Vision and Ophthalmology Statement for the Use of Animals in Ophthalmic and Vision Research. OIR in mice was induced as described (Smith et al., 1994). Briefly, newborn C57BL/6 mice pups along with nursing mother were incubated in a hyperoxia chamber (75% O₂) from postnatal day (P)7 to P12. On day P12, pups were anesthetized using isoflurane and 0.5 µL of vehicle/anti-VEGF/compound was intravitreally injected into each eye under a dissecting microscope. The final estimated concentration of anti-VEGF antibody and compound in the vitreous of each eye was 5 ng and 1 µM respectively. The experimenters were masked to the identity of the treatments throughout experimentation and data analysis. After the injections, pups along with the nursing mother were returned to normoxia (room air) conditions from P12 to P17. On day P17, pups were killed and the eyes were enucleated and fixed in 4% paraformaldehyde for 4 hours. Then retinas were isolated under a dissecting microscope. Retinas were washed twice in PBS and then permeabilized for 2 hours in 0.1% Triton X-100 in 10% goat serum prepared in PBS. Then 1:200 diluted isolectin B4-Alexa 488 in 10% goat serum was added to each retina and incubated overnight at room temperature protected from light. After the incubation, retinas were washed 4 times in PBS with each wash lasting for 15 minutes. Retinas were incised into four sections on a glass slide and mounted using Vectashield mounting medium. Using the LSM700 confocal

microscope, approximately 20 images were taken for each retina with a 10X objective and all of these images were stitched using Adobe Photoshop CS5. Retinal neovascularization was quantified as described (Smith et al., 1994) using Adobe Photoshop CS5 software.

4.3.10 Statistical analysis

The data obtained from all experiments were analyzed by one-way ANOVA with Dunnett's post hoc tests for comparisons between drug treatments and control. All analyses were performed using GraphPad Prism software (v.6.0). A p value of <0.05 was considered statistically significant in all tests.

4.4 RESULTS AND DISCUSSION

4.4.1. Biological Evaluation of A-ring Modified Homoisoflavanones

Our chemist collaborator synthesized a homoisoflavanone series modified on the A ring. Of these, the majority of synthetic compounds except cremastranone exhibited weak inhibitory activity of cell proliferation and poor selectivity for human microvascular retinal endothelial cells (HRECs) compared to macrovascular human umbilical vein endothelial cells (HUVECs) and human ocular tumor cell lines 92-1 (uveal melanoma) and Y79 (retinoblastoma) (Table 4.1). Cremastranone showed potent inhibitory activity of HREC and HUVEC proliferation, as discussed in chapter 3, whereas regioisomers with the different site-combinations of hydroxy and methoxy groups on the A ring had lower activity than the natural compound. Compounds **8** and **9** lost the inhibitory activity on

HREC cell proliferation, while homoisoflavanones **10** and **11** functionalized only with methoxy groups had good activity. Although compound **10** with trimethoxy on C5, C6 and C7 did not show stronger activity than cremastranone, it did show good selectivity for HRECs over other cell types including HUVECs. Thus, it was chosen as the starting point for further analogs in order to discover potent, microvascular endothelial-cell specific, antiangiogenic agents and to expand chemical space.

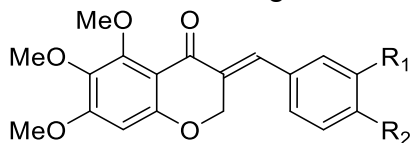
4.4.2. Biological Evaluation of B-ring Modified Homoisoflavanones

A series of homoisoflavanones modified on the B ring were evaluated (Table 4.2). Compared to the 3-benzyl-4-chromanones **10** and **11**, 3-benzylidene-4-chromanones **7b** and **7c** did not exhibit satisfactory activity against HRECs nor selectivity. On the other hand, 3-(3',4'-disubstituted-benzylidene)-4-chromanones (**7d~7h**) with a methoxy group at the C4' position had moderate anti-proliferative activity ($GI_{50} = 3\sim6\ \mu\text{M}$ for HRECs), although still lacked selectivity. 3-Benzylidene-4-chromanones substituted on either C2' or C4' had substantially decreased inhibitory activity on HREC proliferation. Additionally, the bulkier benzyl group at the C4 position led to lower activity than the hydroxyl or methoxy group (**7i** vs **7j**, **7k** vs **7l**).

Table 4.1 Growth inhibitory activity (GI_{50} , μM) of A-ring modified homoisoflavanones on the proliferation of microvascular (HREC), macrovascular (HUVEC) and ocular tumor (92-1 and Y79) Cells. 95% confidence interval shown in parentheses.

Cpd	A ring	HREC	HUVEC	92-1	Y79
1		0.22 (0.12 – 0.39)	0.38 (0.24 – 0.59)	48 (17 – 132)	9.8 (2.1 – 45)
2		45 (26 – 75)	18 (16 – 21)	10 (4.4 – 23)	>100
8		>100	>100	>100	>100
9		>100	44 (34 – 58)	>100	>100
10		2 (0.81 – 5.1)	12 (2.7 – 55)	>100	>100
11		1.6 (1.0 – 2.6)	2.5 (0.87 – 7.1)	>100	4.2 (2.0 – 9.1)

Table 4.2 Growth inhibitory activity (GI₅₀, μ M) of B-ring modified 3-benzylidene-4-chromanone analogs. 95% confidence interval shown in parentheses.

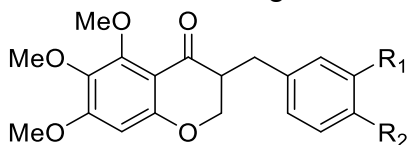


Cpd	B ring	HREC	HUVEC	92-1	Y79
7b		46 (17 – 122)	5.6 (3.2 – 9.8)	0.22 (0.061 – 0.81)	44 (22 – 89)
7c^a		42 (12 – 146)	15 (4.4 – 51)	>100	14 (7.2 – 25)
7d		4.3 (1.9 – 9.7)	16 (5.2 – 49)	3.5 (1.4 – 9.0)	33 (6.1 – 180)
7e		3.9 (1.9 – 8.1)	12 (7.6 – 18)	1.1 (0.34 – 3.6)	2.8 (1.5 – 5.1)
7f		4.8 (2.2 – 11)	15 (7.2 – 31)	12 (6.5 – 24)	2.2 (0.72 – 6.4)
7g		5.6 (2.6 – 12)	3.2 (1.4 – 7.3)	>100	6.1 (3.4 – 11)
7h		2.8 (1.1 – 7.1)	7.6 (3.2 – 18)	7.0 (1.9 – 26)	9.8 (4.1 – 23)
7i		3.3 (1.7 – 6.4)	6.2 (5.1 – 7.7)	26 (8.6 – 77)	5.2 (3.2 – 8.2)
7j		35 (14 – 83)	52 (27 – 100)	68 (25 – 186)	14 (8.7 – 24)
7k		7.6 (2.7 – 22)	5.0 (2.2 – 11)	9.5 (4.8 – 19)	4.0 (0.86 – 19)
7l		72 (18 – 277)	43 (9.1 – 204)	>100	32 (12 – 88)

a. 3-(3'-hydroxy-4'-methoxybenzylidene)-5,7-dimethoxychroman-4-one

In contrast to the 3-benzylidene-4-chromanones with a planar conformation, the freedom of rotation of 3-benzyl-4-chromanones might affect the selectivity for HRECs over human ocular tumor cell lines (Table 4.3). Mainly 3-benzyl-4-chromanones bearing methoxy on C4' of the B ring were evaluated along with **12a**, which shows little antiproliferative activity. Aniline **12b** showed excellent antiproliferative activity, but ester **12c** and acid **12d** showed little or no antiproliferative activity. Benzyl (**12e**) and carbamoyl (**12i**) compounds were found to be weak growth inhibitors. Interestingly, introduction of acyl groups such as benzoyl (**12f**), cinnamoyl (**12g**) and dihydrocinnamoyl (**12h**) strongly increased activity with GI₅₀ values of 0.14~0.65 μ M for HRECs. Moreover **12f~12h** were selective for HREC inhibition over HUVECs, Y79, and 92-1 cells. The antiproliferative activities were obviously dependent on the substitution pattern of the B ring.

Table 4.3 Growth inhibitory activity (GI_{50} , μM) of B-ring modified 3-benzyl-4-chromanone analogs. 95% confidence interval shown in parentheses.



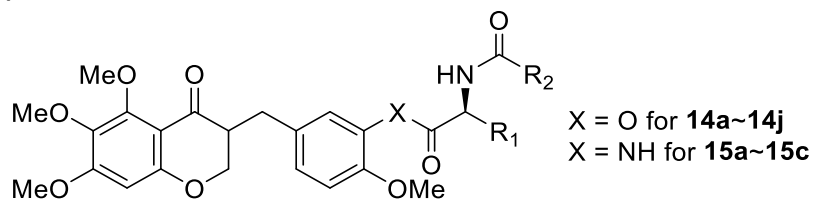
Cpd	B ring	HREC	HUVEC	92-1	Y79
12a		>100	>100	>100	>100
12b		1.1 (0.29 – 4.4)	0.51 (0.11 – 25)	>100	>100
12c		18 (6.1 – 50)	17 (5.1 – 57)	>100	40 (24 – 66)
12d		>100	92 (27 – 317)	>100	>100
12e		22 (13 – 40)	>100	61 (14 – 278)	20 (8.1 – 51)
12f		0.65 (0.26 – 1.6)	>100	>100	>100
12g		0.17 (0.030 – 0.97)	>100	>100	>100
12h		0.22 (0.064 – 0.77)	38 (13 – 109)	>100	>100
12i		49 (17 – 141)	>100	>100	24 (6.1 – 97)

a. *CIN*: cinnamoyl, *DCI*: dihydrocinnamoyl, *DEC*: *N,N*-diethylcarbamoyl.

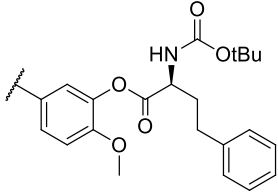
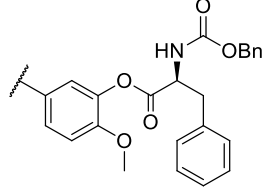
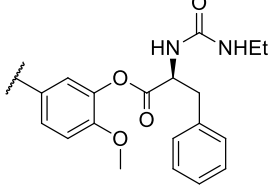
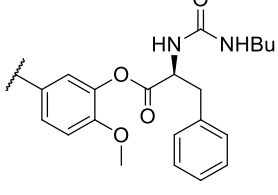
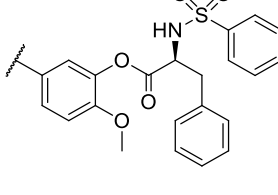
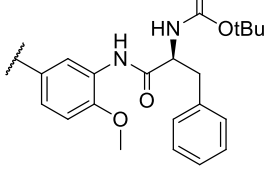
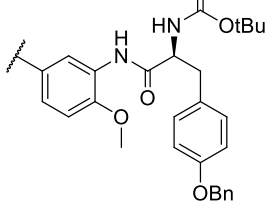
4.4.3. Biological Evaluation of Homoisoflavanones Coupled with Amino Acids on the C3' position

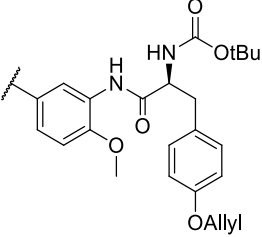
Encouraged by the potent activity of aryl esters (**12f~12h**), phenol **10** and aniline **12b** were coupled with some *N*-protected amino acids to obtain the ester (**14a~14j**) and amide (**15a-15c**) analogs, respectively. Interestingly, **14a** (also called **SH-11037**) which was given by coupling **10** with Boc-Phe-OH showed the most potent activity with $GI_{50} = 55$ nM against HRECs (Table 4.4; Figure 4.2A). Moreover **14a** selectively inhibited HREC proliferation about 14-fold over HUVECs, 218-fold over Y79, and >1000-fold over 92-1, suggestive of cytostatic effects on HRECs rather than general cytotoxicity. The analogs (**14b** and **14c**) for which **10** was coupled with Boc-Tyr(Bn)-OH and Boc-Tyr(Allyl)-OH had similar activity to **14a**, potentially indicating that a bulkier (or longer) chemical spacer to the phenyl ring of the phenylalaninyl moiety is not detrimental to potency. An isoleucinyl analog (**14d**) had lower antiproliferative activity, whereas analogs (**14e**, **14f** and **14g**) generated with Boc-Leu-OH, Boc-homophe-OH and Cbz-Phe-OH have more preferable activity and selectivity to cremastranone. The antiproliferative activity of ethylurea (**14i**), butylurea (**14j**) and sulfonamide (**14j**) analogs was not improved. Noteworthy, the inhibition of HREC proliferation with *N*-arylamide analogs (**15a~15c**) decreased substantially, compared with the corresponding phenyl ester analogs (**14a~14c**). Conversely, *N*-arylamide analogs were considered to be moderate inhibitors against 92-1 and Y79 cells rather than antiangiogenic compounds.

Table 4.4 Growth inhibitory activity (GI₅₀, μ M) of homoisoflavonoids comprising amino acids on the C3' position of the B-ring. 95% confidence interval shown in parentheses.



Cpd	B ring	HREC	HUVEC	92-1	Y79
14a (SH-110 37)		0.055 (0.032 – 0.094)	0.75 (0.37 – 1.5)	>100	12 (5.7 – 25)
14b		0.51 (0.26 – 1.0)	>100	>100	>100
14c		0.16 (0.020 – 1.3)	0.091 (0.013 – 0.63)	>100	52 (17 – 166)
14d		3.1 (1.3 – 7.4)	>100	>100	24 (7.1 – 79)
14e		0.13 (0.026 – 0.69)	>100	>100	>100

14f		0.17 (0.035 – 0.82)	>100	>100	>100
14g		0.14 (0.027 – 0.73)	>100	>100	>100
14h		1.0 (0.031 – 3.6)	34 (7.2 – 165)	98 (37 – 265)	48 (33 – 69)
14i		1.4 (0.73 – 2.4)	>100	>100	64 (26 – 158)
14j		1.5 (0.41 – 5.4)	22 (11 – 43)	>100	>100
15a		22 (16 – 32)	8.6 (1.2 – 6.1)	3.1 (0.93 – 10)	4.7 (1.2 – 18)
15b		>100	>100	>100	0.39 (0.12 – 1.3)

15c		13 (9.7 – 17)	4.5 (1.2 – 17)	1.9 (0.65 – 5.3)	2.5 (1.4 – 4.6)
------------	---	------------------	-------------------	---------------------	--------------------

a. *PB*: *p*-benzyloxybenzyl, *PA*: *p*-allyloxybenzyl, *PT*: *p*-(*tert*-butoxy)benzyl.

4.4.4. Validation of a Potent Cremastranone Derivative In Vitro

In alamarBlue proliferation assays, **14a** (SH-11037) had the highest potency of any compound tested. In addition, it was more potent and endothelial-cell specific than previously described antiangiogenic homoisoflavonoids (Falkenstein et al., 2008; Hasebe et al., 2003; Ivanova et al., 2013; Lee et al., 2014a). Given this, I tested it in a secondary cell proliferation assay, which monitors the incorporation of a thymidine analogue 5-ethynyl-2'-deoxyuridine into DNA of proliferating HRECs. Here, I confirmed the dose-dependent inhibition of HREC proliferation by **14a** (Fig. 4.2a).

After establishing the antiproliferative activity of this promising lead, we further tested its antiangiogenic activities in vitro. First we monitored the migration of HRECs, testing this important property of endothelial cells during blood vessel formation in the presence of **14a** in a scratch wound assay (Fig. 4.2B). **14a** blocked the ability of HRECs to migrate in a dose dependent manner. Then we tested the ability of HRECs to form tubes in the presence of **14a** in a Matrigel tube formation assay, an in vitro assay that recapitulates most of the events of physiological angiogenesis such as migration, proliferation, and cell-cell adhesion. **14a** inhibited the tube formation ability of HRECs in the Matrigel assay at sub micromolar concentrations (Fig. 4.2C). Although **14a** did not induce changes in cell morphology in these assays, since the compound was so potent in inhibiting tube formation, we tested if **14a** induces apoptosis in HRECs. We employed both activated caspase (Fig. 4.2D) and TUNEL assays (Fig. 4.5) to

monitor the apoptosis of HREC cells in the presence of different concentrations of **14a**. We observed less than 10% HREC cells undergoing apoptosis treated with up to 2 μ M **14a**, indicating that the compound may not be cytotoxic at effective concentrations. Furthermore, a trypan blue exclusion assay (Fig. 4.6) confirmed that treated HREC cells retained viability, further implicating a cytostatic rather than cytotoxic mechanism for this compound. This finding was further supported by analysis of the cell cycle profile (Fig. 4.4) in HREC cells treated with **14a**, which revealed a dose-dependent G₂/M phase blockade with few sub-G₀ cells as documented previously for cremastranone. These results established that **14a** is a potent inhibitor of angiogenesis in vitro.

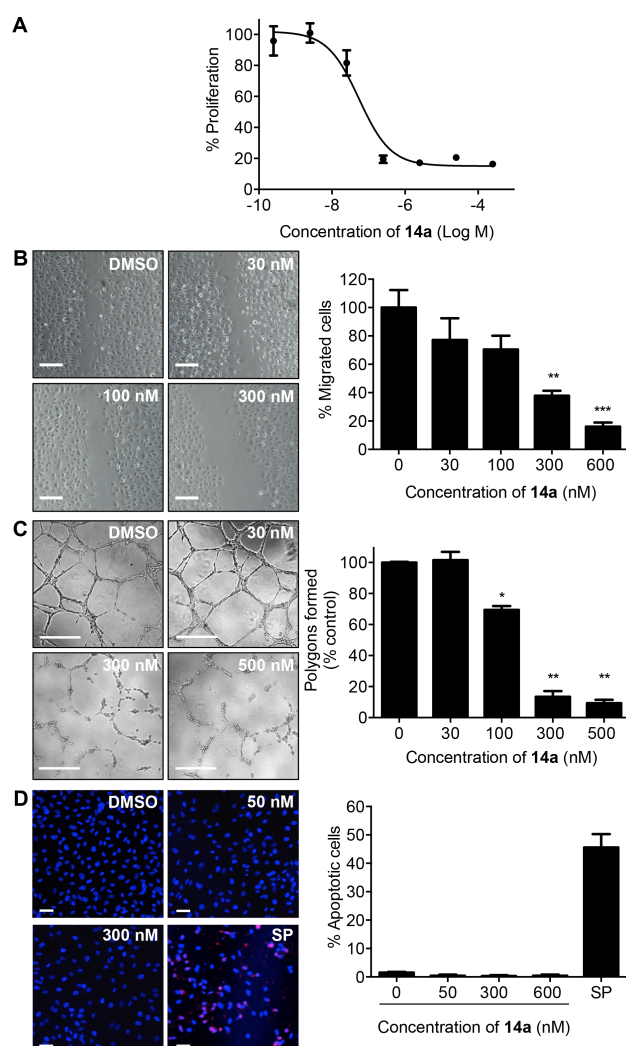


Figure 4.2. Compound 14a (SH-11037) inhibits angiogenic behavior of HRECs in vitro. (A) Dose-response of the effects of **14a** on HREC proliferation as measured by alamarBlue fluorescence. (B) **14a** dose-dependently inhibits migration of HRECs in a scratch-wound assay. (C) **14a** dose-dependently inhibits tube formation of HRECs on Matrigel. (D) **14a** caused negligible apoptosis as assayed by activated caspase 3 (*pink*) immunofluorescence. 1 μ M staurosporine (SP) is positive control. DAPI (*blue*) indicates normal nuclear morphology. Error bars indicate SEM, n=3, representative results from at least triplicate experiments. *P<0.05, **P<0.01 and ***P<0.001. Scale bars = 200 μ m.

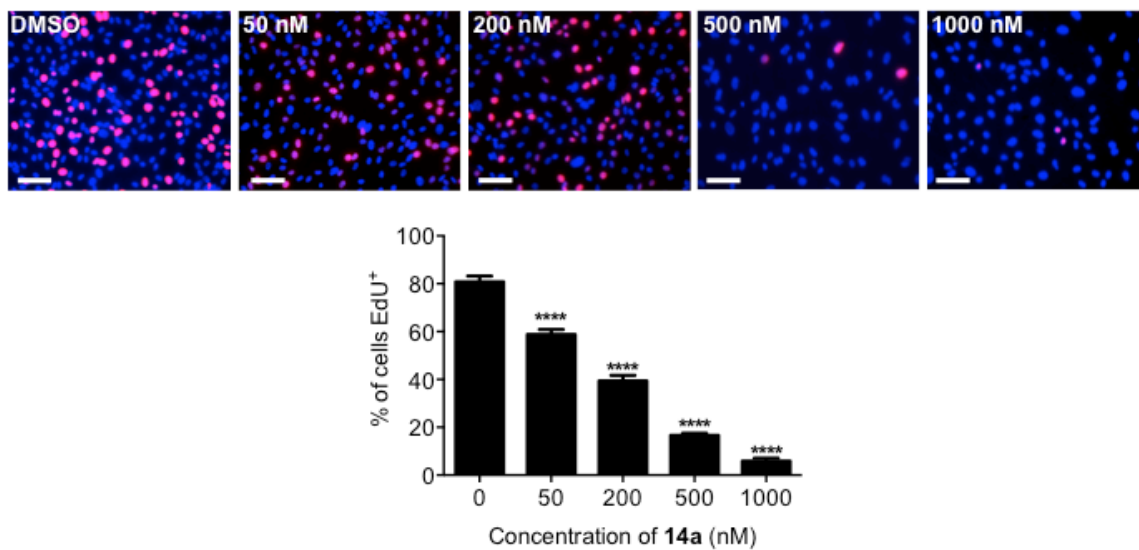


Figure 4.3. Compound 14a (SH-11037) inhibits in vitro proliferation of HRECs as measured by EdU incorporation assay. The nuclei of all cells are labelled with DAPI (blue) and actively dividing cells are labelled with EdU (pink). Error bars indicate SEM, $n = 3$, representative results from at least triplicate experiments. **** $P < 0.0001$.

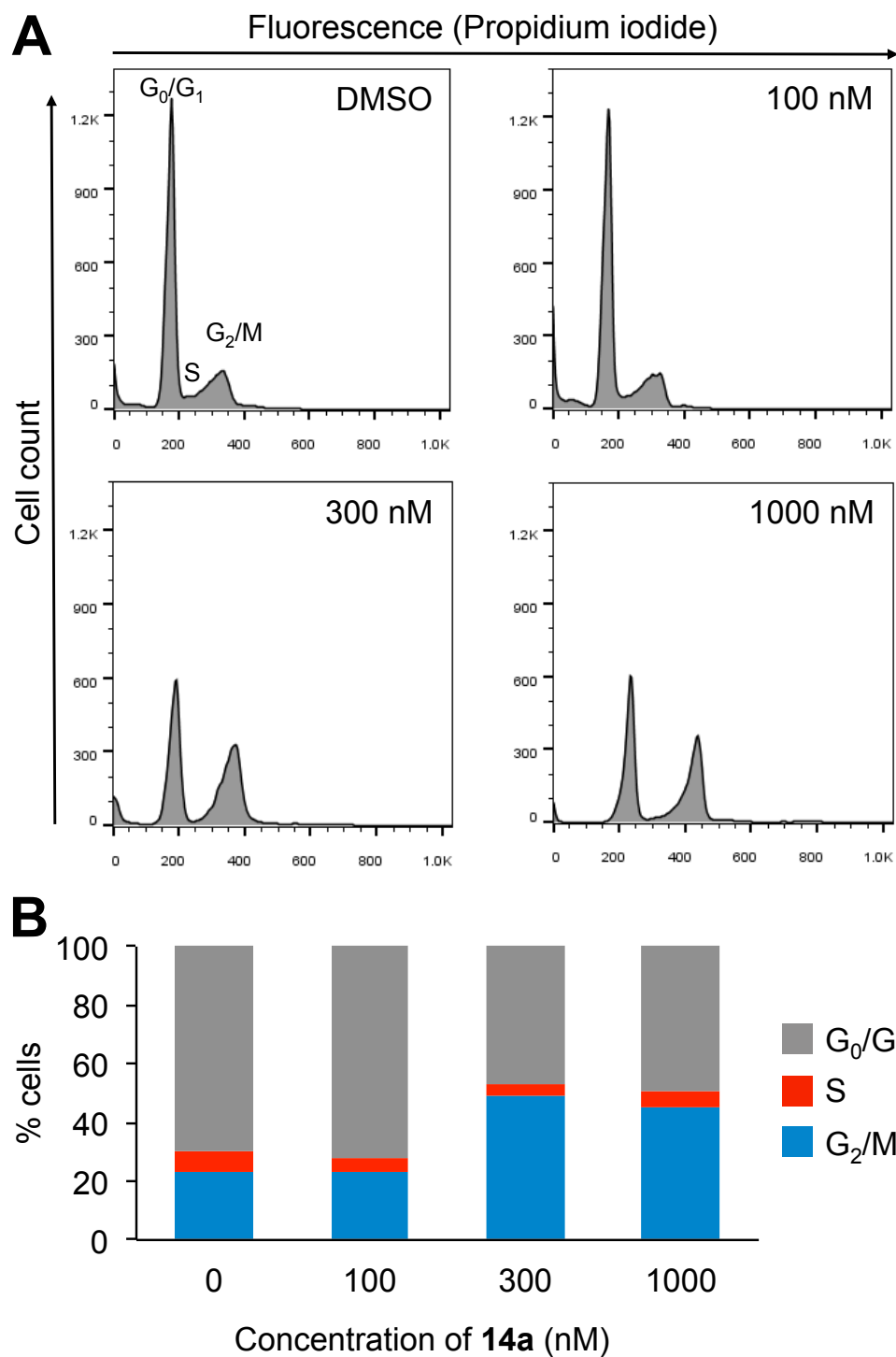


Figure 4.4. Compound 14a (SH-11037) arrests HRECs at G₂/M cell cycle stage as monitored in propidium iodide based flow cytometry assay.

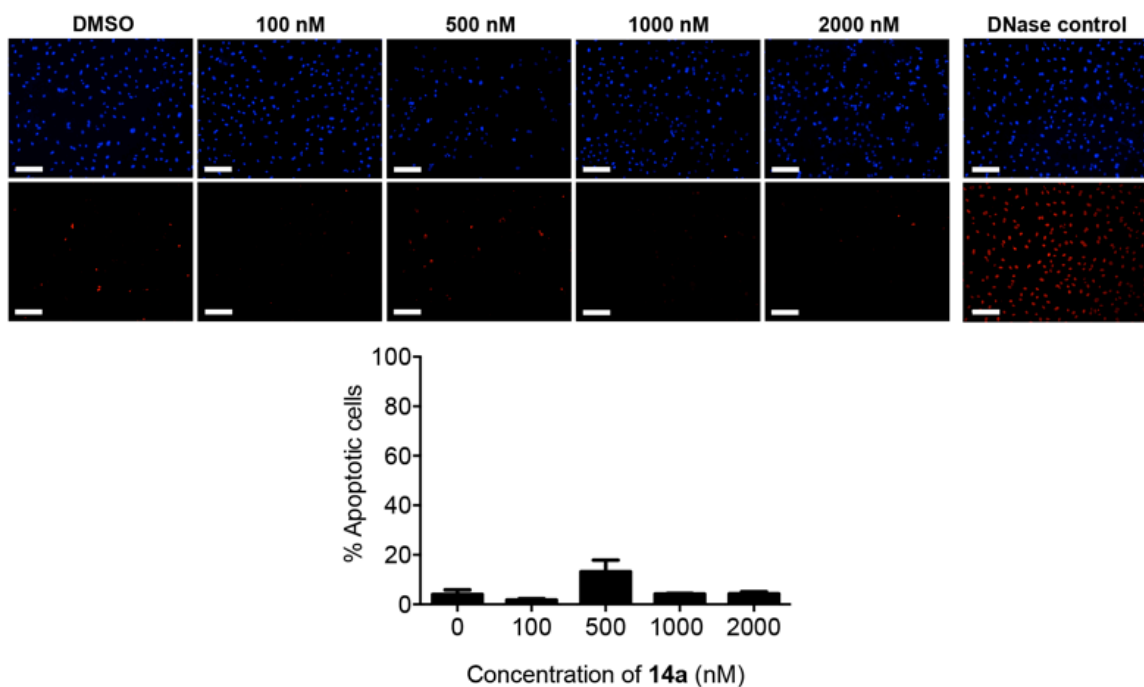


Figure 4.5. Compound 14a does not induce apoptosis significantly, as evidenced by TUNEL assay. The nuclei of all cells are shown in blue (DAPI staining) and TUNEL⁺ cells undergoing apoptosis are shown in red. Error bars indicate SEM, $n = 3$, representative results from at least triplicate experiments. Scale bars = 200 μm .

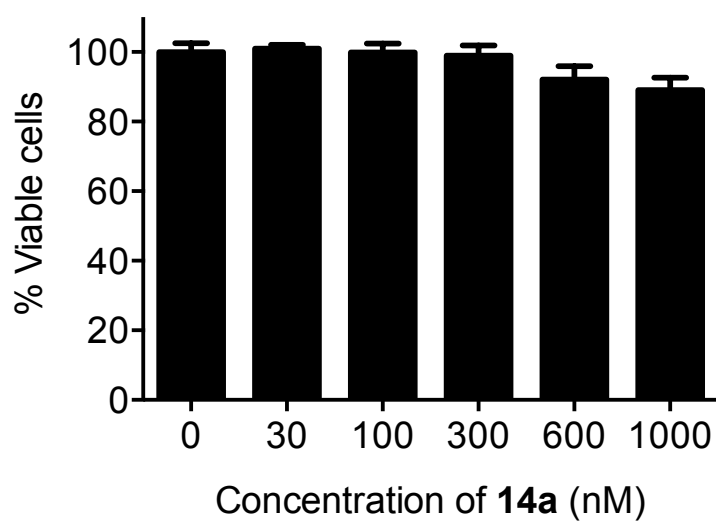


Figure 4.6. Viability of HRECs is not significantly altered by compound **14a** as monitored in Trypan blue exclusion assays. Error bars indicate SEM, $n = 3$, representative results from triplicate experiments.

4.4.5. In vivo efficacy of a Potent Cremastranone Derivative

After establishing antiangiogenic activity of **14a** in vitro, we next explored the in vivo efficacy of this compound in preventing neovascularization in the OIR mouse model. Intravitreal injection of **14a** to a final concentration of 1 μ M in each eye significantly inhibited retinal neovascularization in OIR mice as compared to vehicle. Moreover, efficacy of the compound in vivo was similar to that observed with standard-of-care anti-VEGF antibody treatment (Fig. 4.7). We did not observe any overt systemic or ocular toxicity in mice treated with **14a**, or gross morphological changes in the retinal vasculature. However, more extensive toxicological assessment of **14a** remains to be done.

The in vivo antiangiogenic activity of **14a** observed here provides evidence that novel synthetic homoisoflavonoids that show potent and selective antiangiogenic activity in vitro can be used as lead molecules to develop drugs for treatment of ocular diseases arising from pathological angiogenesis.

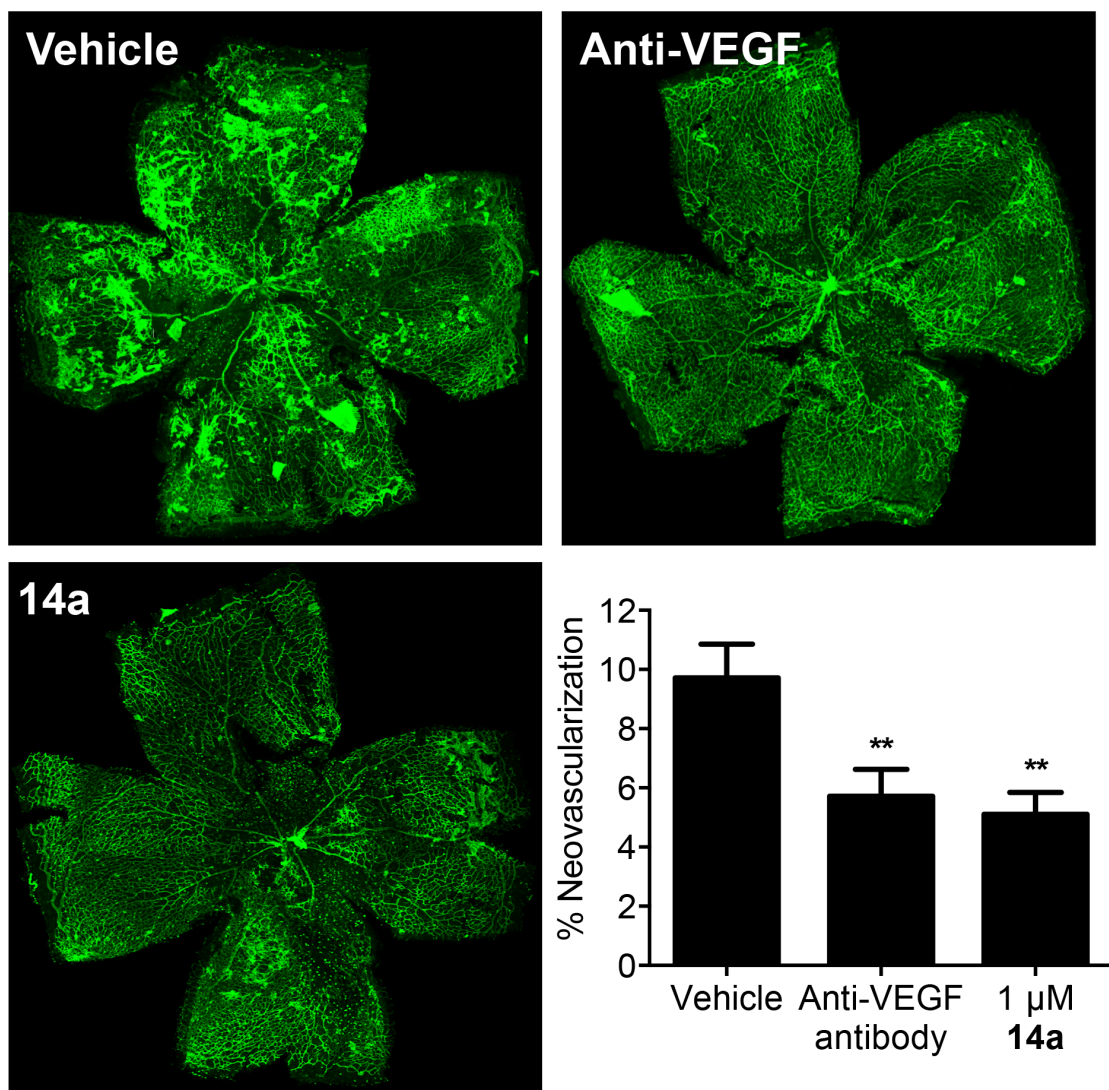


Figure 4.7. Homoisoflavonoid 14a (SH-11037) inhibits retinal neovascularization in the OIR mouse model. Retinal whole mounts from treated mice were stained for blood vessels using Alexa-488-conjugated isolectin and imaged by confocal microscopy; neovascular area was measured using Adobe Photoshop. Error bars indicate SEM, n=6. **P<0.01 vs. vehicle, ANOVA with Dunnett's post hoc tests. Dr. Rajashekar Gangaraju performed intravitreal injections and Alexandra Vayl maintained the animals in the oxygen chamber.

4.5. CONCLUSION

We synthesized a series of homoisoflavonoids from chroman-4-ones, including successfully synthesizing the natural product cremastranone. Antiproliferative compounds with endothelial cell specificity, with a homoisoflavonoid-based scaffold, were developed as potent inhibitors of angiogenesis. The scaffold is sensitive to changes on the substituents on both the A and B rings. Exploring modification at the C3' position revealed that addition of *N*-carbamate amino acids improved inhibitory activity on HREC proliferation. The most potent phenylalanyl-incorporated **14a** showed improved activity and remarkable selectivity for retinal microvascular endothelial cells, with antiangiogenic efficacy in vitro and in the oxygen-induced retinopathy model in vivo.

Now it is very well established that synthetic cremastranone shows similar biological activity to that of its natural counterpart and it can be synthesized in scalable quantities for use in mechanistic studies. Also, during SAR studies potential sites for conjugating the cremastranone analogues to linker-biotin complex have been identified. Using this knowledge, affinity reagents could be synthesized and used in pull-down experiments to identify the cremastranone binding proteins as described in the next chapter.

CHAPTER 5. FERROCHELATASE IS A THERAPEUTIC TARGET FOR OCULAR NEOVASCULARIZATION.

[This chapter forms the following submitted manuscript:

Halesha D. Basavarajappa, Rania S. Sulaiman, Xiaoping Qi, Bit Lee, Judith Quigley, Kamakshi L. Sishtla, Sameerah Alkhairy, Kamna Gupta, Buyun Tang, Mehdi Shadmand, Maria B. Grant, Michael E. Boulton, Seung-Yong Seo & Timothy W. Corson. Ferrochelatase is a therapeutic target for ocular neovascularization, submitted].

5.1. CHAPTER SUMMARY

Using a forward chemical genetic approach to find targets of cremastranone, we identified the heme synthesis enzyme ferrochelatase (FECH) as necessary for angiogenesis in vitro and in vivo. FECH is overexpressed in wet AMD eyes and murine choroidal neovascularization; knockdown modulates endothelial nitric oxide synthase function and VEGF receptor levels. FECH is inhibited by the approved oral antifungal drug griseofulvin, and this compound ameliorated choroidal neovascularization in mice when delivered intravitreally or orally. Thus, FECH inhibition could be used therapeutically to block ocular neovascularization.

5.2. INTRODUCTION

To uncover novel, potentially druggable angiogenesis mediators, here we took a forward chemical genetic approach to find protein targets of an antiangiogenic natural product (Sulaiman et al., 2014), cremastranone (Chapter 3; Kim et al., 2007; Kim et al., 2008; Lee et al., 2014a; Shim et al., 2004). I identified ferrochelatase (FECH) as a target of this compound, and show that it is necessary for angiogenesis in vitro and in vivo and targetable with an FDA-approved small molecule therapeutic. FECH is the terminal enzyme in heme biosynthesis, responsible for catalyzing the insertion of Fe^{2+} ion into protoporphyrin IX (PPIX) (Hamza and Dailey, 2012). To my knowledge, I describe here for the first time FECH's role as a druggable mediator of angiogenesis.

5.3. MATERIALS AND METHODS

5.3.1. *Materials*

Details regarding the cell culture conditions, TUNEL assay reagents, Alamar blue assay, EdU Incorporation assay, in vitro matrigel assay and qRT-PCR materials are already described in chapter 2 (Section 2.3.1). Monoclonal antibody against α -tubulin (DM1A), actin (AC40), protoporphyrin IX, 5-aminolevulinic acid, hemin, hemin agarose beads, griseofulvin and L-arginine were purchased from Sigma-Aldrich (St. Louis, MO, USA). *N*-methyl protoporphyrin (NMPP), the primary antibodies against FECH (A-3) and PDXK (F-12) were obtained from Santa Cruz (Santa Cruz, CA, USA). Antibodies against cleaved caspase 3 (5A1E), phospho-VEGFR2 (Tyr 1175) (19A10), phospho-eIF2 α (Ser 51) (119A11), eIF2 α and eNOS (49G3) were from Cell Signaling (Danvers, MA, USA). Anti-HIF-1 α (241809) antibodies were purchased from R&D systems (Minneapolis, MN, USA). Secondary antibodies were from Thermo Fisher Scientific (Pittsburgh, PA, USA). 4,5-Diaminofluorescein diacetate (DAF-2 diacetate) was purchased from Cayman Chemicals (Ann Arbor, MI, USA). ECL Prime Western Blotting Detection reagent was purchased from GE Healthcare (Buckinghamshire, UK).

5.3.2. *Preparation of photoaffinity reagents*

Synthesis and characterization of affinity reagents **16** and **17** will be reported elsewhere (Lee et al., submitted). Compounds **1** and **4** were synthesized as described (Chapters 2 and 3). For pulldowns, Neutravidin

agarose beads (1 mL of 50 % slurry) were washed three times in buffer A containing 25 mM Tris-HCl pH 7.4, 150 mM NaCl, 2.5 mM sodium pyrophosphate, 1 mM phenylmethylsulfonyl fluoride (PMSF), 0.1 mM sodium orthovanadate, 10 µg/mL aprotinin and 10 µg/mL leupeptin. The beads were then incubated with 100 µM affinity or control reagents **16** or **17** overnight at 4°C with rotation. The beads were blocked using 1 mM biotin solution prepared in buffer A for 1 hour followed by incubation with 1 mg/mL cytochrome c solution for 1 hour at 4°C. The beads were then washed three times with buffer A and resuspended in 1 mL.

5.3.3. Photoaffinity pull down experiments

Flash-frozen porcine brain (20 g) obtained from the Purdue-Indiana University School of Medicine Comparative Medicine Program was homogenized in 50 mL Buffer A using a tissue homogenizer. The homogenate was centrifuged at 2000×g for 5 minutes. The supernatant (S1) was then dounced 50 times followed by 10 min sonication with amplitude of 60% in cycles of 10 sec sonication on and 40 sec sonication off (Q125 from QSonica, Newtown, CT, USA). The lysate was then centrifuged at 11,000×g for 30 min. The resulting supernatant (S2) and pellet (P2) fractions were both collected. The P2 pellet was resuspended in buffer B: 1% Triton X-100 + buffer A and then dounced 25 times and centrifuged at 11,000×g for 30 min; supernatant (S3) was collected. Both S2 and S3 supernatants were equally divided and each fraction was incubated with 500 µL photoaffinity or control reagent conjugated to Neutravidin beads for 75 min at 4°C with shaking.

The beads were collected by centrifugation at 500×g for 5 min, then resuspended in 1 mL of buffer B and irradiated with 365 nm UV light (Mercury bulb H44GS100 from Sylvania in a Blak-Ray 100A long-wave UV lamp) in a 60 mm Petri dish for 30 min at 4°C. The beads were then washed two times in buffer B, followed by three washes in high-salt buffer containing 25 mM Tris-HCl pH 7.4, 350 mM NaCl, 1% Triton X-100 and 1 mM PMSF. The beads were then washed again in salt-free buffer containing 25 mM Tris-HCl, 1% Triton X-100 and 1 mM PMSF. After 5 min incubation, the beads were collected and any residual liquid was removed using a Hamilton syringe. The Neutravidin beads were then boiled in 300 µL of 2× SDS-PAGE gel loading dye containing 30 µL of 2-mercaptoethanol for 10 min at 70°C to release the bound proteins. After boiling, the contents were allowed to cool and after a quick spin the eluate was collected using a Hamilton syringe. The eluates were then analyzed in 4–20% gradient SDS-PAGE and the protein bands were visualized using silver staining (Corson et al., 2011). The protein bands pulled down specifically by photo-affinity reagent were excised from the silver stained SDS-PAGE gel and analyzed by mass spectrometry (IUSM Proteomics Core). Using SequestTM algorithms and the swine database (UniProt), the identities of the pulled down proteins were confirmed (Fig. 5.2).

For competition experiments, S2 and S3 supernatants were incubated with affinity reagent-Neutravidin beads in the presence of 1 mM of cremastranone isomer SH-11052 (**2**) (Chapter 2) and then processed as described above.

5.3.4. Recombinant FECH

Recombinant human FECH protein was purified as described previously (Dailey et al., 1994). Briefly, *Escherichia coli* JM109 cells transformed with plasmid pHDTF20 encoding recombinant human FECH were grown in Circlegrow medium containing 100 µg/mL ampicillin for 20 hours at 30°C. The cells were harvested and resuspended in solubilization buffer (50 mM Tris-MOPS pH 8.0, 1% sodium deoxycholate, 100 mM KCl and 1 mM PMSF). The cell suspension was sonicated and then ultracentrifuged at 45000xg for 30 min. The supernatant was subjected to cobalt-affinity chromatography and the column was washed with solubilization buffer containing 20 mM imidazole. The protein was eluted with 250 mM imidazole in solubilization buffer. The protein eluate was then dialyzed in solubilization buffer containing 10% glycerol before storage at 4°C. Recombinant protein (200 µg) was used in pulldown experiments as above.

5.3.5. Immunoblot assay

Immunoblots were performed as described previously in chapter 2 (Section 2.3.9). Proteins were immunoblotted with antibodies against FECH (1:1000 dilution), α -tubulin (1:1000 dilution), phospho-VEGFR2 (1: 500), VEGFR2 (1:500), phospho-eIF2 α (1:500), eIF2 α (1:500), HIF-1 α (1:500), actin (1:1000) and eNOS (1:500 dilution). All of the dilutions were made in Tris Buffered Saline-0.05% Tween-20 buffer containing 2% bovine serum albumin (BSA).

5.3.6. siRNA knock down of FECH in cells

Cells were grown in 6-well plates until 80% confluency was achieved. Then 7.5 μ L of Lipofectamine RNAiMAX reagent (Life Technologies) mixed with 30 pmol of siRNAs was added to each well according to the protocol recommended by the manufacturer. For *FECH* knockdown, 15 pmol each of two siRNAs (SASI_Hs01_00052189 and SASI_Hs01_00052190; Sigma) and for PDXK knockdown, 30 pmol of siRNA (SASI_Hs01_00053806) were used and for negative control, MISSION[®] siRNA Universal negative control was used. Fresh EGM-2 medium was added to the plate 24 hours after transfection and cells were used 48 hours after transfection for further experiments except for the proliferation time course, for which 24 hours after transfection the cells were trypsinized and seeded in a 96-well plate.

5.3.7. Cell proliferation assay

Proliferation of cells was monitored as described in chapter 2 (Section 2.3.2). The concentration ranges of griseofulvin and NMPP used were 0.5 nM – 500 μ M and 0.1 nM – 100 μ M respectively.

5.3.8. Migration assay

The migration of HRECs was monitored as described in chapter 4 (Section 4.3.7).

5.3.9. *In vitro* Matrigel tube formation assay

The ability of HRECs to form tubes in vitro was monitored as described in chapter 2 (Section 2.3.4).

5.3.10. *Animals*

All animal experiments were approved by the Indiana University School of Medicine Institutional Animal Care and Use Committee and followed the guidelines of the Association for Research in Vision and Ophthalmology Statement for the Use of Animals in Ophthalmic and Visual Research. Wild-type female C57BL/6J mice, 6–8 weeks of age or timed pregnancies, were purchased from Jackson Laboratory (Bar Harbor, ME) and housed under standard conditions (Wenzel et al., 2015). Mice were anesthetized for all procedures by intraperitoneal injections of 17.5 mg/kg ketamine hydrochloride and 2.5 mg/kg xylazine.

5.3.11. *L-CNV model*

L-CNV was generated as described previously (Lambert et al., 2013; Poor et al., 2014; Sulaiman et al., 2015). Briefly, eyes were dilated using 1% tropicamide, then underwent laser treatment using 50 μ m spot size, 50 ms duration, and 250 mW pulses of an ophthalmic argon green laser, wavelength 532 nm, coupled to a slit lamp. Where indicated, intravitreal injections of PBS vehicle, siRNA (1.25 μ M final intravitreal concentrations) or griseofulvin (50 μ M, 100 μ M, final intravitreal concentrations) were given in a 0.5 μ L volume at time of

laser treatment. Eyes were numbed with tetracaine solution before the injection, and triple antibiotic ointment was used immediately after the injection to prevent infection. A masked researcher undertook imaging and analysis to avoid bias. One week after laser treatment, mice underwent optical coherence tomography using a Micron III imager (Phoenix Research Labs, Pleasanton, CA, USA) and CNV lesions were quantified as ellipsoids as described (Sulaiman et al., 2015). Two weeks after laser treatment, eyes were enucleated and fixed, choroidal flatmounts prepared, and vasculature stained with rhodamine labeled *Ricinus communis* agglutinin I (Vector Labs, Burlingame, CA, USA), followed by confocal Z-stack imaging (LSM 700, Zeiss, Thornwood, NY, USA) to estimate lesion volume.

5.3.12. Immunostaining

Human donor eyes were obtained from the National Disease Research Interchange (Philadelphia, PA) with full ethical approval for use in research. Mouse eyes were post induced laser-CNV for 14 days. The eyes were enucleated and fixed in 4% paraformaldehyde/PBS overnight. The anterior segment, lens, and vitreous were removed and the posterior eye cups were prepared for standard paraffin sections or retinal flat mounts. Deparaffinized sections were treated with rodent deblocker (Biocare Medical, Concord, CA, USA) for antigen retrieval. The sections or flat mounts were washed with PBS then permeabilized with 0.3% Triton X-100 and nonspecific binding blocked by 10% normal goat serum plus 1% BSA in PBS. They then received primary antibody (polyclonal anti-FECH (C20, Santa Cruz) at 1:500 for 16 hours at 4°C.

After primary incubation, tissues were washed and incubated for 1.5 hours at room temperature with secondary antibody (Cy3 conjugated goat anti-rabbit IgG, 1:600) at 4°C with 0.1% Triton X-100. We used a vascular specific dye (Ricinus Communis Agglutinin I; Vector Laboratories, Inc.) conjugated to AlexaFluor 488 to label retinal vasculature. This was incubated for 30 minutes at room temperature in 1:400 of 10 mM HEPES plus 150 mM NaCl and 0.1% Tween-20. After washing, specimens were mounted in aqueous mounting medium (VectaShield; Vector Laboratories, Inc.) and coverslipped for observation by confocal microscopy. All microscopic images were acquired with identical exposure settings.

5.3.13. Choroidal sprouting assay

Choroidal sprouting was assessed as described (Sulaiman et al., 2016). Briefly, pieces of choroid-sclera dissected from euthanized mouse eyes were embedded in Matrigel and grown in EGM-2 medium plus antibiotics for 72 hours to allow sprouting to initiate. The indicated concentrations of griseofulvin (in DMSO, final DMSO concentration 1%) were added and growth allowed to proceed for 48 hours. Images were taken and growth quantified by measuring distance from the edge of the choroidal piece to the growth front in 4 directions per sample.

5.3.14. Griseofulvin Feeding

Mice were fed griseofulvin for a total of 3 weeks, with chow changed every 2-3 days. Standard mouse chow (5 g/mouse/day) was mixed in water (2.2 mL H₂O/gram chow), soaked for 15 min, then mashed. Griseofulvin doses were prepared at 0.0% (control), 0.5%, and 1.0% with 0.0 g, 0.5 g, and 1.0 g griseofulvin : 10 mL corn oil : 100 g mouse chow ratio, respectively. Both 0.5% and 1.0% doses were expected to substantially inhibit FeCh and induce a protoporphyria-like phenotype, based on previously published work (Holley et al., 1990; Lochhead et al., 1967; Martinez et al., 2009). The corn oil solutions and mouse chow mixture were manually mixed thoroughly for 10 min. During treatment, the mice were examined and weighed 3 times/week (Fig. 5.11a). On Day 8, mice underwent L-CNV as above, and were imaged by OCT at Day 15 and Day 22, at which time they were euthanized. The eyes were enucleated and flatmounts prepared as above. The livers were dissected out and weighed (Fig. 5.11b).

5.3.15. eNOS assay

eNOS activity was measured in cells as described before (Räthel et al., 2003). Briefly, HRECs (10,000 cells/well) were seeded in 96-well clear bottom black plates and incubated for 24 hours at 37°C and 5% CO₂. Then cells were washed with PBS and incubated for 5 min at 37°C with 100 µL of 100 µM L-arginine prepared in PBS. Subsequently, 100 nM of DAF-2 diacetate was added

to each well and fluorescence readings were taken at excitation and emission wavelengths of 495 nm and 515 nm respectively using the Synergy plate reader.

5.3.16. Hemin pulldown

HRECs were grown in EGM-2 medium in 10 cm plates until ~50% confluent. Cells were then treated with 10 μ M NMPP or DMSO control for 1 week. Medium was changed every 2 days with treatments added to the fresh medium every time. Cells were then lysed with NP-40 lysis buffer containing (20 mM Tris, pH 8.0, 150 mM NaCl, 1% NP-40, 20 μ M leupeptin, 1 mM PMSF, 1 mM NaF, 1 mM β -glycerophosphate, 2 mM sodium orthovanadate, 2 mM EDTA, 10% glycerol) and then centrifuged at 14,000 \times *g* for 10 min at 4°C. Supernatant was collected and samples were pre-cleared by incubation with Neutravidin beads for 1 hour at 4°C followed by centrifugation at 500 \times *g* for 5 min at 4°C. supernatant was then collected and protein concentration was determined using a Bradford assay. Equal amounts of total protein (40 μ g) from each sample were incubated with ~ 50 μ l hemin agarose beads, pre-washed 3 times with lysis buffer, for 1 hour at 4°C.

The beads were then washed two times in NP-40 buffer, followed by two washes in high-salt buffer containing 20 mM Tris-HCl pH 8.0, 350 mM NaCl, and 1 mM PMSF. The beads were then washed once with a very high-salt buffer containing 20 mM Tris-HCl pH 8.0, 500 mM NaCl, and 1 mM PMSF. The beads were then washed again in salt-free buffer containing 20 mM Tris-HCl and 1 mM PMSF. After 5 min incubation, the beads were collected and any residual liquid

was removed using a Hamilton syringe. The hemin agarose beads were then boiled in 30 μ L of 2 \times SDS-PAGE gel loading dye containing 30 μ L of 2-mercaptoethanol for 10 min at 70°C to release the bound proteins. After boiling, the contents were allowed to cool and after a quick spin the eluate was collected using a Hamilton syringe. The eluates were then analyzed in 4–20% gradient SDS-PAGE and then transferred onto PVDF membranes. Proteins were immunoblotted with antibodies against α -tubulin (1:1000 dilution) and eNOS (1:500 dilution). All of the dilutions were made in Tris Buffered Saline-0.05% Tween-20 buffer containing 2% bovine serum albumin (BSA).

5.3.17. PPIX build-up assay

HRECs were grown in a 6-well plate until confluent. Then cells were serum starved overnight in EBM-2 medium. Fresh EGM-2 medium containing DMSO or compounds was added to cells and they were incubated at 37°C for 1 hour followed by addition of 1 mM 5-ALA to increase flux through the heme biosynthetic pathway. After 3 hours of incubation in the dark at 37°C the cells were trypsinized and lysed in buffer containing 25 mM HEPES-NaOH pH 7.4, 150 mM NaCl, 1% NP-40, 10% glycerol and 1 mM PMSF. The cell lysates were incubated in the dark at 4°C for 20 min on a shaker and centrifuged at 12000 $\times g$ for 15 min. Supernatants were collected for analysis. In a 384-well black plate, 20 μ L of supernatant was mixed with 20 μ L of 1:1 solution of 2 M perchloric acid and methanol. After 5 min of incubation, fluorescence readings were taken at excitation and emission wavelengths of 407 nm and 610 nm using the Synergy plate reader.

5.3.18. Iron chelation

Compound or DMSO (1 μ L) was incubated with 2.5 mM freshly prepared ferrous ammonium sulfate in a final volume of 100 μ L for 5 minutes at 37 °C. Then 100 μ L of 2.5 mM ferrozine solution was added to the wells and spectrophotometric readings were taken at 562 nm using the Synergy plate reader. Decrease in absorbance readings at 562 nm represents iron chelation.

5.3.19. Apoptosis assays

Caspase-3 immunofluorescence and TUNEL assays were performed as described previously (Section 2.3.5 and Section 4.3.6, respectively).

5.3.20. qRT-PCR

The assay was performed as described previously in chapter 2 (Section 2.3.8). Primer/probesets used were: *FECH* (Hs01555261_m1), *HIF1A* (Hs00153153_m1), *NOS3* (Hs01574659_m1), *VEGFA* (Hs00900055_m1), *VEGFR2* (Hs00911700_m1), and housekeeping controls *GAPDH* (Hs99999905_m1), *HPRT* (Hs02800695_m1), and *TBP* (Hs00427620_m1). The data were analysed using the $\Delta\Delta C_t$ method. The expression levels of genes were normalized to the 3 housekeeping genes and calibrated to the negative siRNA-treated sample.

5.3.21. Statistical analyses

Both in vitro and in vivo data were analyzed using Student's *t*-test or one-way ANOVA with Dunnett's or Tukey's post hoc tests for comparisons between the groups as appropriate in GraphPad Prism 6 software. The choroidal sprouting assay was analyzed using repeated measures two-way ANOVA with Dunnett's post hoc test. P-values of <0.05 were considered significant in all tests.

5.4. RESULTS

5.4.1. Ferrochelatase is a target of an antiangiogenic compound

To identify potentially novel protein modulators of angiogenesis, we used photoaffinity chromatography to search for targets of the naturally occurring antiangiogenic compound, cremastranone (Fig. 5.1A), which has selective antiproliferative effects on endothelial cells (Chapter 3). Protein binding partners of cremastranone were pulled down from a tissue lysate using immobilized cremastranone-based affinity reagent but not a negative control reagent (Fig. 5.1B). One of the two pulled down proteins was identified using peptide mass fingerprinting as FECH (Fig. 5.1C and Fig. 5.2) and the other as pyridoxal kinase (PDXK) (Fig. 5.2 and Fig. 5.3). Although knock down of PDXK inhibited proliferation and migration of HRECs, tube formation ability of HRECs was not inhibited (Fig. 5.3). Hence PDXK protein was not pursued further.

Immunoblot of eluates from photoaffinity pull down experiments confirmed the identity of the other pulled down protein using an antibody against FECH

(Fig. 5.1D). In order to confirm specificity of binding between cremastranone and pulled down proteins, affinity reagent was incubated with tissue proteins in the presence of excess active cremastranone isomer SH-11052 (**2**) (Fig. 5.1B) (Chapter 2). Under this condition, the binding of FECH to affinity reagent was markedly (87%) decreased, indicating competition for binding to FECH between the cremastranone isomer and the affinity reagent (Fig. 5.1E).

Recombinant FECH also interacted with the affinity reagent (Fig. 5.1F, G), indicating that the interaction does not require eukaryotic accessory proteins.

Some binding to the negative control is likely due to the abundance of recombinant protein present; recent work confirms that cellular FECH does not readily bind benzophenone linkers (Park et al., 2016). Moreover, cremastranone treatment of human retinal endothelial cells (HRECs) caused a dose-dependent buildup of PPIX (Fig. 5.5A), indicative of FECH inhibition, and addition of excess 5-aminolevulinic acid (5-ALA; the first precursor compound in the heme biosynthetic pathway that promotes increased heme production) partially rescued cremastranone's antiproliferative effects on HRECs (Fig. 5.5B). Cremastranone did not chelate iron, suggesting that it does not act indirectly on FECH by sequestering FECH's Fe^{2+} substrate (Fig. 5.5C). The FECH pathway, therefore, is targeted by a known antiangiogenic compound, suggesting that this protein and pathway are important for angiogenesis.

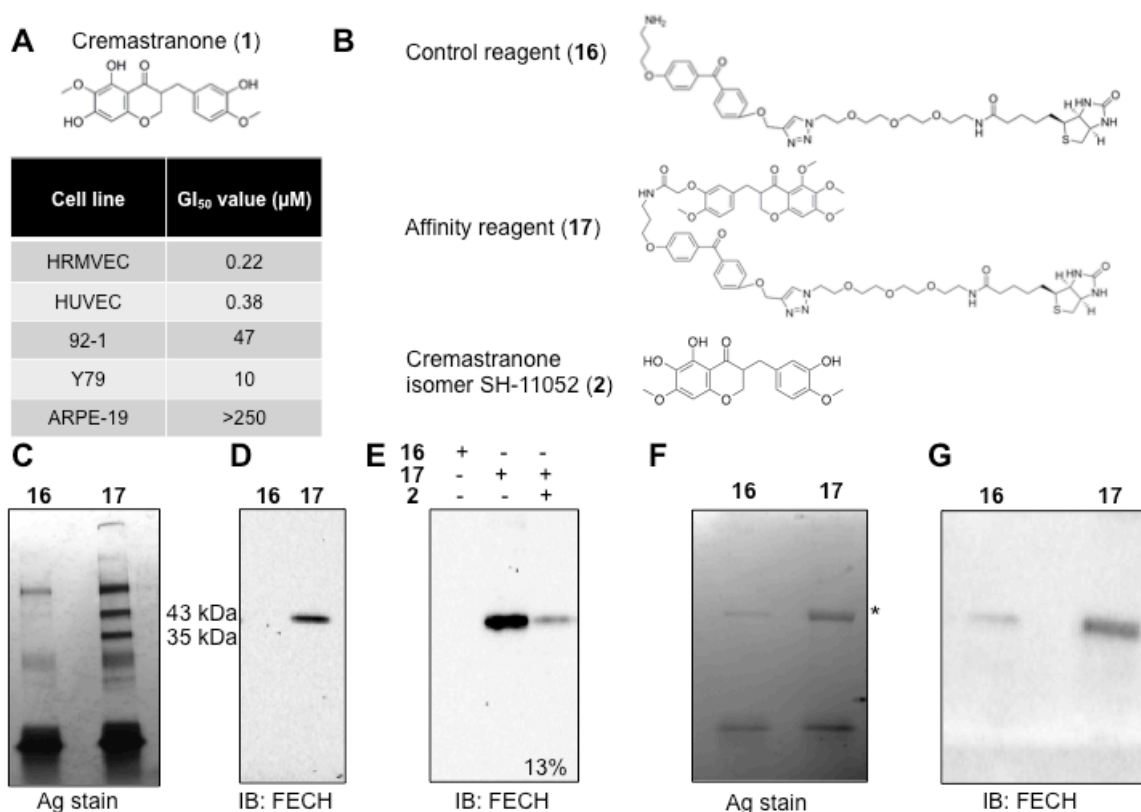


Figure 5.1. Ferrochelatase (FECH) is a target of the antiangiogenic natural product, cremastranone. (A) Chemical structure of cremastranone (1) (top). Anti-proliferative activity of cremastranone (bottom) shown as the 50% growth inhibitory concentration (GI₅₀) on human retinal endothelial cells (HRECs), human umbilical vein endothelial cells (HUVECs) and non-endothelial ocular cells (uveal melanoma 92-1, retinoblastoma Y79, and retinal pigment epithelium ARPE-19). (B) Structures of compounds used in photoaffinity chromatography. (C) Proteins pulled down with indicated reagents in photoaffinity chromatography were separated on SDS-PAGE and silver stained. (D) Immunoblot of pulled down proteins using antibody against ferrochelatase (FECH). (E) Immunoblot of pulled down proteins from competition assay with excess active cremastranone isomer (4); quantification of band intensity shown. (F) Silver stained SDS-PAGE gel of recombinant human FECH protein pulled down using photoaffinity chromatography. (G) Anti-FECH immunoblot of a similar pull-down experiment. All the gel and immunoblot images are representative from at least two independent experiments.

Accession	Description	Score	Coverage	# Unique Peptides	# Peptides	# PSMs*
F1S1X4	Ferrochelatase (Fragment) OS=Sus scrofa GN=FECH PE=3 SV=2 - [F1S1X4_PIG]	62.5	34.4	9	9	59
P00761	Trypsin OS=Sus scrofa PE=1 SV=1 - [TRYP_PIG]	58.0	8.7	1	1	80
F1RUV5	Uncharacterized protein (Fragment) OS=Sus scrofa GN=PC PE=4 SV=2 - [F1RUV5_PIG]	27.0	5.7	3	3	25
I3LVD5	Actin, cytoplasmic 1 OS=Sus scrofa GN=ACTB PE=2 SV=1 - [I3LVD5_PIG]	26.9	14.7	3	3	16
I3LNT6	Uncharacterized protein OS=Sus scrofa GN=KRT77 PE=3 SV=1 - [I3LNT6_PIG]	21.7	3.8	2	2	24
I3LLY8	Uncharacterized protein OS=Sus scrofa GN=KRT79 PE=3 SV=1 - [I3LLY8_PIG]	18.8	4.5	1	2	7
F1SGI7	Uncharacterized protein (Fragment) OS=Sus scrofa GN=LOC100525745 PE=3 SV=2 - [F1SGI7_PIG]	18.2	3.9	1	2	5
F1SHC1	Uncharacterized protein OS=Sus scrofa GN=LOC100127131 PE=3 SV=1 - [F1SHC1_PIG]	12.8	5.6	2	2	5

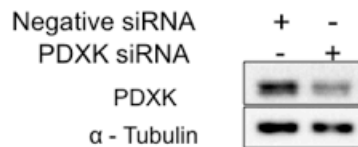
* PSMs → Peptide Spectrum Match

Figure 5.2. Peptide mass fingerprinting analysis of proteins pulled down with a cremastranone affinity reagent from a porcine brain lysate.

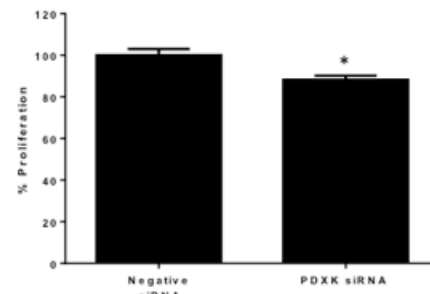
A

Accession	Description	Score	Coverage	# Unique Peptides	# Peptides	# PSMs
I3LV69	Pyridoxal kinase (Fragment) OS=Sus scrofa GN=PDXK PE=4 SV=1 - [I3LV69_PIG]	54.78	21.83	1	5	38
O46560	Pyridoxal kinase OS=Sus scrofa GN=PDXK PE=1 SV=1 - [PDXK_PIG]	64.77	22.98	3	7	43
P00761	Trypsin OS=Sus scrofa PE=1 SV=1 - [TRYP_PIG]	40.61	8.66	1	1	60

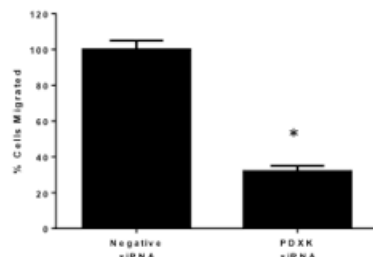
B



C



D



E

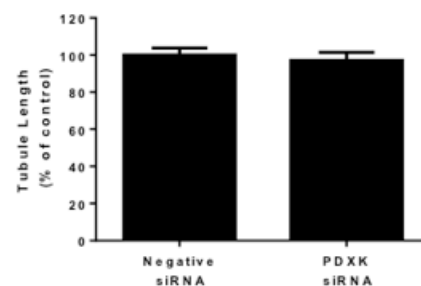


Figure 5.3. Role of PDXK in angiogenesis in vitro. (A) Peptide mass fingerprinting analysis of proteins pulled down with a cremastranone affinity reagent. (B) Knock down of PDXK using siRNA as monitored by immunoblot. (C) Inhibition of proliferation and migration (D) of HRECs after treating with PDXK specific siRNA. (E) effect of knocking down PDXK in HRECs on tube formation ability as monitored by in vitro matrigel experiments. Graphs show mean±SEM, n≥3 samples. Representative results from at least 3 independent experiments. *, p<0.05; relative to negative siRNA controls.

5.4.2. Ferrochelatase is required for angiogenesis in vitro

The role of FECH in angiogenesis has not previously been explored, despite strong evidence linking heme catabolism with angiogenesis (Dulak et al., 2008). To determine if FECH plays a key role in angiogenesis, we knocked FECH down in HRECs using siRNA (Fig. 5.4A & 5.4B) and monitored key angiogenic properties of HRECs in vitro. FECH knockdown significantly reduced the proliferation of HRECs (Fig. 5.4C and Fig. 5.7A). There was also a significant decrease in migration of HRECs treated with *FECH* siRNA in a scratch wound assay (Fig. 5.4D). Further, knocking down FECH in HRECs completely abolished the tube formation ability of HRECs as monitored in a Matrigel assay (Fig. 5.4E). To confirm the knockdown results, we also tested if a known pharmacological inhibitor of FECH shows antiangiogenic properties in vitro. *N*-methylprotoporphyrin (NMPP), a competitive inhibitor of FECH activity (Cole and Marks, 1984), also inhibited proliferation, migration and tube formation ability of HRECs in vitro (Fig. 5.4F-H). However, despite these potent antiproliferative effects, FECH knockdown and low-dose chemical inhibition were not associated with increased apoptosis of these cells (Fig. 5.7B-D), indicating a cytostatic rather than cytotoxic effect. Moreover, FECH knockdown did not inhibit proliferation of non-endothelial ocular cell lines 92-1 and ARPE-19 as well as macrovascular human umbilical vein endothelial cells (HUVECs) (Fig. 5.9), indicating that FECH inhibition is not associated with general cytotoxicity. Together, these experiments confirmed that FECH function is required for angiogenesis in vitro.

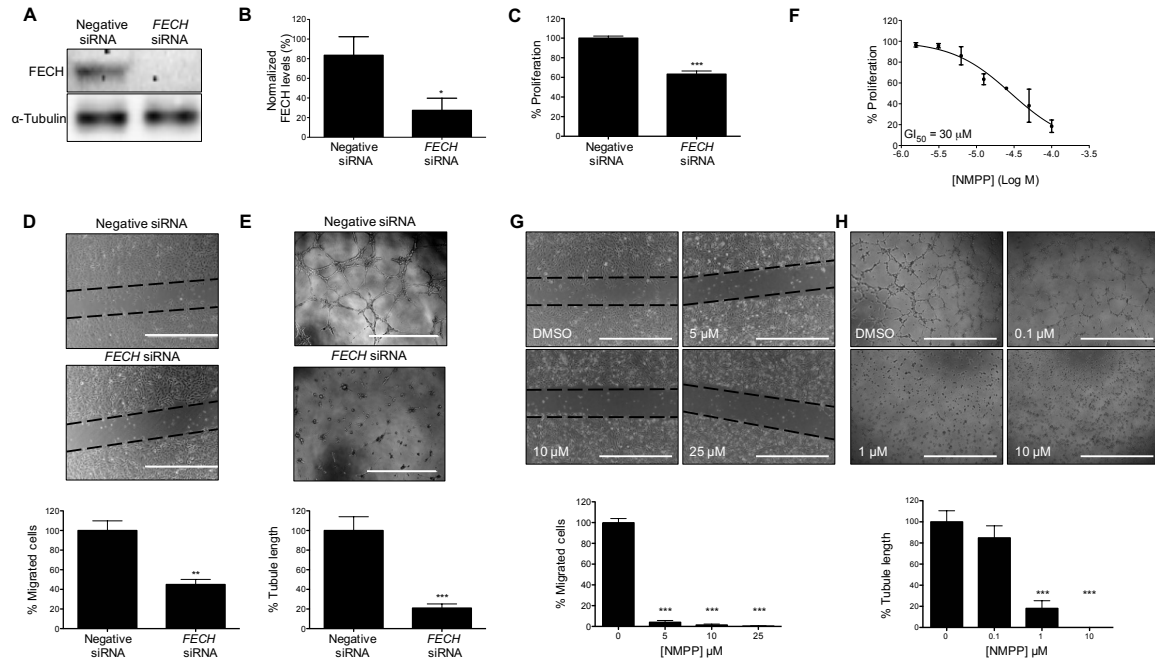


Figure 5.4. FECH is an essential protein for angiogenesis in vitro. (A & B) FECH is knocked down using specific siRNAs as confirmed by immunoblot. (C) Proliferation of HRECs was monitored in presence or absence of *FECH* specific siRNA. (D) Scratch-wound migration assay was performed with or without *FECH* knock down in HRECs. (E) Ability of HRECs to form tubes in vitro on Matrigel was monitored after knocking down FECH. The effect of NMPP, a specific inhibitor of FECH activity, on in vitro proliferation (F), migration (G) and tube formation (H) ability of HRECs was measured. Graphs show mean \pm SEM, $n \geq 3$ samples. Representative results from at least 3 independent experiments. *, $p < 0.05$; **, $p < 0.01$; ***, $p < 0.001$ relative to negative siRNA or DMSO controls. Scale bars = 1 mm.

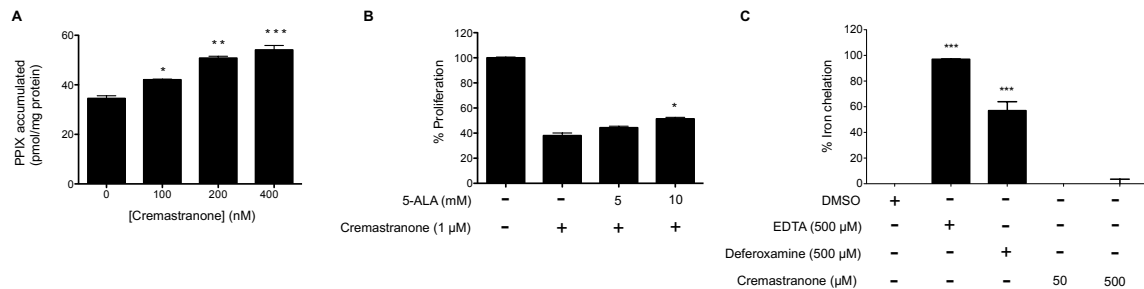


Figure 5.5. Validation of cremastranone's inhibition of FECH. (A) 5-ALA induced protoporphyrin (PPIX) buildup in HRECs after cremastranone treatment. *, $p < 0.05$; **, $p < 0.01$; ***, $p < 0.001$ relative to no cremastranone control. (B) Partial rescue of cremastranone's inhibition of HREC proliferation with 5-ALA, an inducer of heme biosynthesis. HRECs treated with DMSO only are shown as 100% proliferation control. *, $p < 0.05$ relative to cremastranone only. (C) Cremastranone does not bind iron as determined in an iron chelation assay; EDTA and deferoxamine are positive controls. Representative figures from at least three independent experiments. Graphs show mean \pm SEM with $n \geq 3$.

5.4.3. Ferrochelatase is upregulated during neovascularization

Given the potent antiangiogenic effects of FECH knockdown we observed in culture, we then explored whether FECH is associated with neovascularization in vivo. We employed a mouse model of laser-induced choroidal neovascularization (L-CNV). This widely used model recapitulates some of the features of wet AMD (Montezuma et al., 2009). FECH was overexpressed in and around lesions during neovascularization in this model (Fig. 5.6A). More importantly, FECH expression was seen throughout the retinas of human wet AMD patients analyzed postmortem (Fig. 5.6B). In the subretinal layers including the choroid (the origin of neovascularization in wet AMD) expression was significantly increased compared to healthy eyes (Fig. 5.6C).

5.4.4. Ferrochelatase is required for neovascularization in vivo

Since FECH upregulation suggested a role for this protein in neovascularization in the living eye, we asked whether decreased FECH would inhibit this process. When L-CNV mice were treated intravitreally with *Fech*-specific siRNA, there was a significant decrease in choroidal neovascularization as compared with both saline treated control mice as well as control non-coding siRNA treated mice (Fig. 5.6D, E). These in vivo experiments confirm the clinical relevance of FECH in neovascularization, and the value of targeting this enzyme to block this process.

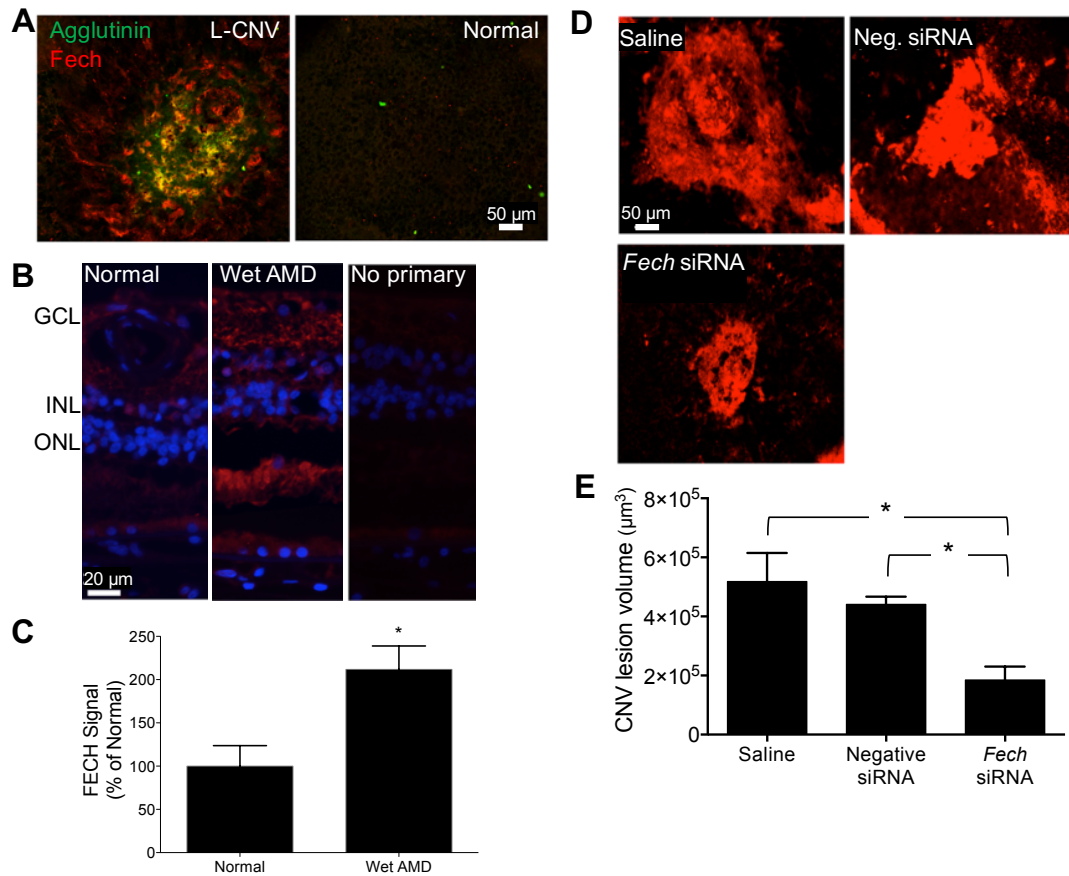


Figure 5.6. FECH is an essential protein for angiogenesis in vivo. (A) Whole mount staining of L-CNV mouse choroid stained with an antibody against Fech (red) and with agglutinin (green) to label neovascularization. (B) Immunostaining of sections of eye sections from a wet AMD patient or an age-matched control using an antibody against FECH (red). The nuclei of cells are stained blue with DAPI. Retinal layers indicated: GCL, ganglion cell layer; INL, inner nuclear layer; ONL, outer nuclear layer. (C) Quantification of the staining intensity of subretinal FECH, where CNV occurs. (D) Whole mount staining of RPE/choroid isolated from L-CNV mice treated with *Fech* specific siRNA. The choroidal vasculature was stained with agglutinin conjugated with Alexafluor 555 (red). *, $p < 0.05$ for comparisons indicated. Graphs show mean \pm SEM, $n \geq 3$ samples. Xiaoping Qi performed immunostaining and laser treatment, and assisted with analysis.

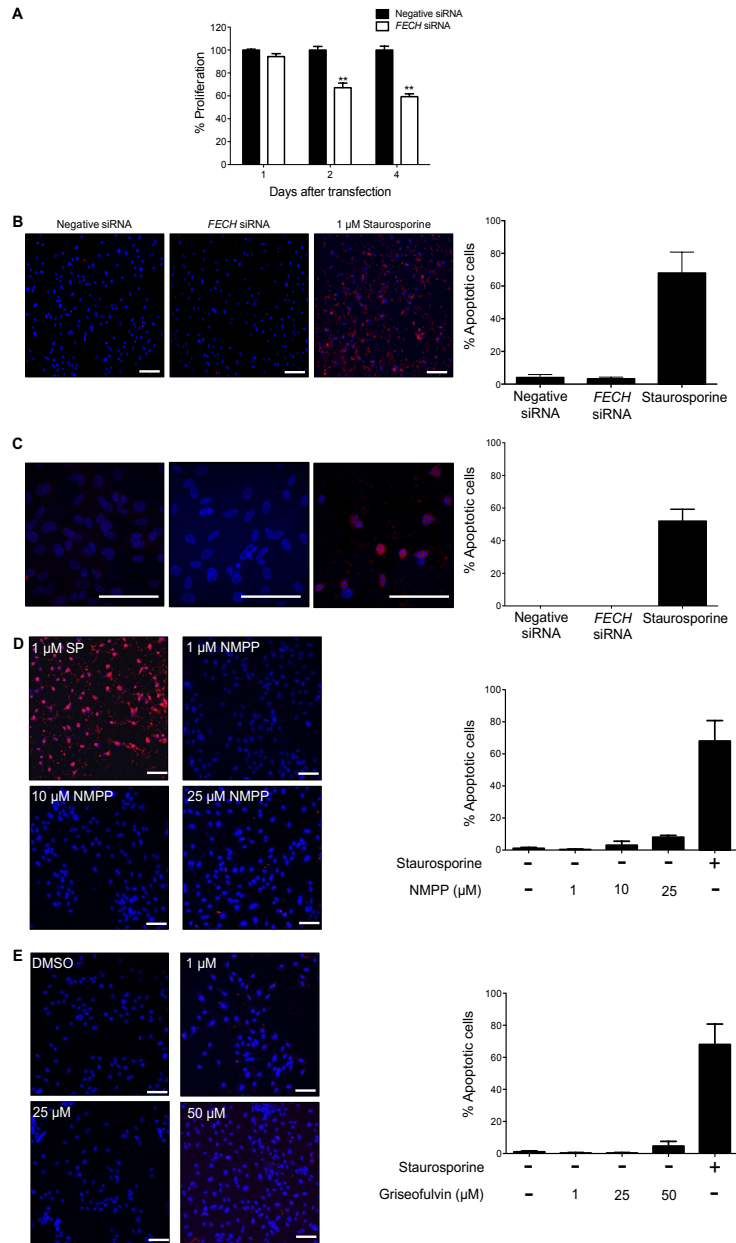


Figure 5.7. Effect of FECH-siRNA, NMPP and griseofulvin on HRECs in apoptosis assays. (A) Time course of the effect of *FECH* siRNA on proliferation of HRECs. The % proliferation calculated are with respect to proliferation with negative control siRNA. **, $p < 0.01$ versus negative siRNA. (B) *FECH* knockdown does not induce apoptosis, as assessed by TUNEL (red). (C) *FECH* knockdown does not induce apoptosis, as assessed by activated caspase-3 immunostaining (red). (D) NMPP and (E) griseofulvin induce minimal apoptosis in HRECs at effective concentrations, as assessed by TUNEL assay. Staurosporine (SP) is positive control. Representative figures from at least three independent experiments. Graphs show mean \pm SEM with $n \geq 3$. Scale bars = 1 mm.

5.4.5. Ferrochelatase-targeting therapy treats neovascularization

The FDA-approved antifungal drug, griseofulvin, has been in clinical use for over half a century (Petersen et al., 2014). The primary antifungal mechanism of this compound is as a microtubule inhibitor (Borgers, 1980). However, an unexpected off-target effect of this drug is inhibition of FECH (Brady and Lock, 1992; Holley et al., 1990; Martinez et al., 2009). Griseofulvin alkylates the heme prosthetic group of cytochrome P450 in vivo, forming NMPP, the active site FECH inhibitor (Liu et al., 2015). Taking advantage of this phenomenon, we treated HRECs with griseofulvin and observed dose-dependent antiproliferative effects, inhibition of migration, and inhibition of tube formation (Fig. 5.8A–C) similar to those observed after FECH knockdown. The concentrations of griseofulvin needed to have effects were higher than those seen with NMPP (Fig. 5.4F–H), likely due to incomplete alkylation of heme in griseofulvin-treated cells. However, this concentration ($\sim 10\ \mu\text{M}$ or $\sim 3.5\ \text{ng/mL}$) is 2.75 logs less than that attained in plasma during antifungal treatment of humans ($1\text{--}2\ \mu\text{g/mL}$) (Epstein et al., 1972), suggesting that efficacy in vitro can be achieved in a clinically attainable concentration range. Moreover, effective antiangiogenic concentrations of griseofulvin were not associated with apoptosis (Fig. 5.7E).

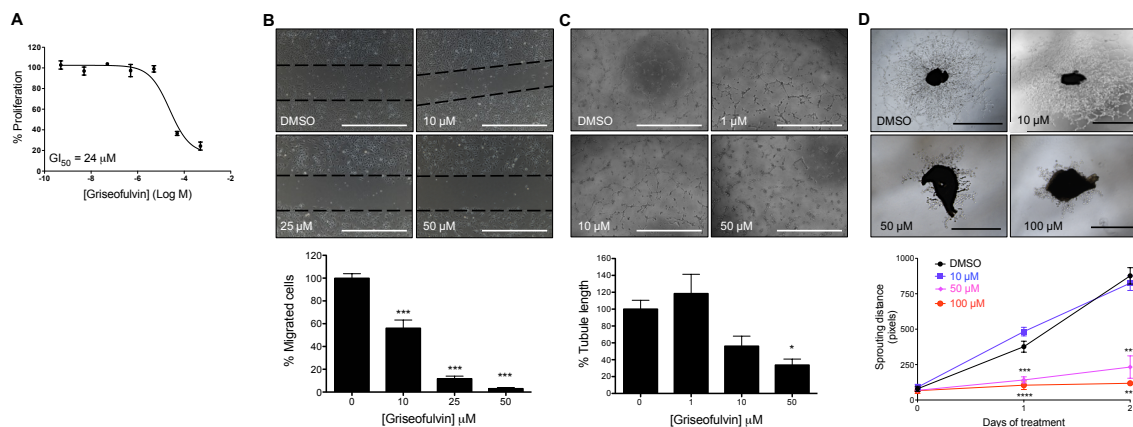


Figure 5.8. Chemical inhibition of FECH inhibits angiogenesis in vitro. The effect of griseofulvin, an FDA-approved drug that inhibits FECH activity, on proliferation (**A**), migration (**B**) and tube formation (**C**) ability of HRECs was monitored in vitro. (**D**) The mouse choroidal sprouting assay was used to further measure the antiangiogenic potential of griseofulvin in vitro. *, $p < 0.05$; ***, $p < 0.001$; ****, $p < 0.0001$ relative to DMSO controls (one- or two-way ANOVA with Dunnett's post hoc tests). Graphs show mean \pm SEM, $n \geq 3$ samples. Representative results from at least 3 independent experiments. Scale bars = 1 mm. Rania Sulaiman did the mouse choroidal sprouting assay.

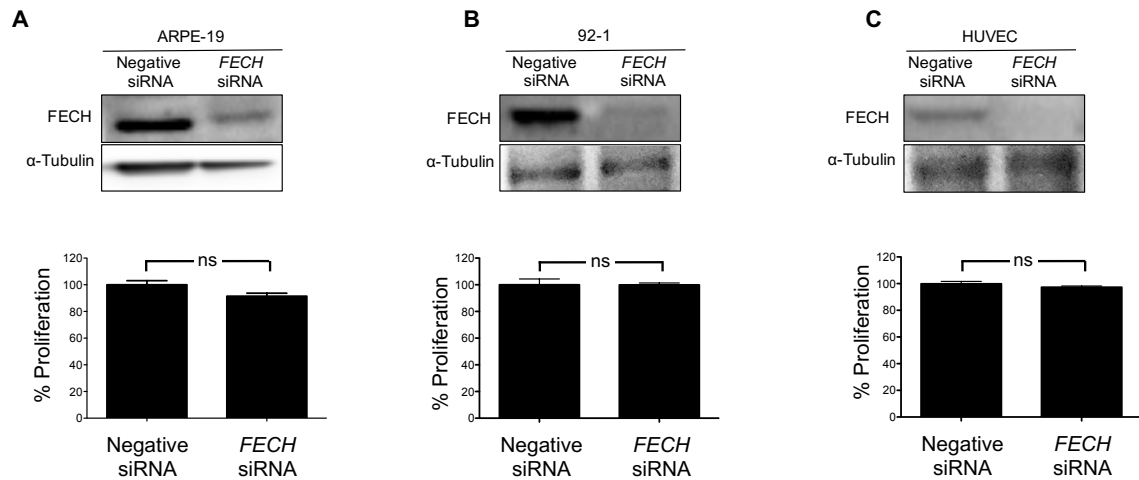


Figure 5.9. FECH knockdown has no significant effects on proliferation of other cell types. (A) ARPE-19 retinal pigment epithelial cells. (B) 92-1 uveal melanoma cells. (C) HUVECs. Graphs show mean \pm SEM with $n \geq 3$. Representative figures from three experiments are shown; ns, non-significant, Student's t-test $p > 0.05$.

Further, griseofulvin inhibited formation of microvascular sprouts in the choroidal sprouting assay, an ex vivo model of choroidal angiogenesis (Fig. 5.8D).

Spurred by these findings, we tested griseofulvin as a therapy for L-CNV. Ad libitum feeding of $\geq 0.5\%$ (w/w) griseofulvin to mice has previously been demonstrated to induce inhibition of FECH (Brady and Lock, 1992). Excitingly, such oral treatment of L-CNV mice decreased neovascularization (Fig. 5.10A–C and Fig. 5.11); similar, dose-dependent results were seen when griseofulvin was intravitreally injected instead; this is the standard delivery route for existing anti-VEGF agents (Fig. 5.10D–F).

5.4.6. Ferrochelatase depletion decreases the VEGF receptor via eNOS

In order to understand how FECH contributes to angiogenesis, we knocked down FECH in HRECs and monitored levels of endothelial nitric oxide synthase (eNOS), a key angiogenesis regulator that requires a heme cofactor for its activity to produce the proangiogenic molecule nitric oxide (NO) (Förstermann and Münzel, 2006). Immunoblot of HRECs treated with *FECH* siRNA showed significantly decreased levels of eNOS (Fig. 5.12A). Further, eNOS activity was decreased in FECH knockdown HRECs as compared to negative control siRNA treated cells (Fig. 5.12B).

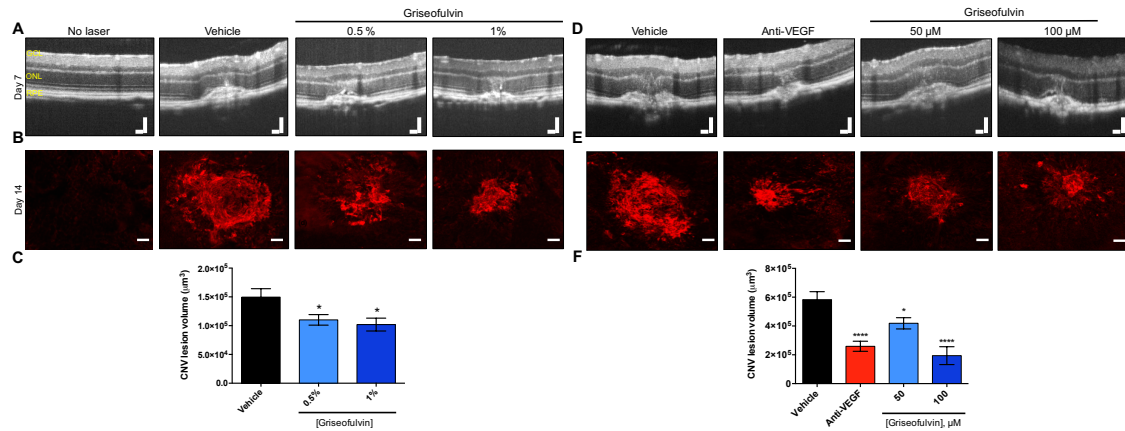


Figure 5.10. Antifungal drug griseofulvin inhibits ocular neovascularization in vivo. Mice were fed ad libitum with 0.5% and 1% griseofulvin for one week prior to, and throughout CNV development. Choroidal neovascularization was monitored by OCT in vivo (**A**) and confocal imaging of CNV lesions ex vivo (**B**). The lesion volumes were measured from confocal images (**C**). The effect of a single intravitreal injection of griseofulvin at time of laser treatment on choroidal neovascularization in the L-CNV model as monitored by OCT (**D**) and confocal imaging of CNV lesions (**E**). The CNV lesion volumes were measured using confocal images (**F**); Anti-VEGF is a positive control antibody therapy. The graphs show mean \pm SEM with $n = 6$ mice per group. *, $p < 0.05$; ****, $p < 0.0001$ versus vehicle. Scale bars for OCT images and immunostained choroids are 100 μm and 50 μm respectively. Sameerah Alkhairy, Kamna Gupta and Rania Sulaiman performed these experiments and analysis.

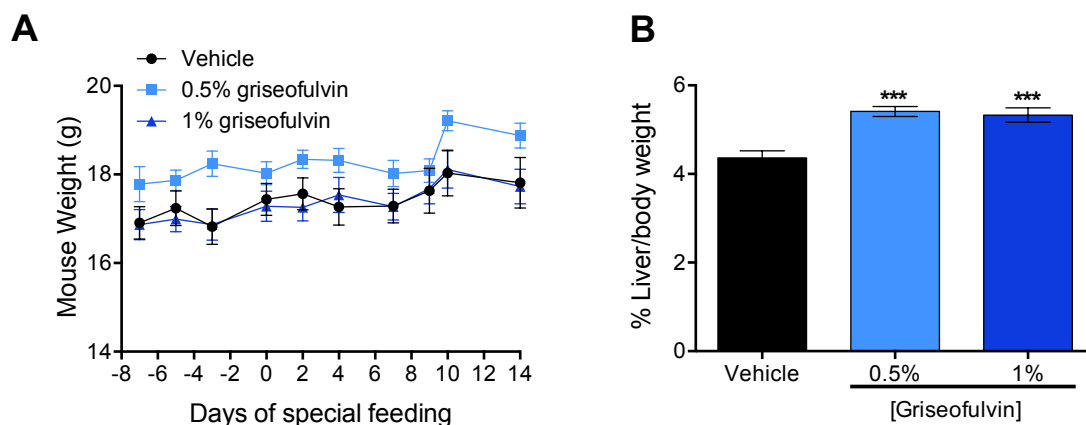


Figure 5.11. Oral griseofulvin's systemic effects. (a) oral griseofulvin treatment did not significantly change mouse weights during the experimental timecourse. (b) griseofulvin increased liver weights as expected with these treatments, confirming drug intake and systemic metabolism. The graphs show mean \pm SEM with $n = 6$ mice for each group. ***, $p < 0.001$. Sameerah Alkhairy, Kamna Gupta and Rania Sulaiman performed these experiments and analysis.

Despite the overall decrease in eNOS levels, we observed that there was an accumulation of *apo*-eNOS lacking the heme co-factor, as demonstrated in a hemin pull down assay (Fig. 5.12C) when HRECs were treated with NMPP, the

specific inhibitor of FECH activity. As nitric oxide, product of eNOS enzyme activity, causes stabilization of hypoxia inducible factor (HIF) 1 α (Sandau et al., 2001), we also monitored levels of this key mediator of angiogenesis after knocking down FECH in HRECS. FECH knockdown decreased protein levels HIF-1 α (Fig. 5.12D).

As VEGF is a major proangiogenic stimulus, we then monitored key events of VEGF signaling after knocking down FECH. We observed a profound decrease in (activating) phosphorylation of the major VEGF receptor VEGFR2 as well as total VEGFR2 protein levels in FECH knockdown cells when cultured in basal medium containing VEGF₁₆₅ as growth factor (Fig. 5.12E); production of *VEGFA* mRNA was unchanged (Fig. 5.13). The protein levels of eNOS and VEGFR2 were rescued after treating FECH knockdown cells with exogenously added hemin (a stable form of heme, the enzymatic product of FECH) (Fig. 5.12E). The decreased protein levels after FECH knockdown were not due to general translational inhibition: there was no difference in phosphorylation levels of eIF-2 α in FECH siRNA treated cells (Fig. 5.12F).

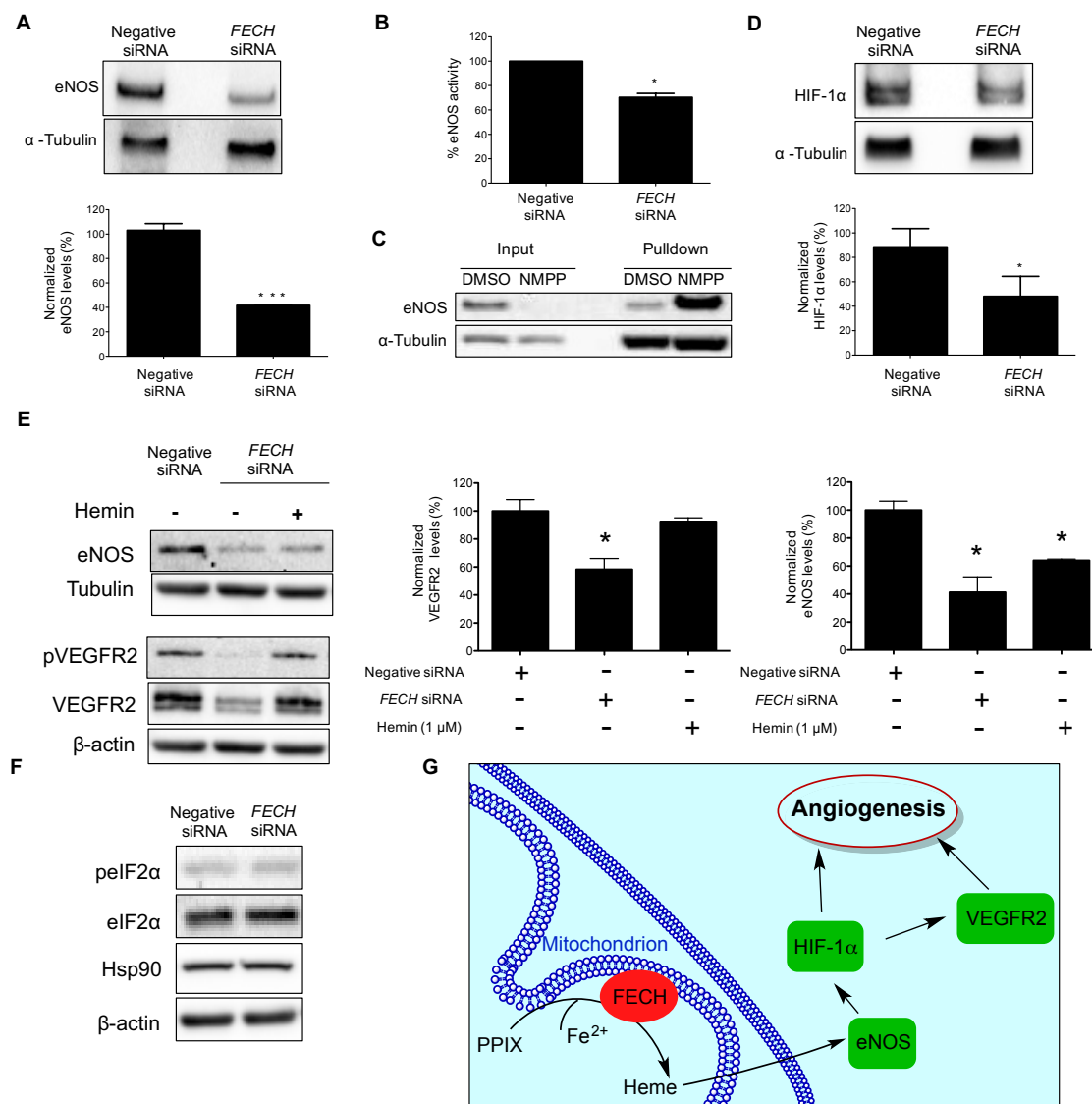


Figure 5.12. FECH depletion suppresses VEGFR2 via eNOS and HIF-1α. (A) Protein levels of eNOS were measured by immunoblot after knocking down FECH in HRECs. (B) Production of NO was monitored using diamino fluorescein-2 diacetate based fluorimetric assay. (C) Immunoblots from hemin pulldown assay using proteins extracted from HRECs treated with DMSO or 10 μ M NMPP. (D) HIF-1 α was measured by immunoblot after knocking down FECH in HRECs. (E) Protein levels of eNOS and phosphorylation of VEGFR2 at Tyr1175 in HRECs after treatment with negative control or FECH siRNAs and/or hemin (1 μ M) were monitored by immunoblotting. (F) Phosphorylation of eIF2 α and protein levels of Hsp90 were measured by immunoblot after knocking down FECH in HRECs to test if general translation is inhibited. (G) Proposed model for FECH regulation of angiogenesis through eNOS, HIF-1 α , and VEGFR2. The figures are representative from at least 3 independent experiments and the graphs show mean \pm SEM with n = 3. *, p<0.05; ***, p<0.001 compared to negative siRNA control.

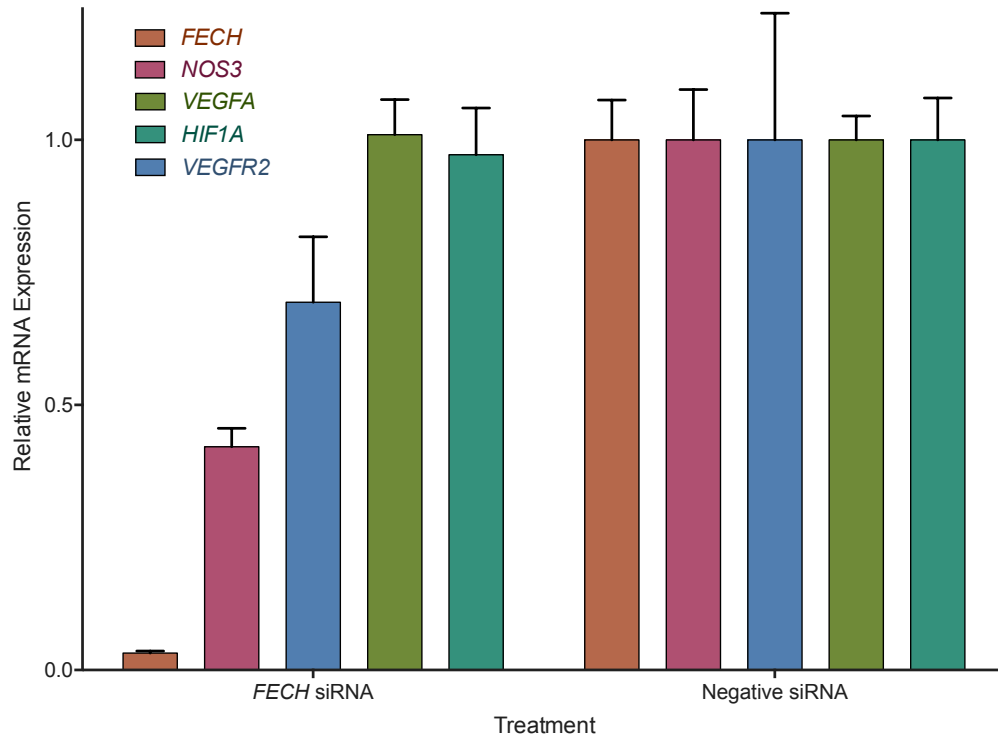


Figure 5.13. Effect of *FECH* knockdown on mRNA expression in HRECs. qRT-PCR analysis shows no decrease in *VEGFA* or *HIF1A* expression while *NOS3* (eNOS) and *VEGFR2* expression is decreased after *FECH* knockdown. Graph shows mean \pm SD with $n = 3$ technical replicates for each group. Representative results of three independent experiments.

5.5. DISCUSSION

Understanding the molecular events of pathological angiogenesis is key to developing novel therapeutics for neovascular eye diseases such as PDR, ROP and wet AMD. Currently, the drug pipeline for these diseases is dominated by anti-VEGF biologics (Kaiser, 2013). Even though these drugs have been successfully used to halt the progression of disease in wet AMD and PDR patients, there is a significant patient population (~30%) who are resistant to these treatments (Folk and Stone, 2010b; Prasad et al., 2010). Hence diversification of the drug pipeline with novel therapeutic agents with different mechanisms of action is required (Smith and Kaiser, 2014). Towards this end, we used a forward chemical genetics approach using an antiangiogenic natural product, cremastranone, to uncover new drug targets for angiogenesis.

Using a series of biochemical, in vitro and in vivo studies we have determined that FECH is a key protein involved in ocular angiogenesis and it can be exploited for developing novel antiangiogenic drugs. A photoaffinity based chromatographic technique identified FECH as a protein binding partner of cremastranone. Although, like other natural products, cremastranone likely exhibits polypharmacology, it exerts its antiangiogenic activity at least partially through inhibition of FECH activity.

Interestingly, FECH is a bona fide mediator of angiogenesis. Lack of FECH activity caused inhibition of angiogenesis both in vitro and in vivo. More importantly, only HREC proliferation was inhibited in vitro while other ocular cell

types tested did not show significant decreases in cell proliferation after FECH knock down. Even macrovascular HUVECs were not as profoundly affected by FECH depletion as the microvascular HRECs. These data reveal that retinal microvascular endothelial cells are particularly sensitive to FECH depletion. The lack of cytotoxic effects of FECH inhibition leads to consideration of FECH as a novel therapeutic target for ocular neovascular disease, possibly with minimal side effects. Supporting this latter assertion, in the genetic disease erythropoietic protoporphyria (EPP), FECH activity is markedly reduced, but EPP patients infrequently present severe symptoms apart from skin photosensitivity (Lecha et al., 2009). Neovascularization in EPP patients has not been studied extensively, although a single case report describes an ocular phenotype of idiopathic optic neuropathy in an EPP patient, not conclusively related to the disease (Tsuboi et al., 2007).

Excitingly, we have shown that the FDA-approved antifungal drug and FECH inhibitor griseofulvin inhibited ocular angiogenesis in the L-CNV mouse model when administered orally. Griseofulvin has been used widely for over half a century to treat fungal infections and is taken orally, often for months or years (Liu et al., 2015; Petersen et al., 2014). An off-target side effect of this therapy is that griseofulvin causes the formation of NMPP, along with other alkylated porphyrins, primarily in the liver (Figure 5.14) (Liu et al., 2015). NMPP in turn acts as an active-site inhibitor of FECH (Cole and Marks, 1984). As with genetic loss of function of FECH, apart from skin photosensitivity, no other major, common side effects are reported with systemic griseofulvin treatment of humans (Elewski

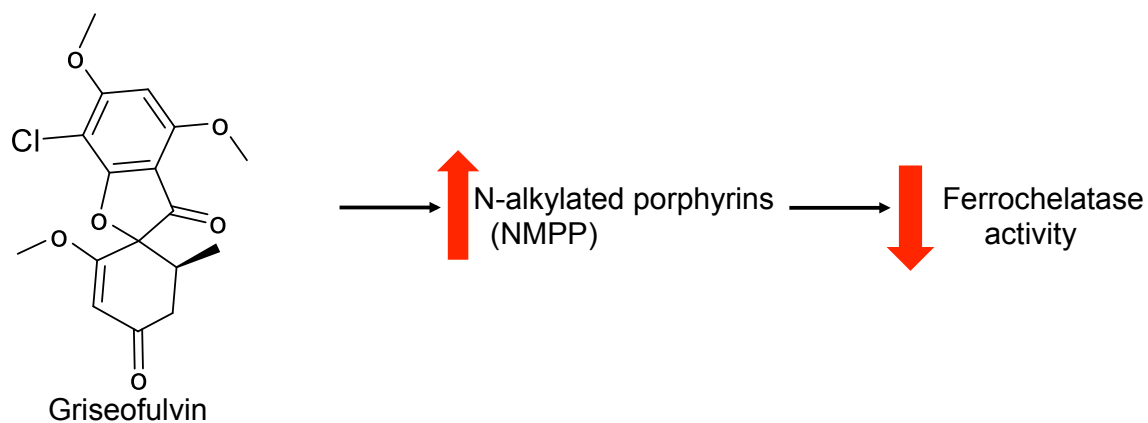


Figure 5.14. Effect of Griseofulvin on FECH activity. Griseofulvin alkylates the heme prosthetic group of cytochrome P450 enzymes to form alkylated porphyrins including NMPP. These alkylated porphyrins then bind to the active site and inhibit the enzyme activity of FECH.

and Tavakkol, 2005; Grover et al., 2012). However, griseofulvin treatment has been very rarely linked to liver injury mainly due to cholestasis. Only 5 % of griseofulvin treated patients experienced elevation of serum aminotransferases, a sign of liver injury. Some patients experience skin rashes due to elevated levels of porphyrins in the blood. Nevertheless, these symptoms are mild in the majority of the patients.

The fact that griseofulvin-fed mice showed decreased ocular neovascularization as compared to control mice is important as currently there are no oral drugs available for the treatment of ocular neovascularization. The current approved drugs (anti-VEGF biologics) are all delivered intravitreally. If side effects were manageable, an oral therapy would be appealing. However, since griseofulvin was also effective when delivered intravitreally, combination intravitreal therapies of this drug with anti-VEGF biologics are also an interesting possibility to increase efficacy and decrease side effects of existing treatments. Moreover, griseofulvin offers the promise of low-cost treatment if shown efficacious in clinical trials. There are also prospects for novel FECH inhibitors as therapy: we have developed cremastranone analogs such as SH-11037 that may also act through FECH (Chapter 4), and recently, the drugs vemurafenib (Savitski et al., 2014) and salicylic acid (Gupta et al., 2013), as well as a lipid-derived probe (Niphakis et al., 2015) compound were all shown to bind to FECH, suggesting that this protein has many potential binding clefts and is therefore likely druggable with novel compounds.

FECH is the only known enzyme in humans to synthesize heme and any loss of activity of this enzyme might result in intracellular heme deficiency (Dailey et al., 2000). Heme serves as either a prosthetic group for many enzymes or as a signaling molecule regulating expression of genes involved in cell differentiation, proliferation and signal transduction (Mense and Zhang, 2006). FECH knock down decreased protein levels of eNOS, HIF-1 α and VEGFR2, key players promoting angiogenesis, in HRECs. As eNOS is a heme dependent enzyme, FECH knock down directly affects the stability and activity of eNOS enzyme. Nitric oxide (NO), product of the eNOS enzyme, induces angiogenesis, (Ziche and Morbidelli, 2000) partly by stabilizing HIF-1 α under normoxia (Sandau et al., 2001). This explains the logic behind the decreased protein levels of HIF-1 α in FECH knock down cells with decreased eNOS activity. HIF-1 α is a transcription factor, which regulates the expression of a range of proangiogenic proteins. VEGFR2, the major tyrosine kinase receptor of VEGF₁₆₅, is up-regulated under hypoxia (Takagi et al., 1996; Tudor et al., 1995), So the decreased levels of VEGFR2 in HRECs after FECH siRNA treatment can be linked to decreased HIF-1 α . Thus low protein levels of VEGFR2 (and thus angiogenesis) in FECH-deficient HRECs can be directly attributed to loss of heme in cells and the resultant decrease in levels of eNOS enzyme (Fig. 5.12g). VEGFR2 depletion in turn further suppresses eNOS levels. The rescue of VEGFR2 and eNOS expression by addition of exogenous hemin, a stable form of heme, further supports this mechanism.

Our findings reveal a previously undocumented, central role of FECH in ocular angiogenesis. They provide a rationale for clinical testing of griseofulvin in neovascular eye disease. In addition, it will be valuable to develop novel, FECH-targeted therapies for treating the debilitating ocular diseases caused by neovascularization.

CHAPTER 6. DISCUSSION

6.1. OVERALL SUMMARY

The primary goal of this study was to understand how cremastranone inhibits ocular angiogenesis by identifying the cellular proteins (targets) with which it interacts and then elucidating the role of the target proteins in angiogenesis. This work encompassed confirming the antiangiogenic activities of synthetic cremastranone **1** and its analogues SH-11052 (**2**) and SH-11037 (**14a**), establishing the SAR of cremastranone and investigating the role of a cremastranone target protein, FECH in ocular angiogenesis (Fig. 6.2). The novelty of this research work is the identification of SH-11037 (compound **14a**) as a highly specific inhibitor of ocular angiogenesis and the discovery of FECH as a key mediator of ocular angiogenesis. I have not come across any small molecule that is very selective against HRECs compared to HUVECs and other ocular non-endothelial cells. This is a significant achievement as it enables us to pursue developing drugs which specifically inhibit ocular angiogenesis without affecting the normal vasculature and angiogenesis taking place elsewhere in the body. Here I will discuss the primary issues addressed in each chapter of my dissertation including how this work impacts the drug discovery program in the ocular angiogenesis field.

SH-11052 (**2**) was synthesized during the preparation of cremastranone as a regioisomer. It differs from cremastranone only in the positions of its methoxy and hydroxyl groups on C-6 and C-7 of the chromanone ring. While the methoxy and hydroxyl groups positions are on C-6 and C-7 respectively in cremastranone, their positions are reversed in SH-11052 (Fig. 2.1). Nonetheless

this minor change significantly altered the potency of the compound and also the selectivity of the compound against non-endothelial cells. Cremastranone has nanomolar GI_{50} values against endothelial cells as compared to high micromolar GI_{50} values against non-endothelial ocular cell lines (Table 6.1). However this difference in selectivity and high potency disappeared by changing the positions of methoxy and hydroxyl groups on the A-ring in SH-11052, indicating the importance of these groups on the A-ring. However even though SH-11052 is less efficacious than cremastranone, it inhibited angiogenic abilities of HRECs and showed similar effects as cremastranone (inhibition of the TNF- α induced NF- κ B pathway). In addition synthesis of a scalable quantity of cremastranone is a significant achievement as it provided us enough material for performing mechanistic studies as well as opened new avenues to synthesize analogues with better potency and specificity.

This work set the stage for establishing the SAR of cremastranone to identify new analogues, which are highly selective against HRECs and more potent than cremastranone. We chose to establish SAR of cremastranone using cell-based proliferation assays as the identity of cremastranone's binding partner was not known and, also, employing both endothelial as well as non-endothelial cells for screening compounds helps us select compounds which are selective against endothelial cells, thereby minimizing the toxicity of lead molecules (Table 6.1). In brief, SAR studies showed that an intact chromanone ring is crucial for activity and further modifications on the C-ring are well tolerated. In fact addition of bulkier groups on the C-ring increased potency as well as selectivity.

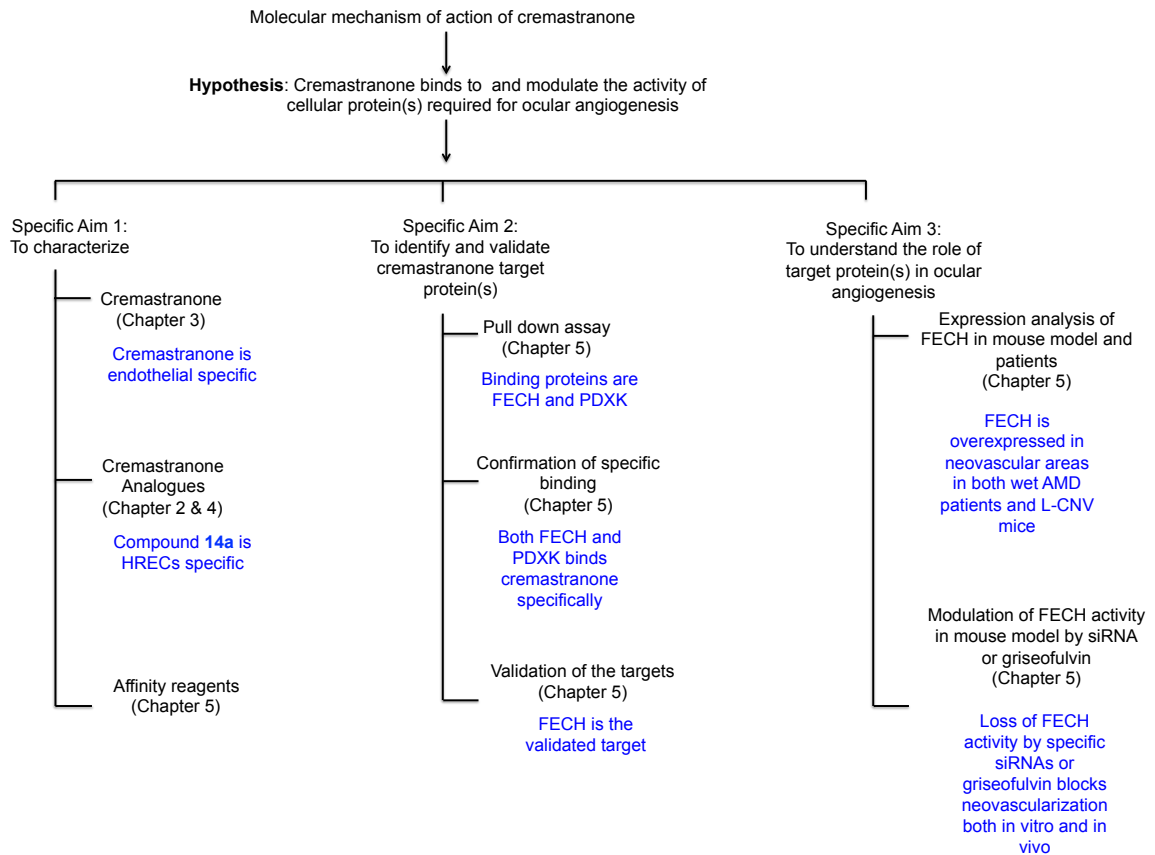


Figure 6.1. Overview of the mechanistic study of cremastranone. The objectives and key findings of each specific aim are described in black and green fonts respectively.

Towards this end, I identified SH-11037 as a potent and selective antiangiogenic molecule. It has GI_{50} values in low nanomolar concentrations against HRECs, 10-fold and >100-fold less potent against HUVECs and non-endothelial ocular cell lines respectively (Table 6.1). This suggests that SH-11037 could be a lead molecule for developing a drug, which is very specific against ocular angiogenesis without marked effects on normal vasculature as well as non-endothelial cells and thus minimizing the side effects of treatment. This is significant as current treatment options for ocular diseases arising from pathological angiogenesis are associated with significant acute systemic side effects, as noted (Chapter 1. Section 1.4.5). Further, I showed the ocular antiangiogenic activity of SH-11037 in preclinical studies in the OIR mouse model (Fig. 4.5). Subsequent work in our lab has shown that SH-11037 also inhibits angiogenesis in the choroidal sprouting assay *ex vivo*, impairs developmental angiogenesis in the eyes of zebra fish larvae and blocks choroidal neovascularization in the L-CNV mouse model. In mice, the antiangiogenic effect of SH-11037 was comparable to that obtained with anti-VEGF antibody and in addition SH-11037 synergized with anti-VEGF antibody both *in vitro* as well as *in vivo*. SH-11037 did not show any signs of ocular toxicity effects even at 100 μ M concentration as there was no difference in the retinal function and retinal vasculature of mice treated with SH-11037 as compared to the placebo treated group (Sulaiman et al., 2016).

Further SAR studies showed potential sites where long chemical linkers can be added to cremastranone derivatives, without affecting their biological

activities. Hence a benzophenone moiety connected to a chemical linker was added on the C-ring (Fig. 5.1). This linker was then connected to biotin. This whole complex reagent is termed an affinity reagent. Using this affinity reagent and a control reagent (Fig. 5.1), I identified FECH as a specific binding partner of cremastranone and then validated it in both in vitro and in vivo mouse models of angiogenesis. To my knowledge this is the first report describing the role of FECH in ocular angiogenesis.

Table 6.1. GI₅₀ values of cremastranone, SH-11052 and SH-11037 on various cell lines tested in AlamarBlue proliferation assay.

Cell type	SH-11052	Cremastranone	SH-11037
HREC	43	0.217	0.055
HUVEC	18	0.377	0.75
Y79	87	9.8	12
92-1	6	47	>100
ARPE-19	>100	>250	>100

6.2 FECH OVERVIEW

FECH is an inner mitochondrial membrane associated enzyme responsible for catalyzing the insertion of ferrous ion into protoporphyrin IX to form heme (Dailey et al., 2000). It is the terminal enzyme in the biosynthesis of heme (Figure 6.2). In humans the biosynthesis of heme starts with the condensation of glycine and succinyl-CoA to yield 5-aminolevulinic acid (ALA). 5-

ALA is the sole contributor of the carbon and nitrogen atoms of heme. Two molecules of 5-ALA are then condensed to yield a pyrrole molecule called porphobilinogen (PBG). Four molecules of PBG undergo oligomerization giving the linear tetrapyrrole molecule, 1-hydroxymethylbilane. Then ring closure happens to yield cyclic tetrapyrrole uroporphyrinogen III. The four acetic acid side chains of this cyclic tetrapyrrole undergo stepwise decarboxylation to form coproporphyrinogen III and oxidative decarboxylation yielding protoporphyrinogen IX. Subsequently oxidation of protoporphyrinogen leads to aromatization of the ring system to form protoporphyrin IX (PPIX). In the final step, insertion of ferrous ion leads to formation of the heme molecule (Layer et al., 2010).

The enzyme FECH was first reported in 1956 (Goldberg et al., 1956) and soon linked to the human genetic disease erythropoietic protoporphyria (EPP) (Dailey et al., 2000; Gouya et al., 1999). In humans a genetic defect that causes reduction in ferrochelatase activity results in EPP. There are over 30 different EPP mutations reported in the human genomic *FECH* gene which cause reduction in FECH activity (Rufenacht et al., 1998). Of these mutations, 18 are missense mutations and six are different exon deletions (exons 3, 4, 5, 7, 9, and 10). Interestingly only two mutations (Y191H and P192T) are located in the active sites and the rest are scattered throughout the protein. In EPP, free protoporphyrin, mainly from erythropoietic tissues, is found to accumulate in the skin resulting in photosensitivity. The disease is not usually life threatening but causes irritation and pain upon exposure to sunlight as protoporphyrins are light

sensitive. Protoporphyrins absorb light and are converted to free radicals, which then damage the cell membrane and proteins. Only in 5 % of the EPP patient population, protoporphyrin accumulates, crystallizes and blocks biliary passages. In very few cases liver failure with cirrhosis may develop. But for the majority of EPP patients the condition is non lethal. However there are no extensive studies on EPP patients with respect to ocular diseases associated with pathological angiogenesis.

Mammalian FECH is a nuclear encoded protein that is synthesized in the cytoplasm in a precursor form and then undergoes proteolytic posttranslational modification to remove the N-terminal organellar targeting sequence while being transported to the inner mitochondrial membrane (Dailey et al., 1994; Karr and Dailey, 1988). The molecular weight of monomeric mature human FECH is 43 kDa. Human FECH is a homodimer with each monomer containing an active site and a [2Fe-2S] cluster. Some EPP mutations in FECH result in the enzyme not having an intact [2Fe-2S] cluster and loss of this feature results in loss of enzyme activity. Both [2Fe-2S] clusters are located at the dimer interface and are required for dimerization of FECH. However the importance of dimerization in the physiological functions of FECH is not yet understood (Dailey et al., 2000).

The gene encoding FECH is located on chromosome 18q21.3 and is composed of 11 exons covering a region of approximately 45 kbp. The promoter region lacks both TATA and CAAT box motifs but contains CpG islands. Also, the FECH promoter contains two HIF-1 binding motifs suggesting that the expression of FECH is modulated by hypoxia, a strong stimulus for angiogenesis.

Only one gene encodes FECH in humans in all the cells even though the expression pattern of FECH is different in different cells. FECH is upregulated in erythroid cells to cope with the production of heme while in other cells its expression is low to provide housekeeping functions. This transcriptional regulation as well as the translational regulation of FECH in different cells is not clearly understood. There are some reports of the FECH gene being transcriptionally regulated by HIF-1 α , HNF-1 α and FKLF-2, a Krüppel-like transcription factor (Asano et al., 2000; Liu et al., 2004; Muppala et al., 2000).

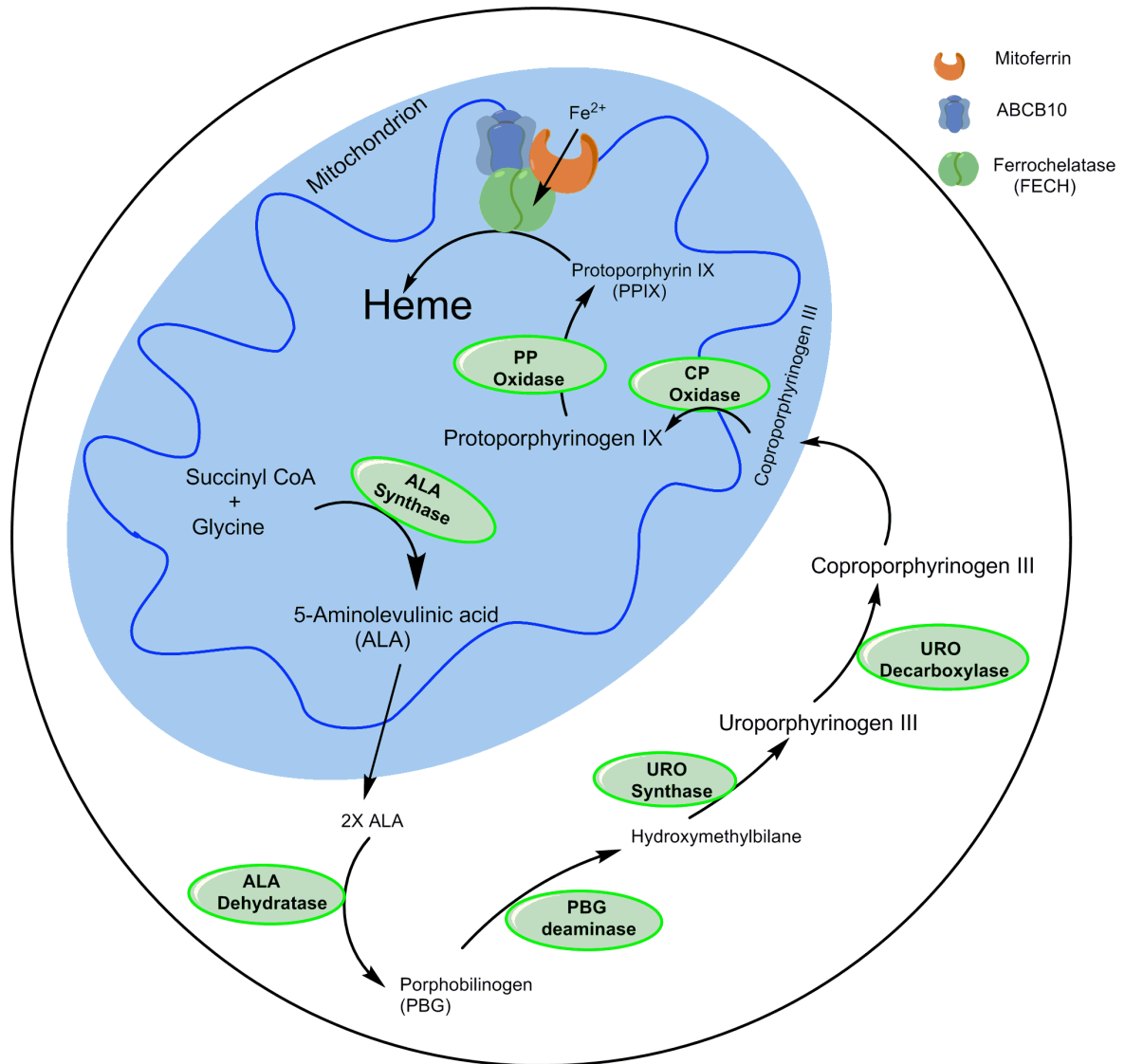


Figure 6.2. The heme biosynthetic pathway in mammals.

6.3. ROLE OF FECH IN ANGIOGENESIS

Apart from its iron insertion activity, no other function has been assigned to FECH. Hence it becomes interesting to understand how FECH affects angiogenesis. One potential clue for the link between FECH and angiogenesis comes from a diagnostic as well as a treatment procedure called photodynamic therapy (PDT) wherein an analogue of PPIX, substrate of FECH, is accumulated specifically in growing endothelial cells. This endothelial-specific accumulation of PPIX analogue has been exploited to destroy neovessels.

Recently, Inoue et al. (2013) showed that PDT involves an antiangiogenic mechanism in urothelial carcinoma and the efficacy of the treatment can be enhanced by inhibition of FECH. PDT involves administration of photosensitizers, including porphyrins such as verteporfin (trade name Visudyne) into the body and then irradiating with light of a particular wavelength (689 nm for Visudyne) to activate the photosensitizer. These activated photosensitizers produce reactive singlet oxygen and reactive oxygen species, which damage nearby cells. PDT was extensively used for treatment of wet AMD and is still being used in certain conditions of wet AMD and in cancer treatments. For some unknown reasons the administered photosensitizer selectively accumulates in growing blood vessels and hence PDT selectively kills neovessels. This concept is used in ALA-PDT wherein 5-ALA, a precursor and inducer of heme synthesis, is administered into the body. This results in accumulation of protoporphyrin IX in growing blood vessels via an unknown mechanism. This PPIX produces reactive oxygen species after exposure to light and selectively destroys growing blood vessels.

The only linkage between PDT and FECH is that the photosensitizer PPIX is a substrate of FECH and there are no extensive studies understanding why PPIX accumulates in growing blood vessels. Inoue et al studied the ALA-mediated PDT in the presence of deferoxamine (an iron chelator) to treat urothelial carcinoma in mice models and showed reduction in growth of abnormal blood vessels after ALA-PDT treatment in the presence of deferoxamine. Even though the group successfully provided proof of concept that PPIX selectively accumulates in growing blood vessels, the treatment strategy involving deferoxamine as a FECH inhibitor is debatable. Deferoxamine is an iron chelator and interferes with a wide range of biological reactions involving iron. Hence the improvement in efficacy of ALA-PDT observed in the presence of deferoxamine might not be due to FECH inhibition only. Thus selective accumulation of porphyrins in growing blood vessels needs to be studied in order to understand the role of FECH in angiogenesis.

However during my dissertation work, the identification of FECH as a protein binding partner of cremastranone led me to the hypothesis that cremastranone might be acting by enhancing the accumulation of PPIX through inhibition of FECH. In support of this, there was an increase in PPIX levels after treatment with cremastranone. However since the majority of in vitro angiogenesis assays are carried out in dark conditions there should not be any photodynamic activation of PPIX and hence no cell death. Consistent with this, there was no induction of cell death as measured in apoptosis assays, when cells were treated with either cremastranone or FECH specific siRNAs (Fig. 5.7). This

led me to hypothesize that the product of FECH, heme, might play a role in angiogenesis either through a signaling pathway or as a crucial cofactor for proangiogenic molecules. There are wide varieties of enzymes, transporters, and receptors that use heme as a cofactor. Among these, I concentrated on endothelial nitric oxide synthase (eNOS) as it is a very well established proangiogenic molecule and needs heme for its stability and activity to produce nitric oxide (NO) (Rafikov et al., 2011). This is supported by the fact that apo-eNOS is accumulated in HRECs treated with FECH specific inhibitor NMPP (Fig. 5.6). NO is required for stabilization of HIF-1 α under normoxic conditions. HIF-1 α , in turn regulates expression of various angiogenic molecules including VEGFR2. Hence loss of FECH activity results in decreased protein levels of HIF-1 α and VEGFR2. Thus the overall angiogenic process is halted as a result of FECH inhibition. The importance of FECH in ocular angiogenesis is further substantiated by the fact that FECH is upregulated in wet AMD patient eyes and in choroidal neovascularized areas in L-CNV mouse eyes (Fig. 5.6).

6.4. FECH INHIBITION AS A THERAPY

Apart from the discovery of FECH as a key mediator of angiogenesis, another important finding of this study is the use of griseofulvin to inhibit choroidal neovascularization. The logic of choosing griseofulvin is that it undergoes metabolic conversion in liver by P450 enzymes to produce alkylated porphyrins including NMPP (Brady and Lock, 1992; Martinez et al., 2009). Thus, FECH activity is decreased in griseofulvin treated animals. We observed that

choroidal neovascularization was significantly reduced in L-CNV mice that received griseofulvin either through oral or intravitreal administration as compared to placebo treated L-CNV mice. This is a significant observation as griseofulvin is already an FDA approved antifungal drug and it can be administered orally, unlike existing anti-VEGF biologics, which are injected into the eye. The toxicity, pharmacokinetic and pharmacodynamic properties of griseofulvin are very well studied so that minimal efforts are needed to take forward this drug to the clinical phase for treating wet AMD patients. As griseofulvin is available at cheaper costs as compared to the current anti-VEGF biologic drugs used, developing this drug for treating ocular diseases arising from pathological angiogenesis could result in a substantial decrease in cost of treatments for wet AMD, PDR and ROP patients.

6.5. EXPERIMENTAL APPROACH

Knowing the cellular targets of cremastranone is helpful if the process of developing antiangiogenic drugs is to be made more efficient. Natural products often interact with several proteins in cells. For drug discovery, an understanding of both protein functions and drug selectivity is highly important. Identification of the full spectrum of targets associated with cremastranone can lead to faster optimization of cremastranone, its effective clinical application as well as understanding of off-target side effects and thereby minimizing the possible toxicities early on in the drug discovery process.

Target identification is traditionally approached using a variety of genetic and biochemical methods such as yeast three hybrid systems, mammalian three-hybrid system, phage display, protein microarrays and affinity chromatography (Schenone et al., 2013; Sleno and Emili, 2008). Each of these techniques has been successfully used to identify target proteins of bioactive small molecules. Of all these techniques I choose affinity chromatography technique, as it is a cost effective and unbiased direct approach of finding target proteins. However some of the drawbacks of this technique are that it can yield non-specific proteins, it requires a large amount of protein to start with and requires synthesis of affinity reagents. Despite these drawbacks this was an ideal approach available to us as we have a synthetic chemist collaborator who could synthesize the affinity reagent.

This technique can yield a full spectrum of target proteins with which cremastranone interacts and thereby allows evaluation of polypharmacology. Moreover this method also allows small molecules to interact with posttranslationally processed, mature proteins under physiologically relevant conditions. I used a slight variation of the affinity approach, photo-affinity based chromatographic technique. The principle of the assay is that the affinity reagent is immobilized on agarose beads by exploiting strong binding affinity of avidin and biotin. The benzophenone moiety helps in covalently “locking” the target proteins bound to affinity reagent upon exposure to UV light. The cremastranone moiety of affinity reagent interacts with target proteins and upon exposure to UV light, because of proximity of target protein and benzophenone moiety in affinity

reagent, both target protein and affinity reagent are locked in covalent bonds. Then the immobilized protein-affinity reagent complex is extensively washed to remove non-specifically bound proteins. Bound proteins were eluted from matrices and separated by SDS-PAGE. The protein bands specifically eluted with the affinity reagent are digested with trypsin and the resulting peptides are analyzed by the LC-MS technique. This is one of the most direct and unbiased approaches for identifying drug targets. However the targets identified might not be the physiologically relevant targets through which cremastranone exerts its antiangiogenic activity. Hence, target validation becomes important. In target validation, we have to ensure that the identified target plays a crucial role in angiogenesis and decrease or increase of the levels of target protein in HRECs affects the angiogenic ability of HRECs.

To validate FECH as a target, I choose both an siRNA-based approach and a specific chemical inhibitor of FECH. This is because I observed inhibition of FECH activity in HRECs by cremastranone. Hence I hypothesized that FECH loss might decrease the angiogenic ability of HRECs. In order to achieve this I first followed an siRNA-based approach, as it is very specific for a gene and the success of the experiments can be analyzed by monitoring the protein levels of FECH using WB technique. Hence, siRNA-based approach gives direct answers.

The reason I chose HRECs for all the in vitro angiogenic assays is that there is a high degree of heterogeneity in endothelial cell behavior. Endothelial cells differ in their physiological functions and response to stimuli in different organs and also between different tissues in order to adapt to the local needs.

HRECs are retinal endothelial cells, which are responsible for retinal neovascularization in the human eye and thus they are perfect in vitro cellular models for ROP and PDR. However there are no readily-available cell lines or primary cells to represent human choroidal neovascularization. I used both HRECs and HUVECs during SAR studies to identify molecules that are selective against HRECs as any molecule targeting HUVECs (macrovascular endothelial cells) might affect general vasculature in the body. The selectivity of SH-11037 against HRECs again substantiates the fact that endothelial cells from different tissues behave differently. Hence HRECs are a convenient in vitro cell model for studying ocular angiogenesis in vitro.

To monitor angiogenic properties of HRECs I chose proliferation, migration and Matrigel-based tube formation assay. During sprouting endothelial cells undergo cell division and hence monitoring proliferation of HRECs is critical. I used the alamar blue based method for measuring proliferation of HRECs as it is reliable, simple, inexpensive and adaptable to high throughput screening (Rampersad, 2012). The principle of the assay is that NADH dehydrogenases reduce resazurin (nonfluorescent) to resorufin (fluorescent). Using this method a large number of compounds can be screened to identify potential antiangiogenic molecules. Once potential candidates were selected then EdU incorporation assay was used to confirm the antiproliferative activities of potential antiangiogenic candidates. Thus using two different proliferation techniques gave us a fail-safe approach to identify antiangiogenic candidates.

Once the antiproliferative activity of compounds were confirmed then the migration ability of HRECs was tested in presence of compounds. For this, I used the scratch wound assay. This is an inexpensive, two-dimensional in vitro assay and cell migration can be monitored over time (Liang et al., 2007). An alternative migration assay is the 'transfilter assay', a modification of the Boyden chamber assay. The transfilter assay is a three-dimensional assay based on migration of endothelial cells towards the chemo-attractant (in this case VEGF) from one chamber to another chamber separated by a filter coated with ECM proteins such as collagen or fibronectin. This assay has several advantages including high sensitivity, high reproducibility, short duration (4-6 h). However it is expensive and scratch wound assay gives as much information as transfilter assays regarding the ability of test compounds to inhibit migration of endothelial cells in vitro (Goodwin, 2007; Liang et al., 2007). Hence the scratch wound assay was used in the project.

Assays that simulate the formation of capillary-like structures are regarded as representative of later stages of angiogenesis (differentiation). The Matrigel-based tube formation assay is a widely used technique for measuring tube formation ability of HRECs. This assay measures attachment, migration and differentiation of endothelial cells into tubule like structures in a manner that simulates the in vivo situation. Matrigel is a mixture of extracellular and basement membrane proteins derived from the mouse Engelbreth-Holm-Swarm sarcoma. Matrigel is the most potent matrix for tubule formation with tubules beginning to form in 1 h and completely formed within 12h following endothelial cell plating.

This assay can be easily adapted to 96-well plate format and free software plugins are available in ImageJ to process and analyze the images. This is a final confirmatory assay to determine the antiangiogenic activity of molecules in vitro (Arnaoutova and Kleinman, 2010; Goodwin, 2007).

In order to monitor antiangiogenic activity of small molecules or FECH-specific siRNAs, L-CNV and OIR mouse models were used to represent choroidal neovascularization (CNV) and retinal neovascularization (RNV) respectively. These two mouse models are standard models recapitulating the majority of the events of wet AMD and ROP respectively (Smith et al., 1994; Tobe et al., 1998). These two models are widely used to develop antiangiogenic molecules for treating ocular diseases and are highly reproducible.

The L-CNV mice model uses breaking of Bruch's membrane using an argon laser. In this model three laser burns are introduced in each eye and the antiangiogenic agent is injected into the eye. After 14 days the choroidal layer is removed and confocal images of the blood vessel stained choroids are taken and analyzed. This model has become the standard model to evaluate the antiangiogenic potential of pharmacologic therapies of CNV. The model can be used to assess gene therapy, siRNA targeting, novel delivery platforms and AAV mediated transfections. The L-CNV mouse model is relatively simple to create, inexpensive, reproducible, efficient and less time consuming than transgenic (VEGF₁₆₄RPE65, Ccr2/Ccl2 deficient, ApoE overexpression) and knock out

(Cp^{-/-} Hep^{-Y}) mice models (Grossniklaus, 2010). The model could also be used with transgenic mice such as Fech mutated mice to assess the pathobiology of CNV under decreased FECH activity. Also, CNV can be monitored using an OCT technique without killing the mice. Disadvantages of the model are that the model is artificial in nature and (unlike humans) mice do not have a macula. Despite this L-CNV is the standard animal model of CNV for most treatment evaluations. We used L-CNV model to test if FECH inhibition can be exploited to block choroidal neovascularization as seen in cell-based models. As expected, administration of siRNAs specific to FECH inhibited choroidal neovascularization. The same model was also used to confirm that chemical inhibition of FECH by griseofulvin leads to blocking of choroidal neovascularization.

In the OIR mouse model pups are placed in an oxygen chamber (75 % O₂) from P7 to P12, then brought back to normal room conditions (21 % O₂) and injected with antiangiogenic agents on P12. The mice pups are sacrificed on P17 and retinal whole mounts are stained for blood vessels and neovascularization is manually counted. This model is the standard animal model to assess pharmacological treatments. The neovascular response in the model is very consistent, reproducible and quantifiable. The major disadvantage of this model is the fact that central retinal vessels, rather than peripheral retinal vessels, are obliterated during hyperoxic exposure. This is different from what happens in ROP where the peripheral retinal vessels fail to develop. Despite this key difference, the mouse OIR model very closely recapitulates the pathologic events

of ROP. Using this model I could establish that compound SH-11037 inhibited ocular angiogenesis in vivo.

In summary, I have used different techniques ranging from purified protein based affinity chromatography to cell-based in vitro approaches to animal based in vivo techniques. All of these techniques helped me develop SAR for cremastranone, selecting a novel and specific ocular antiangiogenic molecule SH-11037 and confirming the role of FECH in ocular angiogenesis both in vitro as well as in vivo.

6.6. POTENTIAL LIMITATIONS OF THE STUDY

Photo-affinity based pull down approach was the basis for identification of targets of cremastranone and the assumption was that the technique pulls down many target proteins considering the polypharmacology of natural products. I optimized the pull down approach and repeatedly pulled down FECH as one of the specific target proteins along with pyridoxal kinase (PDXK) enzyme in at least three independent experiments. However I didn't find any other proteins pulled down with the affinity reagent, suggesting either the affinity between affinity reagent and other target proteins was weak or there was insufficient UV-cross linking. In both cases the loosely bound proteins would have been washed off during rigorous washing steps. Thus FECH might not be the only target through which cremastranone exerts its antiangiogenic activity. I pursued FECH as during the target validation FECH was confirmed to be a specific binding partner of cremastranone and FECH inhibition by siRNA inhibited the angiogenic abilities of

HRECs. Although knock down of PDXK enzyme inhibited the ability of HREC proliferation and migration there was no effect on tube formation ability HRECs in vitro (Fig. 5.3). Hence PDXK was not pursued further for mechanistic studies.

Moreover for protein source I used porcine brain as the protein amount recovered from large scale HREC culturing was minimal, and growth was expensive. Even though I have established that cremastranone inhibits FECH activity in HRECs, it is possible that cremastranone can interact with other proangiogenic proteins specifically in HRECs and modulate their function. Nonetheless identification and validation of FECH itself is a novel work in ocular angiogenesis biology.

Another limitation of the study is the choice of ocular non-endothelial cell lines used in proliferation assays. 92-1 and Y79 are uveal melanoma and retinoblastoma cell lines, respectively. They do not represent the normal, functional non-endothelial ocular cells. Only ARPE-19 represents the non-transformed RPE cells of the eye and in future it would be useful to incorporate one or two more non-endothelial ocular cells which represent the cells of normal eye and are amenable for high-throughput proliferation assay.

6.7. FUTURE DIRECTIONS

I identified FECH as a mediator of ocular angiogenesis and showed that loss of FECH activity results in decreased levels of eNOS, HIF-1 α and VEGFR-2 in HRECs. These findings further raise new questions regarding the functional role of FECH in different cells and its expression under pathological conditions.

6.7.1. *Understanding the role of FECH in angiogenesis*

Using an siRNA based approach combined with immunoblot technique I showed that FECH knock down decreased levels of eNOS. This is used as a basis to rationalize that HIF-1 α levels are decreased, as eNOS is responsible for the stability of HIF-1 α under normoxia (Mateo et al., 2003; Olson and van der Vliet, 2011; Palmer et al., 2000). However it would be good to show this decrease in HIF-1 α in other secondary assays such as luciferase reporter assays wherein we can monitor the transcriptional activity of HIF-1 α after FECH knock down. Also, it needs to be tested if exogenous addition of NO donors will rescue HIF-1 α levels in FECH knock down HRECs. These experiments will confirm if FECH regulates HIF-1 α levels through eNOS. Also it would be interesting to study the effect of overexpression of HIF-1 α in FECH knock down HRECs on the angiogenic abilities of HRECs.

Decreased HIF-1 α results in VEGFR-2 reduction in HRECs (Forsythe et al., 1996). However, it would be interesting to know if HIF-1 α levels are decreased under hypoxia when FECH is knocked down, as HIF-1 α stability is

increased because of reduced activities of PHDs and VHL. This would suggest if there are additional mechanisms through which FECH exerts its angiogenic activities. Also, it would be interesting to delineate if reduction in VEGFR2 is the direct result of decreased HIF-1 α or decreased VEGF production. HIF-1 α is responsible for transcription of VEGF gene (Minchenko et al., 1994) and the VEGF in turn stimulates production of VEGFR2 (Guangqi et al., 2012).

6.7.2. FECH functions in endothelial and non-endothelial cells

To date, there is no satisfactory explanation for why 5-ALA administration results in accumulation of porphyrins in endothelial cells and actively growing cancer cells (Dailey et al., 2000; Inoue et al., 2013). Being an inducer of heme biosynthesis, 5-ALA should have resulted in accumulation of heme or its degradation products such as biliverdin. This suggests that there are additional regulation mechanisms controlling activity of FECH in endothelial cells. It will be interesting to know these control mechanisms and FECH interacting proteins. Identification of FECH interacting proteins both in HRECs as well as non-endothelial ocular cells will help explain why FECH inhibition specifically affects HRECs. Also, identifying other heme-binding proteins which are specifically affected by FECH knock down will give us some clues to the role of these hemoproteins in ocular angiogenesis. This will broaden our knowledge about angiogenesis and open new ways to target angiogenesis specifically.

Also, IHC experiments showed that FECH is upregulated throughout the retina and choroid in wet AMD patients. This corroborates the reports that FECH

expression is induced by hypoxia as choroidal neovascularization in patients is associated with hypoxia. As hypoxia upregulates FECH expression throughout the retina and choroid, it is imperative to understand what are the factors that make retinal endothelial cells specifically vulnerable to FECH inhibition. Hence understanding the FECH interacting partners in both retinal endothelial as well as non-endothelial cells provide the clue for this selected vulnerability and also opens up potential angiogenic pathways in which FECH could participate.

6.7.3. Study of CNV and RNV in *FECH* mutant mice

There are two different mouse models for EPP. Both of these models have a mutated *Fech* gene, and as a result have decreased Fech activity. One of the mouse models, the *Fech*^{m1Pas} mouse, was generated by chemical mutagenesis wherein a missense mutation (M98K) causes less than 10 % residual activity in a homozygous mouse (Boulechfar et al., 1993). However a heterozygous mouse shows 45-65 % of normal FECH activity. In the other mouse model, exon 10 of the *Fech* gene is deleted and 50 % residual enzyme activity is observed in a heterozygous mouse (Magness and Brenner, 1999). While homozygous *Fech*^{m1Pas} display protoporphyria, heterozygous mice have a normal phenotype.

Subjecting these mouse models to OIR and L-CNV and studying neovascularization in these models will confirm the role of FECH in ocular diseases arising from pathological angiogenesis. This will also help understand the molecular mechanism by which FECH exerts its angiogenic activity. Measurement of the levels of eNOS, HIF-1 α and VEGFR2 in these mice under

ischemic conditions will help us to confirm in vitro results and pave the way for further elucidation of the mechanism.

6.7.4 Therapeutic potential of FECH inhibitors

We have shown that FECH is crucial for ocular neovascularization and inhibitors of FECH could be developed to specifically target CNV and RNV. This work reveals three potential molecules for drug development: cremastranone, SH-11037 and griseofulvin.

Cremastranone isolated from extracts of *Cremastra appendiculata* has been tested by others in both L-CNV and OIR mouse models for its antiangiogenic activity and toxicity (Kim et al., 2007; Kim et al., 2008). It inhibited ocular neovascularization in both the mouse models. Considering its high potency and less toxic effects on other cell lines, cremastranone might be developed as a drug to treat ocular diseases such as wet AMD, PDR and ROP. In addition I established SAR for cremastranone along with identification of the more potent compound, SH-11037. Similarly, compound SH-11037 has also been tested in the OIR mouse model and shown to inhibit retinal neovascularization with high potency. The high potency and selectivity against HRECs make SH-11037 a particularly appealing lead molecule for drug discovery. However there are still many pharmacokinetic and pharmacodynamic properties of cremastranone and SH-11037 that need to be established. As both cremastranone and SH-11037 are small molecules, formulating them as eye

drops for treatment would be another possible advantage as a therapy for patients who receive intraocular injection of biologic drugs.

Another important observation from this work is that griseofulvin, an antifungal drug with an off-target effect of inhibiting the mammalian FECH activity (Brady and Lock, 1992; Epstein et al., 1972), blocks ocular neovascularization in the L-CNV model when administered orally and also through intraocular injection. Griseofulvin is an orally administered drug and has very well established pharmacokinetic and pharmacodynamic properties. Its presence in the market for several decades without any major toxicity issues make it an appealing drug for immediate testing in human clinical trials.

6.8. CONCLUSION

Altogether, this research work has encompassed a variety of drug discovery initiatives such as cremastranone target identification, target validation of FECH, establishing SAR of a lead molecule (SH-11037) and testing in preclinical models along with supporting data for repurposing of griseofulvin for treating ocular diseases arising from pathological angiogenesis. This work has revealed FECH as a novel mediator of ocular angiogenesis along with profiling of three small molecules as either lead molecules or drugs for treating ROP, PDR and wet AMD. The hope is that this discovery will help further understanding of the role of FECH in angiogenesis. The greater anticipation from this work is that one day this work may lead to successful new drugs for treating ROP, PDR and wet AMD.

CHAPTER 7. REFERENCES

1. Abouammoh, M., and Sharma, S. (2011). Ranibizumab versus bevacizumab for the treatment of neovascular age-related macular degeneration. *Curr Opin Ophthalmol* 22, 152-158.
2. Alitalo, K., and Carmeliet, P. (2002). Molecular mechanisms of lymphangiogenesis in health and disease. *Cancer Cell* 1, 219-227.
3. Arnaoutova, I., and Kleinman, H.K. (2010). In vitro angiogenesis: endothelial cell tube formation on gelled basement membrane extract. *Nat Protoc* 5, 628-635.
4. Asahara, T., Murohara, T., Sullivan, A., Silver, M., van der Zee, R., Li, T., Witzenbichler, B., Schatteman, G., and Isner, J.M. (1997). Isolation of putative progenitor endothelial cells for angiogenesis. *Science* 275, 964-967.
5. Asano, H., Li, X.S., and Stamatoyannopoulos, G. (2000). FKLf-2: a novel Kruppel-like transcriptional factor that activates globin and other erythroid lineage genes. *Blood* 95, 3578-3584.
6. Avery, R.L., Pieramici, D.J., Rabena, M.D., Castellarin, A.A., Nasir, M.A., and Giust, M.J. (2006). Intravitreal bevacizumab (Avastin) for neovascular age-related macular degeneration. *Ophthalmology* 113, 363-372.e365.
7. Basavarajappa, H.D., Lee, B., Fei, X., Lim, D., Callaghan, B., Mund, J.A., Case, J., Rajashekhar, G., Seo, S.Y., and Corson, T.W. (2014). Synthesis and mechanistic studies of a novel homoisoflavanone inhibitor of endothelial cell growth. *PLoS ONE* 9.
8. Basavarajappa, H.D., Lee, B., Lee, H., Sulaiman, R.S., An, H., Magana, C., Shadmand, M., Vayl, A., Rajashekhar, G., Kim, E.Y., et al. (2015). Synthesis and biological evaluation of novel homoisoflavonoids for retinal neovascularization. *J Med Chem* 58, 5015-5027.
9. Bergers, G., and Song, S. (2005). The role of pericytes in blood-vessel formation and maintenance. *Neuro Oncol* 7, 452-464.
10. Bid, H.K., Oswald, D., Li, C., London, C.A., Lin, J., and Houghton, P.J. (2012). Anti-angiogenic activity of a small molecule STAT3 inhibitor LLL12. *PLoS ONE* 7, 17.
11. Borgers, M. (1980). Mechanism of action of antifungal drugs, with special reference to the imidazole derivatives. *Rev Infect Dis* 2, 520-534.
12. Boulechfar, S., Lamoril, J., Montagutelli, X., Guenet, J.L., Deybach, J.C., Nordmann, Y., Dailey, H., Grandchamp, B., and de Verneuil, H. (1993). Ferrochelatase structural mutant (Fechm1Pas) in the house mouse. *Genomics* 16, 645-648.
13. Brady, A.M., and Lock, E.A. (1992). Inhibition of ferrochelatase and accumulation of porphyrins in mouse hepatocyte cultures exposed to porphyrinogenic chemicals. *Arch Toxicol* 66, 175-181.

14. Brennan, C.M., and Steitz, J.A. (2001). HuR and mRNA stability. *Cell Mol Life Sci* 58, 266-277.
15. Carmeliet, P. (2000). Mechanisms of angiogenesis and arteriogenesis. *Nat Med* 6, 389-395.
16. Carmeliet, P. (2003). Angiogenesis in health and disease. *Nat Med* 9, 653-660.
17. Carmeliet, P., Dor, Y., Herbert, J.M., Fukumura, D., Brusselmans, K., Dewerchin, M., Neeman, M., Bono, F., Abramovitch, R., Maxwell, P., et al. (1998). Role of HIF-1alpha in hypoxia-mediated apoptosis, cell proliferation and tumour angiogenesis. *Nature* 394, 485-490.
18. Carmeliet, P., Ferreira, V., Breier, G., Pollefeyt, S., Kieckens, L., Gertsenstein, M., Fahrig, M., Vandenhoek, A., Harpal, K., Eberhardt, C., et al. (1996). Abnormal blood vessel development and lethality in embryos lacking a single VEGF allele. *Nature* 380, 435-439.
19. Carmeliet, P., and Jain, R.K. (2011). Molecular mechanisms and clinical applications of angiogenesis. *Nature* 473, 298-307.
20. Chen, G., and Goeddel, D.V. (2002). TNF-R1 signaling: a beautiful pathway. *Science* 296, 1634-1635.
21. Chen, J., and Smith, L.E. (2007). Retinopathy of prematurity. *Angiogenesis* 10, 133-140.
22. Cole, S.P., and Marks, G.S. (1984). Ferrochelatase and N-alkylated porphyrins. *Mol Cell Biochem* 64, 127-137.
23. Corson, T.W., Cavga, H., Aberle, N., and Crews, C.M. (2011). Triptolide directly inhibits dCTP pyrophosphatase. *Chembiochem* 12, 1767-1773.
24. Corson, T.W., and Crews, C.M. (2007). Molecular understanding and modern application of traditional medicines: triumphs and trials. *Cell* 130, 769-774.
25. Crouch, N.R., Bangani, V., and Mulholland, D.A. (1999). Homoisoflavanones from three South African: *Scilla* species. *Phytochemistry* 51, 943-946.
26. Dailey, H.A., Dailey, T.A., Wu, C.K., Medlock, A.E., Wang, K.F., Rose, J.P., and Wang, B.C. (2000). Ferrochelatase at the millennium: structures, mechanisms and [2Fe-2S] clusters. *Cell Mol Life Sci* 57, 1909-1926.
27. Dailey, H.A., Sellers, V.M., and Dailey, T.A. (1994). Mammalian ferrochelatase. Expression and characterization of normal and two human protoporphyrin ferrochelatases. *J Biol Chem* 269, 390-395.
28. Das, A., and McGuire, P.G. (2003). Retinal and choroidal angiogenesis: pathophysiology and strategies for inhibition. *Prog Retin Eye Res* 22, 721-748.

29. du Toit, K., Drewes, S.E., and Bodenstein, J. (2010). The chemical structures, plant origins, ethnobotany and biological activities of homoisoflavanones. *Nat Prod Res* 24, 457-490.
30. du Toit, K., Elgorashi, E.E., Malan, S.F., Drewes, S.E., van Staden, J., Crouch, N.R., and Mulholland, D.A. (2005). Anti-inflammatory activity and QSAR studies of compounds isolated from Hyacinthaceae species and *Tachiadenus longiflorus* Griseb. (Gentianaceae). *Bioorg Med Chem* 13, 2561-2568.
31. Dulak, J., Deshane, J., Jozkowicz, A., and Agarwal, A. (2008). Heme oxygenase-1 and carbon monoxide in vascular pathobiology: focus on angiogenesis. *Circulation* 117, 231-241.
32. E, Guangqi, Cao, Y., Bhattacharya, S., Dutta, S., Wang, E., and Mukhopadhyay, D. (2012). Endogenous Vascular Endothelial Growth Factor-A (VEGF-A) maintains endothelial cell homeostasis by regulating VEGF Receptor-2 transcription. *J Biol Chem* 287, 3029-3041.
33. Economopoulou, M., Bdeir, K., Cines, D.B., Fogt, F., Bdeir, Y., Lubkowski, J., Lu, W., Preissner, K.T., Hammes, H.P., and Chavakis, T. (2005). Inhibition of pathologic retinal neovascularization by alpha-defensins. *Blood* 106, 3831-3838.
34. Ehrlich, R., Kheradiya, N.S., Winston, D.M., Moore, D.B., Wirostko, B., and Harris, A. (2009). Age-related ocular vascular changes. *Graefes Arch Clin Exp Ophthalmol* 247, 583-591.
35. Elewski, B., and Tavakkol, A. (2005). Safety and tolerability of oral antifungal agents in the treatment of fungal nail disease: a proven reality. *Ther Clin Risk Manag* 1, 299-306.
36. Englander, M., and Kaiser, P.K. (2013). Combination therapy for the treatment of neovascular age-related macular degeneration. *Curr Opin Ophthalmol* 24, 233-238.
37. Epstein, W.L., Shah, V.P., and Riegelman, S. (1972). Griseofulvin levels in stratum corneum. Study after oral administration in man. *Arch Dermatol* 106, 344-348.
38. Faia, L.J., and Trese, M.T. (2011). Retinopathy of prematurity care: screening to vitrectomy. *Int Ophthalmol Clin* 51, 1-16.
39. Falkenstein, I.A., Cheng, L., Wong-Staal, F., Tammewar, A.M., Barron, E.C., Silva, G.A., Li, Q.X., Yu, D., Hysell, M., Liu, G., et al. (2008). Toxicity and intraocular properties of a novel long-acting anti-proliferative and anti-angiogenic compound IMS2186. *Curr Eye Res* 33, 599-609.
40. Farkas, L., Gottsegen, Á., Nógrádi, M., and Strelisky, J. (1971). Synthesis of homoisoflavanones—II: Constituents of *Eucomis autumn alis* and *E. Punctata*. *Tetrahedron* 27, 5049-5054.

41. Farkas, L., and Strelisky, J. (1970). The direct synthesis of 5,7-dihydroxy-6-methoxyflavones I. synthesis of 4',6-dimethoxy-3',5,7-trihydroxyflavone and pectolinarigenin. *Tetrahedron Letters* 11, 187-190.
42. Ferrara, N. (1999). Role of vascular endothelial growth factor in the regulation of angiogenesis. *Kidney Int* 56, 794-814.
43. Ferrara, N., Carver-Moore, K., Chen, H., Dowd, M., Lu, L., O'Shea, K.S., Powell-Braxton, L., Hillan, K.J., and Moore, M.W. (1996). Heterozygous embryonic lethality induced by targeted inactivation of the VEGF gene. *Nature* 380, 439-442.
44. Fine, S.L., Berger, J.W., Maguire, M.G., and Ho, A.C. (2000). Age-Related Macular Degeneration. *N Engl J Med* 342, 483-492.
45. Folk, J.C., and Stone, E.M. (2010). Ranibizumab therapy for neovascular age-related macular degeneration. *N Engl J Med* 363, 1648-1655.
46. Förstermann, U., and Münzel, T. (2006). Endothelial nitric oxide synthase in vascular disease: from marvel to menace. *Circulation* 113, 1708-1714.
47. Forsythe, J.A., Jiang, B.H., Iyer, N.V., Agani, F., Leung, S.W., Koos, R.D., and Semenza, G.L. (1996). Activation of vascular endothelial growth factor gene transcription by hypoxia-inducible factor 1. *Mol Cell Biol* 16, 4604-4613.
48. Fotsis, T., Pepper, M.S., Aktas, E., Breit, S., Rasku, S., Adlercreutz, H., Wahala, K., Montesano, R., and Schweigerer, L. (1997). Flavonoids, dietary-derived inhibitors of cell proliferation and in vitro angiogenesis. *Cancer Res* 57, 2916-2921.
49. Friedlander, M. (2009). Combination angiostatic therapies: targeting multiple angiogenic pathways. *Retina* 29, S27-29.
50. Gilbert, C., Rahi, J., Eckstein, M., O'Sullivan, J., and Foster, A. (1997). Retinopathy of prematurity in middle-income countries. *Lancet* 350, 12-14.
51. Gilbert, R.E., Vranes, D., Berka, J.L., Kelly, D.J., Cox, A., Wu, L.L., Stacker, S.A., and Cooper, M.E. (1998). Vascular endothelial growth factor and its receptors in control and diabetic rat eyes. *Lab Invest* 78, 1017-1027.
52. Goldberg, A., M., A., E., C.G., and M., W.M. (1956). Studies on the Biosynthesis of Heme In Vitro by Avian Erythrocytes. *Blood* 11, 821-833.
53. Goodwin, A.M. (2007). In vitro assays of angiogenesis for assessment of angiogenic and anti-angiogenic agents. *Microvasc Res* 74, 172-183.
54. Gouya, L., Puy, H., Lamoril, J., Da Silva, V., Grandchamp, B., Nordmann, Y., and Deybach, J.-C. (1999). Inheritance in erythropoietic protoporphyria: a common wild-type ferrochelatase allelic variant with low expression accounts for clinical manifestation. *Blood* 93, 2105-2110.

55. Gragoudas, E.S., Adamis, A.P., Cunningham, E.T.J., Feinsod, M., and Guyer, D.R. (2004). Pegaptanib for neovascular age-related macular degeneration. *N Engl J Med* 351, 2805-2816.
56. Grant, M.B., May, W.S., Caballero, S., Brown, G.A., Guthrie, S.M., Mames, R.N., Byrne, B.J., Vaught, T., Spoerri, P.E., Peck, A.B., et al. (2002). Adult hematopoietic stem cells provide functional hemangioblast activity during retinal neovascularization. *Nat Med* 8, 607-612.
57. Gridley, T. (2010). Notch signaling in the vasculature. *Curr Top Dev Biol* 92, 277-309.
58. Grossniklaus, H.E. (2010). Animal models of choroidal and retinal neovascularization. *Prog Retin Eye Res* 29, 500-519.
59. Grover, C., Arora, P., and Manchanda, V. (2012). Comparative evaluation of griseofulvin, terbinafine and fluconazole in the treatment of tinea capitis. *Int J Dermatol* 51, 455-458.
60. Gupta, S.C., Sundaram, C., Reuter, S., and Aggarwal, B.B. (2010). Inhibiting NF- κ B activation by small molecules as a therapeutic strategy. *Biochim Biophys Acta* 1799, 775-787.
61. Gupta, V., Liu, S., Ando, H., Ishii, R., Tateno, S., Kaneko, Y., Yugami, M., Sakamoto, S., Yamaguchi, Y., Nureki, O., et al. (2013). Salicylic acid induces mitochondrial injury by inhibiting ferrochelatase heme biosynthesis activity. *Mol Pharmacol* 84, 824-833.
62. Hamza, I., and Dailey, H.A. (2012). One ring to rule them all: trafficking of heme and heme synthesis intermediates in the metazoans. *Biochim Biophys Acta* 1823, 1617-1632.
63. Hanneken, A., de Juan, E., Jr., Luttly, G.A., Fox, G.M., Schiffer, S., and Hjelmeland, L.M. (1991). Altered distribution of basic fibroblast growth factor in diabetic retinopathy. *Arch Ophthalmol* 109, 1005-1011.
64. Hanout, M., Ferraz, D., Ansari, M., Maqsood, N., Kherani, S., Sepah, Y.J., Rajagopalan, N., Ibrahim, M., Do, D.V., and Nguyen, Q.D. (2013). Therapies for neovascular age-related macular degeneration: current approaches and pharmacologic agents in development. *Biomed Res Int* 830837, 11.
65. Hasebe, Y., Egawa, K., Yamazaki, Y., Kunimoto, S., Hirai, Y., Ida, Y., and Nose, K. (2003). Specific inhibition of hypoxia-inducible factor (HIF)-1 α activation and of vascular endothelial growth factor (VEGF) production by flavonoids. *Biol Pharm Bull* 26, 1379-1383.
66. Heier, J.S., Brown, D.M., Chong, V., Korobelnik, J.F., Kaiser, P.K., Nguyen, Q.D., Kirchhof, B., Ho, A., Ogura, Y., Yancopoulos, G.D., et al. (2012). Intravitreal aflibercept (VEGF trap-eye) in wet age-related macular degeneration. *Ophthalmology* 119, 2537-2548.

67. Hellstrom, M., Kalen, M., Lindahl, P., Abramsson, A., and Betsholtz, C. (1999). Role of PDGF-B and PDGFR-beta in recruitment of vascular smooth muscle cells and pericytes during embryonic blood vessel formation in the mouse. *Development* 126, 3047-3055.
68. Hesse, B., and Moser, R. (2003). Health Information National Trends Survey (HINTS), 2003 (Ann Arbor, MI: Inter-university Consortium for Political and Social Research).
69. Hodge, W., Brown, A., Kymes, S., Cruess, A., Blackhouse, G., Hopkins, R., McGahan, L., Sharma, S., Pan, I., Blair, J., et al. (2010). Pharmacologic management of neovascular age-related macular degeneration: systematic review of economic evidence and primary economic evaluation. *Can J Ophthalmol* 45, 223-230.
70. Hoeben, A., Landuyt, B., Highley, M.S., Wildiers, H., Van Oosterom, A.T., and De Bruijn, E.A. (2004). Vascular endothelial growth factor and angiogenesis. *Pharmacol Rev* 56, 549-580.
71. Holley, A., King, L.J., Gibbs, A.H., and De Matteis, F. (1990). Strain and sex differences in the response of mice to drugs that induce protoporphyria: role of porphyrin biosynthesis and removal. *J Biochem Toxicol* 5, 175-182.
72. Hughes, S., and Chan-Ling, T. (2004). Characterization of smooth muscle cell and pericyte differentiation in the rat retina in vivo. *Invest Ophthalmol Vis Sci* 45, 2795-2806.
73. Hur, S., Lee, Y.S., Yoo, H., Yang, J.H., and Kim, T.Y. (2010). Homoisoflavanone inhibits UVB-induced skin inflammation through reduced cyclooxygenase-2 expression and NF- κ B nuclear localization. *J Dermatol Sci* 59, 163-169.
74. Ikeda, Y., Nonaka, H., Furumai, T., and Igarashi, Y. (2005). Cremastrine, a pyrrolizidine alkaloid from *Cremastra appendiculata*. *Journal of natural products* 68, 572-573.
75. Inoue, K., Fukuhara, H., Kurabayashi, A., Furihata, M., Tsuda, M., Nagakawa, K., Fujita, H., Utsumi, K., and Shuin, T. (2013). Photodynamic therapy involves an antiangiogenic mechanism and is enhanced by ferrochelatase inhibitor in urothelial carcinoma. *Cancer Sci* 104, 765-772.
76. Ivanova, L., Varinska, L., Pilatova, M., Gal, P., Solar, P., Perjesi, P., Smetana, K., Jr., Ostro, A., and Mojzis, J. (2013). Cyclic chalcone analogue KRP6 as a potent modulator of cell proliferation: an in vitro study in HUVECs. *Mol Biol Rep* 40, 4571-4580.
77. Ji, H.F., Li, X.J., and Zhang, H.Y. (2009). Natural products and drug discovery. Can thousands of years of ancient medical knowledge lead us to new and powerful drug combinations in the fight against cancer and dementia? *EMBO reports* 10, 194-200.

78. Kaiser, P.K. (2013). Emerging therapies for neovascular age-related macular degeneration: drugs in the pipeline. *Ophthalmology* 120, S11-15.
79. Kang, Y.J., Mbonye, U.R., DeLong, C.J., Wada, M., and Smith, W.L. (2007). Regulation of intracellular cyclooxygenase levels by gene transcription and protein degradation. *Prog Lipid Res* 46, 108-125.
80. Karr, S.R., and Dailey, H.A. (1988). The synthesis of murine ferrochelatase in vitro and in vivo. *Biochem J* 254, 799-803.
81. Kim, J.H., Kim, K.H., Yu, Y.S., Kim, Y.M., Kim, K.W., and Kwon, H.J. (2007). Homoisoflavanone inhibits retinal neovascularization through cell cycle arrest with decrease of cdc2 expression. *Biochem Biophys Res Commun* 362, 848-852.
82. Kim, J.H., Lee, Y.M., Ahn, E.M., Kim, K.W., and Yu, Y.S. (2009). Decursin inhibits retinal neovascularization via suppression of VEGFR-2 activation. *Mol Vis* 15, 1868-1875.
83. Kim, J.H., Yu, Y.S., Jun, H.O., Kwon, H.J., Park, K.H., and Kim, K.W. (2008). Inhibition of choroidal neovascularization by homoisoflavanone, a new angiogenesis inhibitor. *Mol Vis* 14, 556-561.
84. Kimura, H., Spee, C., Sakamoto, T., Hinton, D.R., Ogura, Y., Tabata, Y., Ikada, Y., and Ryan, S.J. (1999). Cellular response in subretinal neovascularization induced by bFGF-impregnated microspheres. *Invest Ophthalmol Vis Sci* 40, 524-528.
85. Klein, S., de Fougerolles, A.R., Blaikie, P., Khan, L., Pepe, A., Green, C.D., Koteliansky, V., and Giancotti, F.G. (2002). $\alpha 5 \beta 1$ integrin activates an NF- κ B-dependent program of gene expression important for angiogenesis and inflammation. *Mol Cell Biol* 22, 5912-5922.
86. Koehn, F.E., and Carter, G.T. (2005). The evolving role of natural products in drug discovery. *Nat Rev Drug Discov* 4, 206-220.
87. Lai, S.L., Cheah, S.C., Wong, P.F., Noor, S.M., and Mustafa, M.R. (2012). In vitro and in vivo anti-angiogenic activities of Panduratin A. *PLoS ONE* 7, 30.
88. Lallena, M.J., Diaz-Meco, M.T., Bren, G., Paya, C.V., and Moscat, J. (1999). Activation of I κ B kinase β by protein kinase C isoforms. *Mol Cell Biol* 19, 2180-2188.
89. Lally, D.R., Gerstenblith, A.T., and Regillo, C.D. (2012). Preferred therapies for neovascular age-related macular degeneration. *Curr Opin Ophthalmol* 23, 182-188.
90. Lambert, V., Lecomte, J., Hansen, S., Blacher, S., Gonzalez, M.L., Struman, I., Sounni, N.E., Rozet, E., de Tullio, P., Foidart, J.M., et al. (2013). Laser-induced choroidal neovascularization model to study age-related macular degeneration in mice. *Nat Protoc* 8, 2197-2211.

91. Layer, G., Reichelt, J., Jahn, D., and Heinz, D.W. (2010). Structure and function of enzymes in heme biosynthesis. *Protein Sci* 19, 1137-1161.
92. Lecha, M., Puy, H., and Deybach, J.C. (2009). Erythropoietic protoporphyria. *Orphanet J Rare Dis* 4, 1750-1172.
93. Lee, B., Basavarajappa, H.D., Sulaiman, R.S., Fei, X., Seo, S.Y., and Corson, T.W. (2014). The first synthesis of the antiangiogenic homoisoflavanone, cremastranone. *Org Biomol Chem* 28, 28.
94. Lee, Y.S., Hur, S., and Kim, T.Y. (2014). Homoisoflavanone prevents mast cell activation and allergic responses by inhibition of Syk signaling pathway. *Allergy* 69, 453-462.
95. Li, J.W., and Vederas, J.C. (2009). Drug discovery and natural products: end of an era or an endless frontier? *Science* 325, 161-165.
96. Liang, C.-C., Park, A.Y., and Guan, J.-L. (2007). In vitro scratch assay: a convenient and inexpensive method for analysis of cell migration in vitro. *Nat Protocols* 2, 329-333.
97. Lin, M., Sun, W., Gong, W., Zhou, Z., Ding, Y., and Hou, Q. (2015). Methylophiopogonanone A protects against cerebral ischemia/reperfusion injury and attenuates blood-brain barrier disruption in vitro. *PLoS One* 10, e0124558.
98. Liu, K., Yan, J., Sachar, M., Zhang, X., Guan, M., Xie, W., and Ma, X. (2015). A metabolomic perspective of griseofulvin-induced liver injury in mice. *Biochem Pharmacol* 98, 493-501.
99. Liu, R.Y., Fan, C., Liu, G., Olashaw, N.E., and Zuckerman, K.S. (2000). Activation of p38 mitogen-activated protein kinase is required for tumor necrosis factor- α -supported proliferation of leukemia and lymphoma cell lines. *J Biol Chem* 275, 21086-21093.
100. Liu, Y.L., Ang, S.O., Weigent, D.A., Prchal, J.T., and Bloomer, J.R. (2004). Regulation of ferrochelatase gene expression by hypoxia. *Life Sci* 75, 2035-2043.
101. Lochhead, A.C., Dagg, J.H., and Goldberg, A. (1967). Experimental griseofulvin porphyria in adult and foetal mice. *Br J Dermatol* 79, 96-102.
102. Lux, A., Llacer, H., Heussen, F.M., and Joussen, A.M. (2007). Non-responders to bevacizumab (Avastin) therapy of choroidal neovascular lesions. *Br J Ophthalmol* 91, 1318-1322.
103. Maehara, K., Hasegawa, T., and Isobe, K.I. (2000). A NF- κ B p65 subunit is indispensable for activating manganese superoxide dismutase gene transcription mediated by tumor necrosis factor- α . *J Cell Biochem* 77, 474-486.

104. Magness, S.T., and Brenner, D.A. (1999). Targeted disruption of the mouse ferrochelatase gene producing an exon 10 deletion. *Biochim Biophys Acta* 1453, 161-174.
105. Majumdar, S., and Srirangam, R. (2010). Potential of the bioflavonoids in the prevention/treatment of ocular disorders. *J Phar Pharmacol* 62, 951-965.
106. Manach, C., Scalbert, A., Morand, C., Remesy, C., and Jimenez, L. (2004). Polyphenols: food sources and bioavailability. *Am J Clin Nutr* 79, 727-747.
107. Martinez, M.C., Afonso, S.G., Meiss, R.P., Buzaleh, A.M., and Batlle, A. (2009). Hepatic damage and oxidative stress induced by griseofulvin in mice. *Cell Mol Biol* 55, 127-139.
108. Mateo, J., Garcia-Lecea, M., Cadenas, S., Hernandez, C., and Moncada, S. (2003). Regulation of hypoxia-inducible factor-1 α by nitric oxide through mitochondria-dependent and -independent pathways. *Biochem J* 376, 537-544.
109. Mense, S.M., and Zhang, L. (2006). Heme: a versatile signaling molecule controlling the activities of diverse regulators ranging from transcription factors to MAP kinases. *Cell Res* 16, 681-692.
110. Meyer, R.D., Latz, C., and Rahimi, N. (2003). Recruitment and activation of phospholipase Cy1 by vascular endothelial growth factor receptor-2 are required for tubulogenesis and differentiation of endothelial cells. *J Biol Chem* 278, 16347-16355.
111. Miller, J.W., Adamis, A.P., and Aiello, L.P. (1997). Vascular endothelial growth factor in ocular neovascularization and proliferative diabetic retinopathy. *Diabetes Metab Rev* 13, 37-50.
112. Minchenko, A., Bauer, T., Salceda, S., and Caro, J. (1994). Hypoxic stimulation of vascular endothelial growth factor expression in vitro and in vivo. *Lab Invest* 71, 374-379.
113. Mishra, B.B., and Tiwari, V.K. (2011). Natural products: an evolving role in future drug discovery. *Eur J Med Chem* 46, 4769-4807.
114. Mitchell, P., Annemans, L., White, R., Gallagher, M., and Thomas, S. (2011). Cost effectiveness of treatments for wet age-related macular degeneration. *Pharmacoeconomics* 29, 107-131.
115. Mohan, R., Hammers, H.J., Bargagna-Mohan, P., Zhan, X.H., Herbstritt, C.J., Ruiz, A., Zhang, L., Hanson, A.D., Conner, B.P., Rougas, J., et al. (2004). Withaferin A is a potent inhibitor of angiogenesis. *Angiogenesis* 7, 115-122.
116. Montezuma, S.R., Vavvas, D., and Miller, J.W. (2009). Review of the ocular angiogenesis animal models. *Semin Ophthalmol* 24, 52-61.

117. Mulholland, D.A., Schwikkard, S.L., and Crouch, N.R. (2013). The chemistry and biological activity of the Hyacinthaceae. *Nat Prod Rep* 30, 1165-1210.
118. Muppala, V., Lin, C.S., and Lee, Y.H. (2000). The role of HNF-1alpha in controlling hepatic catalase activity. *Mol Pharmacol* 57, 93-100.
119. Newman, D.J., Cragg, G.M., and Snader, K.M. (2003). Natural products as sources of new drugs over the period 1981-2002. *J Nat Prod* 66, 1022-1037.
120. Niphakis, M.J., Lum, K.M., Cognetta, A.B., 3rd, Correia, B.E., Ichu, T.A., Olucha, J., Brown, S.J., Kundu, S., Piscitelli, F., Rosen, H., et al. (2015). A global map of lipid-binding proteins and their ligandability in cells. *Cell* 161, 1668-1680.
121. Oh, H., Takagi, H., Takagi, C., Suzuma, K., Otani, A., Ishida, K., Matsumura, M., Ogura, Y., and Honda, Y. (1999). The potential angiogenic role of macrophages in the formation of choroidal neovascular membranes. *Invest Ophthalmol Vis Sci* 40, 1891-1898.
122. Olson, N., and van der Vliet, A. (2011). Interactions between nitric oxide and hypoxia-inducible factor signaling pathways in inflammatory disease. *Nitric Oxide* 25, 125-137.
123. Omar, H.A., Arafa el, S.A., Salama, S.A., Arab, H.H., Wu, C.H., and Weng, J.R. (2013). OSU-A9 inhibits angiogenesis in human umbilical vein endothelial cells via disrupting Akt-NF-kappaB and MAPK signaling pathways. *Toxicol Appl Pharmacol* 272, 616-624.
124. Ozaki, H., Okamoto, N., Ortega, S., Chang, M., Ozaki, K., Sadda, S., Vinore, M.A., Derevjani, N., Zack, D.J., Basilico, C., et al. (1998). Basic fibroblast growth factor is neither necessary nor sufficient for the development of retinal neovascularization. *Am J Pathol* 153, 757-765.
125. Ozes, O.N., Mayo, L.D., Gustin, J.A., Pfeffer, S.R., Pfeffer, L.M., and Donner, D.B. (1999). NF-kappaB activation by tumour necrosis factor requires the Akt serine-threonine kinase. *Nature* 401, 82-85.
126. Palmer, L.A., Gaston, B., and Johns, R.A. (2000). Normoxic stabilization of hypoxia-inducible factor-1 expression and activity: redox-dependent effect of nitrogen oxides. *Mol Pharmacol* 58, 1197-1203.
127. Papetti, M., and Herman, I.M. (2002). Mechanisms of normal and tumor-derived angiogenesis. *Am J Physiol Cell Physiol* 282, C947-970.
128. Park, J., Koh, M., Koo, J.Y., Lee, S., and Park, S.B. (2016). Investigation of specific binding proteins to photoaffinity linkers for efficient deconvolution of target protein. *ACS Chem Biol* 11, 44-52.
129. Penn, J.S., Madan, A., Caldwell, R.B., Bartoli, M., Caldwell, R.W., and Hartnett, M.E. (2008). Vascular endothelial growth factor in eye disease. *Prog Retin Eye Res* 27, 331-371.

130. Petersen, A.B., Ronnest, M.H., Larsen, T.O., and Clausen, M.H. (2014). The chemistry of griseofulvin. *Chem Rev* 114, 12088-12107.
131. Ponce, M.L. (2001). In vitro matrigel angiogenesis assays. *Methods Mol Med* 46, 205-209.
132. Poor, S.H., Qiu, Y., Fassbender, E.S., Shen, S., Woolfenden, A., Delpero, A., Kim, Y., Buchanan, N., Gebuhr, T.C., Hanks, S.M., et al. (2014). Reliability of the mouse model of choroidal neovascularization induced by laser photocoagulation. *Invest Ophthalmol Vis Sci* 55, 6525-6534.
133. Potente, M., Gerhardt, H., and Carmeliet, P. (2011). Basic and therapeutic aspects of angiogenesis. *Cell* 146, 873-887.
134. Prasad, P.S., Schwartz, S.D., and Hubschman, J.P. (2010). Age-related macular degeneration: current and novel therapies. *Maturitas* 66, 46-50.
135. Raffioni, S., Thomas, D., Foehr, E.D., Thompson, L.M., and Bradshaw, R.A. (1999). Comparison of the intracellular signaling responses by three chimeric fibroblast growth factor receptors in PC12 cells. *Proc Natl Acad Sci U S A* 96, 7178-7183.
136. Rafikov, R., Fonseca, F.V., Kumar, S., Pardo, D., Darragh, C., Elms, S., Fulton, D., and Black, S.M. (2011). eNOS activation and NO function: Structural motifs responsible for the posttranslational control of endothelial nitric oxide synthase activity. *J Endocrinol* 210, 271-284.
137. Rajashekhar, G., Grow, M., Willuweit, A., Patterson, C.E., and Clauss, M. (2007). Divergent and convergent effects on gene expression and function in acute versus chronic endothelial activation. *Physiol Genomics* 31, 104-113.
138. Rajashekhar, G., Kamocka, M., Marin, A., Suckow, M.A., Wolter, W.R., Badve, S., Sanjeevaiah, A.R., Pumiglia, K., Rosen, E., and Clauss, M. (2011). Pro-inflammatory angiogenesis is mediated by p38 MAP kinase. *J Cell Physiol* 226, 800-808.
139. Rajashekhar, G., Willuweit, A., Patterson, C.E., Sun, P., Hilbig, A., Breier, G., Helisch, A., and Clauss, M. (2006). Continuous endothelial cell activation increases angiogenesis: evidence for the direct role of endothelium linking angiogenesis and inflammation. *J Vasc Res* 43, 193-204.
140. Rampersad, S.N. (2012). Multiple Applications of Alamar Blue as an Indicator of Metabolic Function and Cellular Health in Cell Viability Bioassays. *Sensors (Basel)* 12, 12347-12360.
141. Räthel, T.R., Leikert Jü, F., Vollmar, A.M., and Dirsch, V.M. (2003). Application of 4,5-diaminofluorescein to reliably measure nitric oxide released from endothelial cells in vitro. *Biol Proced Online* 5, 136-142.
142. Ratner, M. (2004). Genentech discloses safety concerns over Avastin. *Nat Biotechnol* 22, 1198.

143. Resnikoff, S., Pascolini, D., Etya'ale, D., Kocur, I., Pararajasegaram, R., Pokharel, G.P., and Mariotti, S.P. (2004). Global data on visual impairment in the year 2002. *Bull World Health Organ* 82, 844-851.
144. Rosenfeld , P.J., Brown , D.M., Heier , J.S., Boyer , D.S., Kaiser , P.K., Chung , C.Y., and Kim , R.Y. (2006). Ranibizumab for Neovascular Age-Related Macular Degeneration. *N Engl J Med* 355, 1419-1431.
145. Roskoski, R., Jr. (2007). Sunitinib: a VEGF and PDGF receptor protein kinase and angiogenesis inhibitor. *Biochem Biophys Res Commun* 356, 323-328.
146. Royds, J.A., Dower, S.K., Qwarnstrom, E.E., and Lewis, C.E. (1998). Response of tumour cells to hypoxia: role of p53 and NFkB. *Mol Pathol* 51, 55-61.
147. Rufenacht, U.B., Gouya, L., Schneider-Yin, X., Puy, H., Schafer, B.W., Aquaron, R., Nordmann, Y., Minder, E.I., and Deybach, J.C. (1998). Systematic analysis of molecular defects in the ferrochelatase gene from patients with erythropoietic protoporphyria. *Am J Hum Genet* 62, 1341-1352.
148. Sagar, S.M., Yance, D., and Wong, R.K. (2006a). Natural health products that inhibit angiogenesis: a potential source for investigational new agents to treat cancer-Part 1. *Curr Oncol* 13, 14-26.
149. Sagar, S.M., Yance, D., and Wong, R.K. (2006b). Natural health products that inhibit angiogenesis: a potential source for investigational new agents to treat cancer-Part 2. *Curr Oncol* 13, 99-107.
150. Sandau, K.B., Fandrey, J., and Brune, B. (2001). Accumulation of HIF-1alpha under the influence of nitric oxide. *Blood* 97, 1009-1015.
151. Sapienza, P., Joyal, J.S., Rivera, J.C., Kermorvant-Duchemin, E., Sennlaub, F., Hardy, P., Lachapelle, P., and Chemtob, S. (2010). Retinopathy of prematurity: understanding ischemic retinal vasculopathies at an extreme of life. *J Clin Invest* 120, 3022-3032.
152. Savitski, M.M., Reinhard, F.B., Franken, H., Werner, T., Savitski, M.F., Eberhard, D., Martinez Molina, D., Jafari, R., Dovega, R.B., Klaeger, S., et al. (2014). Tracking cancer drugs in living cells by thermal profiling of the proteome. *Science* 346, 1255784.
153. Schenone, M., Dancik, V., Wagner, B.K., and Clemons, P.A. (2013). Target identification and mechanism of action in chemical biology and drug discovery. *Nat Chem Biol* 9, 232-240.
154. Schmidt, B.M., Ribnicky, D.M., Lipsky, P.E., and Raskin, I. (2007). Revisiting the ancient concept of botanical therapeutics. *Nat Chem Biol* 3, 360-366.
155. Shalaby, F., Ho, J., Stanford, W.L., Fischer, K.D., Schuh, A.C., Schwartz, L., Bernstein, A., and Rossant, J. (1997). A requirement for Flk1 in

- primitive and definitive hematopoiesis and vasculogenesis. *Cell* 89, 981-990.
156. Shi, Q., Rafii, S., Wu, M.H., Wijelath, E.S., Yu, C., Ishida, A., Fujita, Y., Kothari, S., Mohle, R., Sauvage, L.R., et al. (1998). Evidence for circulating bone marrow-derived endothelial cells. *Blood* 92, 362-367.
 157. Shim, J.S., Kim, J.H., Lee, J., Kim, S.N., and Kwon, H.J. (2004). Anti-angiogenic activity of a homoisoflavanone from *Cremastra appendiculata*. *Planta Med* 70, 171-173.
 158. Sivalingam, A., Kenney, J., Brown, G.C., Benson, W.E., and Donoso, L. (1990). Basic fibroblast growth factor levels in the vitreous of patients with proliferative diabetic retinopathy. *Arch Ophthalmol* 108, 869-872.
 159. Sleno, L., and Emili, A. (2008). Proteomic methods for drug target discovery. *Curr Opin Chem Biol* 12, 46-54.
 160. Smith, A.G., and Kaiser, P.K. (2014). Emerging treatments for wet age-related macular degeneration. *Expert Opin Emerg Drugs* 19, 157-164.
 161. Smith, L.E., Wesolowski, E., McLellan, A., Kostyk, S.K., D'Amato, R., Sullivan, R., and D'Amore, P.A. (1994). Oxygen-induced retinopathy in the mouse. *Invest Ophthalmol Vis Sci* 35, 101-111.
 162. Sulaiman, R.S., Basavarajappa, H.D., and Corson, T.W. (2014). Natural product inhibitors of ocular angiogenesis. *Exp Eye Res* 129, 161-171.
 163. Sulaiman, R.S., Merrigan, S., Quigley, J., Qi, X., Lee, B., Boulton, M.E., Kennedy, B., Seo, S.Y., and Corson, T.W. (2016). A novel small molecule ameliorates ocular neovascularisation and synergises with anti-VEGF therapy. *Sci Rep* 6, 25509.
 164. Sulaiman, R.S., Quigley, J., Qi, X., O'Hare, M.N., Grant, M.B., Boulton, M.E., and Corson, T.W. (2015). A simple optical coherence tomography quantification method for choroidal neovascularization. *J Ocul Pharmacol Ther* 31, 447-454.
 165. Swift, M.R., and Weinstein, B.M. (2009). Arterial-venous specification during development. *Circ Res* 104, 576-588.
 166. Tahergorabi, Z., and Khazaei, M. (2012). A review on angiogenesis and its assays. *Iran J Basic Med Sci* 15, 1110-1126.
 167. Tak, P.P., and Firestein, G.S. (2001). NF- κ B: a key role in inflammatory diseases. *J Clin Invest* 107, 7-11.
 168. Takagi, H., King, G.L., Ferrara, N., and Aiello, L.P. (1996). Hypoxia regulates vascular endothelial growth factor receptor KDR/Flk gene expression through adenosine A2 receptors in retinal capillary endothelial cells. *Invest Ophthalmol Vis Sci* 37, 1311-1321.
 169. Tobe, T., Ortega, S., Luna, J.D., Ozaki, H., Okamoto, N., Derevjani, N.L., Vinore, S.A., Basilico, C., and Campochiaro, P.A. (1998). Targeted

- disruption of the FGF2 gene does not prevent choroidal neovascularization in a murine model. *Am J Pathol* 153, 1641-1646.
170. Tomita, K., Chikumi, H., Tokuyasu, H., Yajima, H., Hitsuda, Y., Matsumoto, Y., and Sasaki, T. (1999). Functional assay of NF- κ B translocation into nuclei by laser scanning cytometry: inhibitory effect by dexamethasone or theophylline. *Naunyn Schmiedeberg's Arch Pharmacol* 359, 249-255.
 171. Tsuboi, H., Yonemoto, K., and Katsuoka, K. (2007). Erythropoietic protoporphyria with eye complications. *J Dermatol* 34, 790-794.
 172. Tuder, R.M., Flook, B.E., and Voelkel, N.F. (1995). Increased gene expression for VEGF and the VEGF receptors KDR/Flk and Flt in lungs exposed to acute or to chronic hypoxia. Modulation of gene expression by nitric oxide. *J Clin Invest* 95, 1798-1807.
 173. Vanderslice, P., Munsch, C.L., Rachal, E., Erichsen, D., Sughrue, K.M., Truong, A.N., Wygant, J.N., McIntyre, B.W., Eskin, S.G., Tilton, R.G., et al. (1998). Angiogenesis induced by tumor necrosis factor- α is mediated by α 4 integrins. *Angiogenesis* 2, 265-275.
 174. Webster, G.A., and Perkins, N.D. (1999). Transcriptional cross talk between NF- κ B and p53. *Mol Cell Biol* 19, 3485-3495.
 175. Welti, J., Loges, S., Dimmeler, S., and Carmeliet, P. (2013). Recent molecular discoveries in angiogenesis and antiangiogenic therapies in cancer. *J Clin Invest* 123, 3190-3200.
 176. Wenzel, A.A., O'Hare, M.N., Shadmand, M., and Corson, T.W. (2015). Optical coherence tomography enables imaging of tumor initiation in the TAg-RB mouse model of retinoblastoma. *Mol Vis* 21, 515-522.
 177. Yancopoulos, G.D., Davis, S., Gale, N.W., Rudge, J.S., Wiegand, S.J., and Holash, J. (2000). Vascular-specific growth factors and blood vessel formation. *Nature* 407, 242-248.
 178. Yang, H.T., Papoutsopoulou, S., Belich, M., Brender, C., Janzen, J., Gantke, T., Handley, M., and Ley, S.C. (2012). Coordinate regulation of TPL-2 and NF- κ B signaling in macrophages by NF- κ B1 p105. *Mol Cell Biol* 32, 3438-3451.
 179. Yoshida, A., Yoshida, S., Ishibashi, T., Kuwano, M., and Inomata, H. (1999). Suppression of retinal neovascularization by the NF- κ B inhibitor pyrrolidine dithiocarbamate in mice. *Invest Ophthalmol Vis Sci* 40, 1624-1629.
 180. Yoshida, A., Yoshida, S., Khalil, A.K., Ishibashi, T., and Inomata, H. (1998). Role of NF- κ B-mediated interleukin-8 expression in intraocular neovascularization. *Invest Ophthalmol Vis Sci* 39, 1097-1106.

181. Yoshida, S., Ono, M., Shono, T., Izumi, H., Ishibashi, T., Suzuki, H., and Kuwano, M. (1997). Involvement of interleukin-8, vascular endothelial growth factor, and basic fibroblast growth factor in tumor necrosis factor α -dependent angiogenesis. *Mol Cell Biol* 17, 4015-4023.
182. Zhang, F., Yu, W., Hargrove, J.L., Greenspan, P., Dean, R.G., Taylor, E.W., and Hartle, D.K. (2002). Inhibition of TNF- α induced ICAM-1, VCAM-1 and E-selectin expression by selenium. *Atherosclerosis* 161, 381-386.
183. Zhang, M.S., Peng, S.W., and Wang, W. (2010). Macro research on growth and development of *Cremastra appendiculata* (D. Don.) Makino (Orchidaceae). *J Med Plants Res* 4, 1837-1842.
184. Ziche, M., and Morbidelli, L. (2000). Nitric oxide and angiogenesis. *J Neurooncol* 50, 139-148.

CURRICULUM VITAE

Halesha Dhurvigere Basavarajappa

Education:

PhD **2011 – 2016**
Department of Biochemistry and Molecular Biology, Indiana University, USA.

Dissertation title: Molecular mechanism of action of an antiangiogenic natural product, cremastranone.

MSc **2003 – 2005**
Department of Biochemistry, Bangalore University, Bangalore, India.

Industrial Work Experience **2011 – 2016**
Assistant Research Scientist
AstraZeneca Pharmaceuticals India Pvt Ltd (R&D), Bangalore, India

Research Experience:

As a graduate student in Dr Timothy Corson's lab, I was involved in identifying novel antiangiogenic small molecules as well as understanding the mechanism of action of cremastranone, an antiangiogenic molecule. During my dissertation, I identified ferrochelatase, an enzyme required for synthesizing heme, as an important mediator of ocular angiogenesis using various biochemical (spectrophotometric enzyme assays, recombinant protein production and purification), biophysical (ITC), cell culture (in vitro angiogenesis assays, immunoblot, qPCR) and in vivo techniques (oxygen induced retinopathy mouse model).

As an assistant research scientist in AstraZeneca Pharmaceuticals I was involved in developing and optimizing enzyme assays (spectrophotometric, spectrofluorimetric, HPLC-based) and protein binding assays (thermal melt and ITC) for drug targets as well as identifying potent, novel enzyme inhibitors for development of anti-mycobacterial drugs.

Research scholarship and Travel grants:

- | | |
|------|---|
| 2015 | Received "Elizabeth Anderson travel grant" to attend ARVO-2015 annual meeting. |
| 2015 | Best poster presentation award from Dept. of Biochemistry & Molecular biology (IUSM) |
| 2013 | Received "Ausich graduate student research scholarship" for two years (2013 and 2014, \$15000 p.a.) from Kemin Health industries to study the mechanism of action of cremastranone. |

Honors and Awards:

2010	Award of Excellence for Best Project team – 2009 by AstraZeneca (R &D).
2009	Award for “developing XTT-based assay for monitoring the enzymatic activity of one of the protein drug target” by AstraZeneca (R & D).
2008	Award for “developing and optimizing modified malachite green reagent to monitor the ATPase activity in High Throughput Screening-format” by AstraZeneca (R&D).
2007	Award for “Establishing methods to purify some of the challenging proteins of <i>E.coli</i> and <i>M.tuberculosis</i> ” by AstraZeneca (R&D).
2007	Promoted to Assistant research scientist 2.
2005	Qualified in the “National eligibility test” conducted at the national level for entry into PhD programs and/or as a lecturer to undergraduate degree colleges.

Patents:

1. Corson TW, Seo SY, Basavarajappa HD, Lee B, Fei X. Compounds for treatment of angiogenesis mediated diseases. U.S. National Patent Application 14/888,117, filed 30 October 2015.
2. Corson TW, Basavarajappa HD. Inhibition of Ferrochelatase as an Antiangiogenic Therapy. US Patent Application Serial No. 15/009,339. Filed January 28, 2016.

Mentorship experience:

I have trained two high school students, one undergraduate and one PhD rotation student in learning various biochemical techniques required for completing their research projects.

Technical skills:

Molecular DNA cloning, Protein expression in both Prokaryotic and Eukaryotic cells, Protein purification using affinity, Ion-exchange, Size-exclusion column chromatography, HPLC based enzyme assays, Spectrophotometric, Florescence polarization and Spectrofluorimetric enzyme assays, ELISA based assays, Western Blot, Aseptic Bacterial techniques, Mammalian cell culture techniques, Cell migration assay, Matrigel-based tube formation assay, Confocal Microscopy, Flow cytometry, Basic mouse handling techniques, qRT-PCR, Protein Thermal shift assay, Isothermal Titration Calorimetry (ITC).

Published abstracts:

- 2015 Poster presentation at ARVO-2016 annual meeting in Seattle, Washington, USA.
Title: "Ferrochelatase is required for retinal neovascularization". Invest Ophthalmol Vis Sci 57, E-abstract 3639, (2016).
- 2015 Oral presentation at ARVO-2015 annual meeting in Denver, Colorado, USA.
Title: "Ferrochelatase as a novel mediator of ocular angiogenesis". Invest Ophthalmol Vis Sci 56, E-abstract 5854, (2015).
- 2014 Oral presentation at ARVO-2014 annual meeting in Orlando, Florida, USA.
Title: "Identification and characterization of a novel synthetic homoisoflavonoid as an inhibitor of retinal angiogenesis." Invest Ophthalmol Vis Sci 55, E-abstract 1266, (2014).
- 2013 Poster presentation at ARVO-2013 annual meeting in Seattle, Washington, USA.
Title: "Structure-activity relationship studies of a natural product inhibitor of choroidal angiogenesis. Invest Ophthalmol Vis Sci 54, E-abstract 3282, (2013)

Publications:

1. Basavarajappa HD, Qi X, Sulaiman RS, Lee B, Quigley J, Sishtla K, Alkhairy S, Gupta K, Shadmand M, Grant MB, Boulton ME, Seo SY & Corson TW. Ferrochelatase is a therapeutic target for ocular neovascularization. (Submitted).
2. Basavarajappa HD, Lee B, Lee H, Sulaiman RS, An H, Magaña C, Shadmand M, Vayl A, Rajashekar G, Kim EY, Suh YG, Lee K, Seo SY, Corson TW. Synthesis and biological evaluation of novel homoisoflavonoids for retinal neovascularization. J Med Chem. 2015 Jun 25; 58(12):5015-27. PubMed PMID: 26035340.
3. Sulaiman RS, Basavarajappa HD, Corson TW. Natural product inhibitors of ocular angiogenesis. Exp Eye Res. 2014 Dec; 129:161-71. PubMed PMID: 25304218.
4. Humnabadkar V, Madhavapeddi P, Basavarajappa H, Sheikh MG, Rane R, Basu R, Verma P, Sundaram A, Mukherjee K, de Sousa SM. Assays, surrogates, and alternative technologies for a TB lead identification program targeting DNA gyrase ATPase. J Biomol Screen. 2015 Feb; 20(2):265-74. PubMed PMID: 25300873.

5. Lee B, Basavarajappa HD, Sulaiman RS, Fei X, Seo SY, Corson TW. The first synthesis of the antiangiogenic homoisoflavanone, cremastranone. *Org Biomol Chem*. 2014 Oct 21; 12(39):7673-7. PubMed PMID: 25167470.
6. Basavarajappa HD, Lee B, Fei X, Lim D, Callaghan B, Mund JA, Case J, Rajashekhar G, Seo SY, Corson TW. Synthesis and mechanistic studies of a novel homoisoflavanone inhibitor of endothelial cell growth. *PLoS One*. 2014 Apr 21; 9(4):e95694. PubMed PMID: 24752613.
7. Thériault BL, Basavarajappa HD, Lim H, Pajovic S, Gallie BL, Corson TW. Transcriptional and epigenetic regulation of KIF14 overexpression in ovarian cancer. *PLoS One*. 2014 Mar 13; 9(3):e91540. PubMed PMID: 24626475.
8. Kale RR, Kale MG, Waterson D, Raichurkar A, Hameed SP, Manjunatha MR, Kishore Reddy BK, Malolanarasimhan K, Shinde V, Koushik K, Jena LK, Menasinakai S, Humnabadkar V, Madhavapeddi P, Basavarajappa H, Sharma S, Nandishaiah R, Mahesh Kumar KN, Ganguly S, Ahuja V, Gaonkar S, Naveen Kumar CN, Ogg D, Boriack-Sjodin PA, Sambandamurthy VK, de Sousa SM, Ghorpade SR. Thiazolopyridone ureas as DNA gyrase B inhibitors: optimization of antitubercular activity and efficacy. *Bioorg Med Chem Lett*. 2014 Feb 1; 24(3):870-9. PubMed PMID: 24405701.
9. Kale MG, Raichurkar A, P SH, Waterson D, McKinney D, Manjunatha MR, Kranthi U, Koushik K, Jena Lk, Shinde V, Rudrapatna S, Barde S, Humnabadkar V, Madhavapeddi P, Basavarajappa H, Ghosh A, Ramya VK, Gupta S, Sharma S, Vachaspati P, Kumar KN, Giridhar J, Reddy J, Panduga V, Ganguly S, Ahuja V, Gaonkar S, Kumar CN, Ogg D, Tucker JA, Boriack-Sjodin PA, de Sousa SM, Sambandamurthy VK, Ghorpade SR. Thiazolopyridine ureas as novel antitubercular agents acting through inhibition of DNA Gyrase B. *J Med Chem*. 2013 Nov 14; 56(21):8834-48. PubMed PMID: 24088190.
10. Shirude PS, Madhavapeddi P, Tucker JA, Murugan K, Patil V, Basavarajappa H, Raichurkar AV, Humnabadkar V, Hussein S, Sharma S, Ramya VK, Narayan CB, Balganesht TS, Sambandamurthy VK. Aminopyrazinamides: novel and specific GyrB inhibitors that kill replicating and nonreplicating *Mycobacterium tuberculosis*. *ACS Chem Biol*. 2013 Mar 15; 8(3):519-23. PubMed PMID: 23268609.
11. Basavarajappa HD, Corson TW. KIF14 as an oncogene in retinoblastoma: a target for novel therapeutics? *Future Med Chem*. 2012 Nov; 4(17):2149-52. PubMed PMID: 23190103.